Gravity Field Uncertainty Analysis for Ganymede Orbit Phase of The JUICE mission.

Parameter Error Propagation

B.N. Kiyani

Delft University of Technology

Gravity Field Uncertainty Analysis for Ganymede Orbit Phase of The JUICE mission.

Parameter Error Propagation

MSc Thesis

by

B.N. Kiyani

to obtain the degree of Master of Science
at the Delft University of Technology.

Department of Astrodynamics and Space missions

Cover Image from: https://www.nasa.gov/image-feature/jpl/juno-s-ganymede-close-up
NASA's Juno spacecraft during its 07 June 2021 flyby of Ganymede
at closest approach of 1038 km.

Graduation Committee TU Delft:	Dr. ir. E. Mooij	Committee chairperson
	Dr. ir. D. Dirkx	Daily supervisor
	Dr. ir. A. Cervone	External member

TU Delft

”The sun, too, runs its determined course laid down for it by the almighty, the all knowing.

As for the moon, We have ordained (precise) phases for it, until it finally becomes like an old date-stalk.

The sun cannot overtake the moon, nor can the night outrun the day: each floats in [its own] orbit.”

Qur’an [36:37-36:40]

Preface

”Whether one moves slowly or with speed, the one who is a seeker will be a finder.” Rumi

As I write the final words to conclude my MSc. Thesis and therefore my study period at TU Delft, I can’t help but remember this quote which pretty much sums up how I feel about this journey. Despite all obstacles, I am greatly humbled to have come so far and have the opportunity to successfully complete the journey that I started some long time ago. At times I thought I would not make it and I doubted my own capabilities, but I don’t give up easily and this piece of document is proof of that. It would be selfish to think that I was alone. I met so many inspiring students, friends, researchers, mentors and teachers, too many to name all of you here. I would like to thank each one of you from the bottom of my heart, you have made my life pleasant in one way or the other.

This work would not have come to fruition if it weren’t for my supervisor Dominic. I can rightfully say that you did not give up either and endured with me through the difficult phases at the start of the project. I would like to thank you for everything. You carefully guided me through this project and accepted my personal shortcomings. And thank you even more for taking out the time to explain things in detail several times when needed and pushing me through the obstacles.

Last but not least, my sincere gratitude to student advisor Susan. You have always been there for me. I am truly grateful to have received your support in the most difficult of times. I couldn’t have made it without you!

B.N. Kiyani
Delft, April 2022

Abstract

The Ganymede Circular Orbit Phase (GCO-500) of the JUICE (JUpiter ICy moon Explorer) mission will be the first time a moon beyond Earth's will be orbited for an extended period of 9 months. This orbit phase, due to its close proximity, opens the window to more accurately determine the spacecraft position and thereby unambiguously characterize the interiors of the Galilean moons. Ganymede is believed to harbor an internal ocean and will help understand the habitability of icy worlds in the outer solar system. Gravity field coefficients of Ganymede are known for $C_{2,0}$ and $C_{2,2}$ with an underlying assumption of hydrostatic equilibrium. One of the objectives of the JUICE mission at Ganymede is to improve the degree 2 gravity field (without relying on the assumption of hydrostatic equilibrium). Furthermore, the JUICE mission will allow to determine gravity field coefficients up to degree and order 12.

In this thesis results of a sensitivity analysis are presented which investigate the settings of a basic model developed for the GCO-500 phase of the JUICE mission. The basic model aims to realistically emulate the JUICE mission concept, by specifically focusing on the radio science experiment 3GM and the PRIDE experiment, which are responsible for estimating the gravity field. The model also includes non-gravitational accelerations which are accounted for by the High Accuracy Accelerometer (HAA) onboard the JUICE mission. The sensitivity analysis quantitatively evaluates the robustness of the finding by means of the output of a covariance analysis, namely formal errors and correlations of parameters. The covariance analysis propagates the error in simulated observations with respect to (a priori) uncertainty in estimated parameters. These parameters include gravity field coefficients uncertainty up to and including degree and order 12, spacecraft (initial) states, Gravitational Parameter of Ganymede and empirical accelerations from the on-board accelerometer.

The sensitivity analysis will help identify sensitive variables or settings which aids in accurate predictions and recommendations with regards to mission operations in the future. An extensive set of setting is investigated, which include Data types & weights, observation interval & planning, arc length & number of arcs as well as mission duration. The results shows that in general the gravity field is hardly sensitive to any settings that were investigated. Increasing the arc length of (initial) states influences the spacecraft initial uncertainty more than it does the gravity field uncertainty. On the other hand, changing the arc length of empirical accelerations affects the gravity field more than other settings (but still less than 1% overall change) and the affect of it is again largest on the states. For range only measurements, decreasing the range noise from 20 cm to 1 cm show a significant influence in formal error for both gravity field and (initial) states. The correlation coefficient between gravity field parameters, compared to some previous studies is significantly lower.

In conclusion, the indifference of the gravity field to the chosen settings means that a stable model has been developed which is a good foundation to investigate the error propagation of parameters for the JUICE mission in the future. It is recommended to include range measurements with data noise of 1 cm, to missions which previously only relied on Doppler measurements. Operation of the on-board accelerometer shows room for freedom as the formal error of gravity field is hardly sensitive to the arc length of empirical accelerations. However, when considering (initial) states, the large change in formal error will be reason to efficiently manage accelerometer operations on board the JUICE mission.

Contents

1

Introduction

The JUpiter ICy moons Explorer (JUICE) will perform detailed investigations of Jupiter and its four largest moons, known as the Galilean moons. The Galilean moons were discovered by Galileo in 1610 and spotted by a telescope due to their massive sizes, Ganymede being the largest moon in the solar system. The JUICE mission will study the three icy moons of the Jovian system (Ganymede, Callisto and Europa) in close proximity. The secondary target of the mission is to study other bodies in the Jovian system including volcanic Io, inner moons and rings of Jupiter as well as Jupiter itself. Jupiter has a composition similar to that of the sun and a total of 68 moons making it a small solar system in itself. With this mission ESA (European Space Agency) aims to understand the formation of the solar system and interaction of bodies within the solar system as well as characterize the possibility of life on the icy moons where possible forms of life may exist due to the presence of water (Magnanini (2021)). The Jovian tour encompasses gravity assists, flybys and finally the Ganymede orbit phase (GCO-500) at 500km (ESA (2014)). In terms of relevance to orbit determination this tour becomes challenging as there are discontinuities in down link periods to the ground station which leads to uncertainties in the initial conditions for the start of each subsequent leg of the mission. The Ganymede orbit phase however will provide a continuous set of data for the entire orbit phase, the down link period is set to 8 hours per day to earth ground stations, enabling post-processing of data to determine spacecraft trajectory and physical parameters in a batch, by control centres on earth. JUICE's 3GM and Pride experiment primarily are responsible for the orbit determination (Cimò et al. (2017)) and an onboard High Accuracy Accelerometer will measure the non-gravitational forces acting on the spacecraft.

Although Esa's JUICE mission is yet to be launched, the possibility of predicting the outcome of the mission by numerical simulations is an admirable aspect of modern techniques of numerical simulations. Once the results of the simulations are compared to the actual data, improvements can be made in modelling techniques and hence parameter estimation as well as uncertainty estimation. This insight can then be applied to estimate better physical parameters for all other solar system bodies and beyond for which it might not always be possible to send a planetary mission. In this work, the JUICE mission is used as a case study to investigate the sensitivity of the developed model to certain inputs, hence quantifying the affect of changing certain assumptions and providing high level of credibility to the model by testing it across a wide set of possibilities. The sensitivity analysis helps to evaluate the underlying assumptions and aid in better decision making about model development in the future. The JUICE spacecraft will tour Ganymede for a total of 9 months and eventually crash into Ganymede to terminate the JUICE mission. This tour starts with an elliptical orbit phase followed by a 5000km circular orbit phase (Cappuccio et al. (2018)). The second elliptical orbit phase starts at this altitude to eventually reach a low altitude orbit of 500km. This orbit is low enough to study in detail the interior composition as well exterior (exosphere) of Ganymede and will enable to determine gravity field coefficients up to and including degree and order 12 as per JUICE mission requirements.

Parameter estimation due to orbit determination is one aspect of accurately determining the position and velocity of a spacecraft from a ground station, reducing the uncertainty of the determined parameters is equally important to determine the error bounds within which the estimated parameter is expected to lie in. At present measurements can determine the position and velocity of a spacecraft within 20cm and 0.1 m/s uncertainty respectively (Dirkx et al. (2017)). This uncertainty in spacecraft

state is then used to propagate the uncertainty in estimated parameters. These parameters help better characterize the exterior and interior of a planetary body and reveal mysteries about the formation of these bodies and other phenomena in the solar system (ESA (2014)). While the position of the spacecraft is constantly changing and is prone to perturbations, parameters such as gravity field coefficients and gravitational parameters are not sensitive to short term perturbations and their estimation will not lead to significant changes in their currently defined universal values, it is the uncertainty which can be propagated with short time periods such as the JUICE mission to detect any changes compared to previous missions and add to the existing knowledge about the error bounds of these parameters. The sensitivity analysis quantitatively evaluates the robustness of the finding by means of the output of a covariance analysis, namely formal errors and correlations of parameters. A covariance analysis has the advantage that it is computationally less demanding since state estimation is not performed, therefore the best estimate of the trajectory is not computed, instead only the uncertainty associated with states and parameters is computed. This simplicity in covariance analysis further makes it easier to estimate the uncertainties in a large set of parameters. The formal errors are statistical values which indicate the magnitude of the uncertainty of the parameters, however these values might be optimistic and therefore not entirely realistic. A disadvantage of the covariance analysis is that the true error can not be calculated, because true error is the difference between estimated state and apriori state, while the state is not estimated in a covariance analysis (Dirkx et al. (2016)).

Since the announcement of the JUICE mission various preliminary investigations have been performed to theoretically quantify the improvement that JUICE instruments will achieve in for example measuring the gravity filed and spacecraft orbit. One such study is done by (Di Benedetto et al. (2021)) where the role of the 3GM experiment of the JUICE mission is investigated in the accurate estimation of the tidal love number (k_2), for flyby phase of Callisto. Here a covariance analysis is performed using the JUICE mission as a case study.

The present thesis work uses the same foundation of the covariance analysis to study the sensitivity of the model to certain input settings/parameters. The goal of this study is to build a spacecraft dynamic model as accurate as possible based on mission and instrument specifications of the JUICE mission and perform a sensitivity study which determines the affects of changing simulation settings on the quality of the parameter uncertainty estimation. A wide range of settings are tested which help identify optimal data acquisition strategies as well as areas of improvement. This will help define a simulation model which is close to reality and help predict the real outcome of the JUICE mission and give useful recommendations to the actual mission operations before it flies.

The main **research objective** is as follows:

Determine the influence of model settings and parameters on the quality of the gravity field uncertainty estimation of Ganymede during the orbit phase of the JUICE mission.

To achieve the desired sensitivity analysis, three **research questions** are defined:

- How well is the gravity field uncertainty of Ganymede simulated during GCO-500 phase of the JUICE mission.
- What are the most sensitive settings/parameters and to what extent do they influence error estimation of gravitational and non-gravitational parameters.
- How do the sensitivity results contribute to future mission operations of the JUICE mission.

Following this introduction, the main research is presented in the form of a scientific paper in chapter 2. The scientific paper will present the results as well as its own conclusion. The answers to the research question as described above are presented in the conclusion of the main report (Chapter 3). In chapter 4 the recommendations stemming from this work are given. Model development and the results, which have been omitted in the scientific paper are presented in Appendix A. Appendix B deals with the verification of the model and validation of the results.

2

Scientific Paper

Gravity Field Uncertainty Analysis for Ganymede Orbit Phase of The JUICE Mission. Parameter Error Propagation

B. N. Kiyani[a,]

[a] *Delft University of Technology, Kluyverweg 1, 2629HS Delft, The Netherlands*

Abstract

Context: The Ganymede Circular Orbit Phase (GCO-500) of the JUICE (JUpiter ICy moon Explorer) mission will be the first time a moon beyond Earth's will be orbited for an extended period of 9 months. This orbit phase, due to its close proximity, opens the window to more accurately determine the spacecraft orbit and thereby unambiguously characterize the interiors of the Galilean moons. Ganymede is believed to harbor an internal ocean and will help understand the habitability of icy worlds in the outer solar system.

Aim: In this paper results of a sensitivity analysis are presented which investigate the settings of a basic model developed for the GCO-500 phase of the JUICE mission. The basic model aims to realistically emulate the JUICE mission concept, by specifically focusing on the radio science experiment 3GM and the PRIDE experiment, which are responsible for estimating the gravity field. The model also includes non-gravitational accelerations which are accounted for by the High Accuracy Accelerometer (HAA) onboard the JUICE mission.

Method: The sensitivity analysis quantitatively evaluates the robustness of the finding by means of the output of a covariance analysis, namely formal errors and correlations of parameters. These parameters include gravity field coefficients up to and including degree and order 12, spacecraft (initial) states, gravitational parameter of Ganymede and empirical accelerations from the on-board accelerometer.

Results: The results shows that in general the gravity field is hardly sensitive to any settings that were investigated. Increasing the arc length of (initial) states influences the spacecraft initial uncertainty more than it does the gravity field uncertainty. On the other hand, Changing the arc length of empirical accelerations affects the gravity field more than other settings (but still less than 1% overall change) and the affect of it is again largest on the states. For range only measurements, decreasing the range noise from 20 cm to 1 cm show a significant influence in formal error for both gravity field and (initial) states. The correlation coefficient between gravity field parameters, compared to some previous studies is significantly lower.

Conclusion: The indifference of the gravity field to the chosen settings means that a stable model has been developed which is a good foundation to investigate the error propagation of parameters for the JUICE mission in the future. Also sensitivity analysis have successfully quantified the influence of arc length, data noise and other parameters. It is recommended to include range measurements with data noise of 1 cm, to missions which previously only relied on Doppler measurements. Operation of the on-board accelerometer shows room for freedom as the formal error of gravity field is hardly sensitive to the arc length of empirical accelerations. However, when considering (initial) states, the large increase in formal error will be reason to efficiently manage accelerometer operations.

Keywords: Degree Variance; Arc-wise States; Empirical Accelerations; Gravity field uncertainty; Covariance

1. Introduction

Although the closest approach of Nasa's Galileo mission of 261 km from Ganymede's surface in September 1996 (Frank et al. (1997)) lead to numerous discoveries about the interior of the largest moon in the solar system including a first estimate of the gravity field coefficients up to degree and order 2 (namely $C_{2,0}$ and $C_{2,2}$) (Anderson et al. (1996)), no mission however has orbited the Galilean moon or any other moon beyond Earth's and therefore the gravity field of Ganymede remains largely unexplored. The extended GCO-500 phase (Ganymede Circular Orbit at 500 km altitude) is the last leg of ESA's (European Space Agency) JUICE (JUpiter ICy moon Explorer) mission and the first time a moon beyond earth's moon will be orbited for 4 months(ESA (2014)), with the total Ganymede orbit phase being 9 months.

The extended orbit phase will provide extensive amount of continuous data at close proximity to the surface of Ganymede. Even though at closest approach of a flyby,

Email address: bushraky8@gmail.com (B. N. Kiyani)

the spacecraft is at close proximity to the surface, but this is for a very short period of time, due to high velocity at closest approach the spacecraft is soon bound outwards. Secondly, spacecraft dynamics at closest approach will be influenced by a small area of Ganymede, therefore numerous flybys are needed for a wider coverage of the gravity field. In case of the JUICE mission the extended orbit phase will provide almost global coverage of Ganymede enabling more accurate gravity field estimation.

The degree 2 field is a point of interest as it enables determining indirectly the moment of inertia of the body (and hence thickness of ice crust and internal differentiation). The degree 2 determination of Ganymede's gravity field as of yet (By the Galileo mission) are based on the underlying assumption of the 'hydro-static equilibrium' (ESA (2014)). The consequence of which is that the degree 2 field coefficients cannot be determined independently. Hydro-static equilibrium is the state that is reached when the gravitational force that holds the body together is equal to the internal pressure, hence the body does not expand or shrink any more (Luciuk and Carlo (2019)). The concept of hydro-static equilibrium is more applicable to giant bodies such as the Sun, Jupiter and in this case safe to assume Ganymede because the force that prevents these bodies from collapsing is internal fluid pressure (De Pater and Lissauer (2015)). If one is to imagine a dissection of a differentiated body, for any two layers of the body the hydro-static equilibrium is due to the balance between the thermal pressure from the inside being equal to the weight of the layer from above. This internal differentiation in planetary body is due to layers of different materials and densities separating from each other and the layers of higher density normally move towards the centre of the body, during the formation period of the planet or body (Hussmann et al. (2006)). Hydro-static equilibrium is assumed when the internal differentiated layers of the body are ambiguous and have yet to be estimated to characterize the internal layers of the body. In the past to estimate gravity field coefficients, it is normally assumed that all coefficients are zero except for $C_{2,0}$ and $C_{2,2}$ which are fixed to a hydrostatic equilibrium ratio of -10/3 respectively (Nimmo et al. (2011)). Whether this ratio will hold for the estimated coefficients with results obtained from the JUICE mission will be an interesting and coincidental result to look out for, hopefully resulting in deviation of this presumption. Also once the gravity 2 field coefficients are estimated with a higher precision this will help to assess the extent of differentiation better.

Most recently NASA's Juno spacecraft performed a flyby of Ganymede with closest approach of about 1050 km (Casajus et al. (2021)). This approach with more accurate data acquisition with current instruments will add to the existing estimates of the degree-2 gravity fields. How and to what extent the previous estimates for the degree-2 coefficients are improved from Juno's recent closest approach in June 2021 might be ongoing and is yet to be seen. Juno's mission remains a flyby and the output from JUICE is expected to deliver more clues to the mysteries of the icy moons than Juno mission.

The JUICE mission is a so called L-Class (Large) mission, ones which are selected for launch once every decade (Dougherty et al. (2012)). Ganymede is the main target and the final leg around Ganymede after a set of flybys and gravity assists around the other Galilean moons (Callisto, Io and Europa). Ganymede is the largest moon in the solar system and the only moon with its own intrinsic magnetic field (Kivelson et al. (1996)). The discovery of the magnetic field hints towards an outer silicate core and inner (partially) liquid iron or iron sulphide core (Schubert et al. (1996)). The metallic core is predicted to have a radius of 400-1300km (Anderson et al. (1996)). Surrounding the silicate mantle is a thick layer of ice with a predicted radius of 800km (Anderson et al. (1996)). It is this surface ice crust which makes Ganymede different from Io. Io also appears to have an intrinsic magnetic field due to a metallic core (Schubert et al. (1996)) but no ice crust. Measurements from Hubble Telescope have confirmed the presence of a subsurface ocean (Saur et al. (2015)) in Ganymede which could be potential reason to believe in the emergence of habitable worlds around Gas giants. JUICE mission will further unambiguously characterize the internal structure of Ganymede. There is still ambiguity about the thickness of the inner core as mentioned above, but also the depth of the subsurface ocean (Saline or dissolved electrolytes) which according to some estimate could be about 150km below the icy crust. Below the subsurface ocean is another layer of ice (icy mantle), the composition and depth of which need to be constrained as well. The JUICE mission will in this way help further characterize the Jovian system and eventually help to answer fundamental question about the conditions for planet formation and emergence of life. For more details about this and other science goals of the JUICE mission, the interested reader can consult ESA (2014).

The JUICE mission hosts a total of 10 instruments as well as a science experiment (PRIDE), together they comprise of three packages namely the remote sensing package, the geophysics package and the *in situ* package. The radio science instrument 3GM (Gravity and Geophysics of Jupiter and the Galilean Moons) is part of the geophysics package. The 3GM is mainly responsible for estimating the gravity fields. This is supported by the PRIDE experiment (which does not have its own hardware on-board), using ground based VLBI (Very Long Baseline Interferometry) measurements to improve the orbits of the spacecraft and the moons (ESA (2014)). The radio science package of JUICE (3GM) allows improving the gravity field compared to previous missions. While Galileo mission was equipped with a radio science system, due to failure of deployment this system failed, resulting in data loss. The 3GM ka/ka radio link of the JUICE mission is highly immune to interplanetary plasma noise. Combining this with the X/X and X/Ka band radio links provided by the Deep Space Transponder, will almost eliminate (Dis-

persive) plasma noise ESA (2014). This improved mission design combined with an ambitious 4 month orbit of Ganymede at low altitude of 500km will lead to unprecedented accuracy in gravity field determination which in turns leads to better characterization of the interior and exterior of the icy moon. Adding to this accuracy is the on-board accelerometer. While the Galileo mission did not house an on-board accelerometer, the JUICE mission is equipped with a High Accuracy Accelerometer (HAA) which accounts for the non-gravitational (empirical) forces due to radiation pressure, atmospheric drag and propellant sloshing.

Since the announcement of the JUICE mission various preliminary investigations have been performed to theoretically quantify the improvement that JUICE instruments will achieve in for example measuring the gravity filed and spacecraft orbit. One such study is done by Di Benedetto et al. (2021) where the role of the 3GM experiment of the JUICE mission is investigated in the accurate estimation of the tidal love number (k_2). Here a covariance analysis is performed using the JUICE mission as a case study. A covariance analysis is the process of propagating the error or uncertainty in observations with respect to uncertainty of parameters, where the simulation model, a priori uncertainty in observations and parameters are a basis for the propagation. The obtained (numerical) uncertainty is the margin or bound within which the value of the parameter lies or could lie, which in turn is needed in a sensitivity analysis to assess the confidence in obtained results and hence limitations or triumphs of the developed model's input (variables) and design. Therefore a sensitivity analysis is performed in tandem with a covariance analysis. The present thesis work uses the same foundation of the covariance analysis as done by (Di Benedetto et al. (2021)) to study the sensitivity of the model to certain input settings/parameters. In the numerical model which is developed in this study, covariance analysis will quantify the achievable accuracy of the parameters and will provide insight into whether deviations from the hydrostatic equilibrium will be detected by JUICE. The estimated uncertainties include gravitational as well as non-gravitational parameters and spacecraft states. The gravity field uncertainty is estimated up to degree 12 for the GCO-500 phase of the JUICE mission, this is in accordance with JUICE instrument requirements. Hydro-static equilibrium condition as mentioned above will not be applied when setting a priori uncertainties for the degree 2 gravity field coefficients ($C_{2,0}$ and $C_{2,2}$). Once the nominal model is set up, the next step is to investigate the factors which affect these error bounds by varying the settings and assessing how influential each setting is. This will eventually help understand the underlying reasons for any observable outputs and lead to further improvement of the model. These reasons may include errors in instrumentation (3GM or accelerometer) or (numerical) Dynamic model assumptions and limitations.

The aim of this paper is to present the results of a sensitivity analysis which determines the affects of changing simulation settings on the quality of the parameter uncertainty estimation. A wide range of settings are tested which help provide credibility to the nominal model and the results. This is crucial in assessing the robustness of the findings and the ability to make better decisions regarding mission design and identifying optimal data acquisition strategies as well as areas of improvement. This will help define a simulation model which is close to reality and help predict the real outcome of the JUICE mission and give useful recommendations to the actual mission operations before or after it flies.

In the sensitivity analysis two steps are taken. A first set of settings/parameters are investigated to come to a nominal model. These simulation runs include the influence of data quality (noise and type of data), a priori uncertainty of parameters and mission duration among other settings. This nominal model is developed to rule out the need to further investigate settings which are predicted to not influence the model if was to be run with additional settings and to higher degree and order. Once the nominal model is consolidated, further settings/parameters are investigated which need a proper/complete model to start with. These settings include addition of gravitational parameter of Ganymede, different settings for the empirical accelerations (hence accelerometer operations during flight) and estimating the centre of mass of Ganymede. The final results are eventually run to degree 60 as to explore possibilities of higher degree uncertainty estimation and validity of the model at higher degrees.

This paper has the following structure: In section 2 the mission environment relating to this study as well as the outline of the research context are specified in detail. In section 3: The methodology of setting up the nominal simulation model and its limitations and specifications are provided. In section 4 the results of the sensitivity analysis are presented in order to show how the uncertainty in the gravity field is influenced by different model parameters and settings. In section 5, the insights from this study are summarized in the form of a conclusion.

2. Mission Environment & Research Formulation

In this section two aspects of the problem definition are explained in detail. Firstly the Instrumental background of the JUICE mission are presented under the "Mission Environment" in section 2.1. This is followed by an introduction to the mathematical methods used to formulate the research question in section 2.2.

2.1. Mission Environment

Essential for this study are the onboard accelerometer and the following two instruments/experiments of the JUICE mission.

2.1.1. Radio Science (3GM) & PRIDE Experiment

The radio science experiment (3GM) will collect highly precise Doppler and two-way range signals in the GCO-500 orbit of Ganymede to determine the spacecraft orbit as well as moon ephemeris (Giuseppe et al. (2021)). The 3GM comprises of a Ka Band Transponder (KaT) which enables two-way range and Doppler measurements. Radio signals in X-band (7.2-8.4 GHz) and Ka-band (34.3-32.5) are transmitted in parallel from a ground station on earth and then sent back coherently by separate tansponders on the spacecraft. These radio signals are in the microwave range and are picked up by ESA ESTRACK station on earth, in this case Malargue DSA3 which supports Ka-band uplink and down-link. The accuracy of the range and Doppler measurements is respectively 20cm and 1-3 μm/s (Iess et al. (2009))(Iess and Boscagli (2001)). The Ka/Ka radio link enabled by the KaT is mainly responsible for gravity measurements (range and Doppler), which in turn will help to characterize the interior of Ganymede by performing Precise orbit determination (POD) (See section 2.2). Measuring the moon's gravity field and tidal response will help constrain the depth of the global subsurface ocean and help to reconsider the dependence on the hydrostatic equilibrium condition (Di Benedetto et al. (2017)). The 3GM system is virtually immune to interplanetary plasma noise (propagation noise) which is a dispersive noise. Non-dispersive noise due to Earth troposphere require installing advanced water vapour radiometers at the ground station (Asmar et al. (2005)).

The PRIDE experiment will use VLBI to measure the angular position (right ascension and declination). VLBI measures the time difference in arrival of a radio wave front emitted by a distant quasar, by two different earth ground stations. VLBI measurements generally contribute to ephemerides of planets due to their long term measurement period. Including VLBI measurements in spacecraft orbit determination for a far away mission such as JUICE is perhaps more reasonable than for a nearby orbit such as that of the earth. Hence, all three measurements types (Doppler, range and VLBI) will be investigated in this study to see whether range and VLBI measurements contribute less or significantly less compared to Doppler measurements only.

2.1.2. High Accuracy Accelerometer (HAA)

The HAA onboard of the JUICE mission is part of the inertial navigation system (Just like gyroscopes and other sensors) and helps to correct the path of the spacecraft in order to follow its designed trajectory, which might deviate due to perturbations. Within the orbit determination of 3GM, the empirical accelerations can also be estimated, which calibrate for the non-gravitational forces of the HAA including atmospheric drag, solar radiation pressure and propellant sloshing (Alessi et al. (2012)). The propellant sloshing is caused by maneuvers that align the spacecraft to the moon or planet, the result being shift in the centre of mass of the spacecraft, causing instability. Estimating the empirical acceleration uncertainty w.r.t the centre of mass of the spacecraft in the covariance analysis helps to mitigate these perturbations. This way the behaviour of the accelerometer noise can be modelled and the parameters which are affected most by this perturbation can be identified. The accelerometer is therefore an essential addition to the JUICE mission instruments. The empirical accelerations collectively quantify the disturbance caused by non-gravitational accelerations, as opposed to including each one of them individually. It simplifies the simulation to a great extent by replacing individual models that would be required to mitigate propellant sloshing, atmospheric drag or solar radiation pressure (Cappuccio and Cascioli (2019)).

Just like other instruments the accelerometer has intrinsic noise such as random noise and biases. To account for this imperfection, uncertainty in empirical accelerations are included in the covariance analysis. How this is done depends upon how often the accelerometer will be used and hence calibrated, because each time the accelerometer is turned on it will need to be calibrated. Therefore, this is an aspect which can be explored in the covariance analysis keeping in mind that this parameter can be investigated independently without showing any correlation with the gravity field.

The magnitude for the uncertainty in empirical accelerations is determined during the covariance analysis process [Section 2.2.4]. These are estimated as a constant term for each direction (Radial (R), along-track(S) and across-track(W)) in the RSW reference frame.

2.2. Research Formulation

This section explains the research formulation in steps. First the theoretical background is briefly summarized in subsections 2.2.1 and 2.2.2. This is followed by the practical implementation process of Multiple arcs (subsection 2.2.3) and Covariance Analysis (subsection 2.2.4) in the simulation model.

2.2.1. Dynamical Model

The motion of the spacecraft is described by the equations of motion. The equations of motion (Equation 1) are propagated w.r.t centre of mass of the spacecraft and are second-order differential equations relating spacecraft movement to the accelerations that perturb the orbit. The first term in equation 1 is the gravitational acceleration, which is the main force that keeps the spacecraft in a circular orbit. The second term in equation 1 represents all the physical forces (a_p) which are secondary compared to the main gravitational force. The physical forces are either gravitational (due to third body perturbations) or non-gravitational (as represented by the empirical accelerations). This gravitational acceleration that the spacecraft experiences due to a planet or moon in a two-body system is given as follows (Allahvirdi-Zadeh et al. (2022)):

$$a = \frac{\mu_G}{||r_{GS}||^3 r_{GS}} + a_P \tag{1}$$

the position is a relative position given by:

$$r_{GS} = r_S - r_G \tag{2}$$

here r_{GS} stands for Spacecraft position with respect to Ganymede.

2.2.2. Gravity Field

The gravity field is derived from the spherical harmonic expansion of the gravity potential. The potential of a point mass of body i, evaluated at point j is $U_{\bar{i}}(r_j)$ and that of its extended body is $U_{\hat{i}}(r_j)$. The total potential of the body i is then given as follows (Di Benedetto et al. (2021)) (Konopliv et al. (2002)):

$$U_i(r_j) = \mu_i(U_{\bar{i}}(r_j) + U_{\hat{i}}(r_j)) \tag{3}$$

$$U_{\bar{i}}(r_j) = \frac{1}{r_{ij}} \tag{4}$$

$$U_{\hat{i}}(r_j) = \frac{1}{r_{ij}} \sum_{l=1}^{\infty} \sum_{m=0}^{l} \left(\frac{R_{e,i}}{r_{ij}}\right)^l \bar{P}_{lm}(sin\phi_{ij})(\bar{C}^i_{lm} cos(m\lambda_{ij}) \tag{5}$$

$$+ \bar{S}^i_{lm} sin(m\lambda_{ij}) = \sum_{l=0}^{\infty} \sum_{m=0}^{l} U_{\hat{i},lm}(r_j) \tag{6}$$

where:

r_{ij} is the distance from the centre of body i to point j.
ϕ_{ij} is the latitude of point j measured from the body fixed frame of body i.
λ_{ij} is the longitude of point j measured from the body fixed frame of body i.
μ_i is the gravitational parameter of body i.
$R_{e,i}$ is the reference (equatorial) radius of the spherical harmonic expansion.
$\bar{P}_{lm}$ is the associated Legendre polynomial of degree l and order m.
$\bar{C}_{lm} : \bar{S}_{lm}$ are the normalized cosine and sine gravity field spherical harmonic coefficients which are estimated during orbit determination and the formal uncertainties and correlations of which can be propagated during the Covariance analysis (See section 2.2.4).

2.2.3. Single & Multiple arcs

In a numerical model position calculation is done in steps with the previous position being the input for the next position. For values of the position there will be a build up in error and that will accumulate when reaching the final destination giving a highly inaccurate orbit, to compensate for this the arc-wise state and empirical acceleration are used. Arc wise estimation is where the estimation or propagation of an orbit or covariance respectively, is divided into manageable time intervals instead of one single arc for the entire mission duration (Serra et al. (2018)). The smaller the time step the more accurate the orbit state will be.

Just like the (initial) States, the empirical accelerations uncertainty can also be implemented in an arc-wise fashion. In the simulation model the arc length is one of the settings which is investigated to quantify the improvement in spacecraft state or the empirical accelerations, if any. For the empirical accelerations are first modeled with a single arc and then the arc length is reduced eventually till it has the same length as the arc length for the spacecraft states. This is done to see how often the accelerometer (Section 2.1.2) needs to be turned on or how long downtime can be permitted to not jeopardize the quality of the estimation, keeping in mind constant equipment operation or the fact that calibration is needed every time the equipment is restarted.

2.2.4. Covariance Analysis

The process of covariance analysis as performed by the simulation during any simulation run is illustrated in detail in figure 1. The JUICE mission will determine the gravity field of Ganymede by means of precise orbit determination (POD). POD is the process of determining the orbit of a spacecraft with high accuracy. POD starts by defining the dynamical model (section 2.2.1). This step is necessary to generate the observations (measurements) which are needed for the covariance analysis. As summarized in figure 1, the covariance analysis can be split into two main steps. The first step is the "Observation Generation" where the Spice Kernels provide the initial conditions to solve for the differential equations (See Equation of motion in section 2.2.1). Once the equations of motion are solved, the observations (range, Doppler and VLBI) are calculated by the "Observation Simulator", after which the covariance analysis can be performed, given a set of a priori model constraints (in parameters). The second step is the "Error propagation" where the output from the previous step (observations) combined with a priori covariance of parameters the covariance analysis is performed. The final results are the formal errors and correlations for the parameters of interest. The covariance analysis has the underlying assumptions that there is no correlation between the uncertainty in parameters and that the relation between inputs and the final covariance is linear.

The covariance matrix of parameters P_{qq} is computed as follows (Montenbruck et al. (2002)):

$$\mathbf{P}_{qq}(t) = (\mathbf{P}^{-1}_{qq,0} + \mathbf{H}^T(t)\mathbf{W}(t)\mathbf{H}(t))^{-1} \tag{7}$$

$$\mathbf{W} = \begin{bmatrix} \frac{1}{w}^2_{1,1} & 0 & ... & 0 \\ 0 & . & & : \\ : & & . & 0 \\ 0 & ... & 0 & \frac{1}{w}^2_{i,i} \end{bmatrix} \tag{8}$$

Here $P^{-1}_{qq,0}$ is the a priori covariance of parameters. Adding the a priori uncertainty makes the covariance more

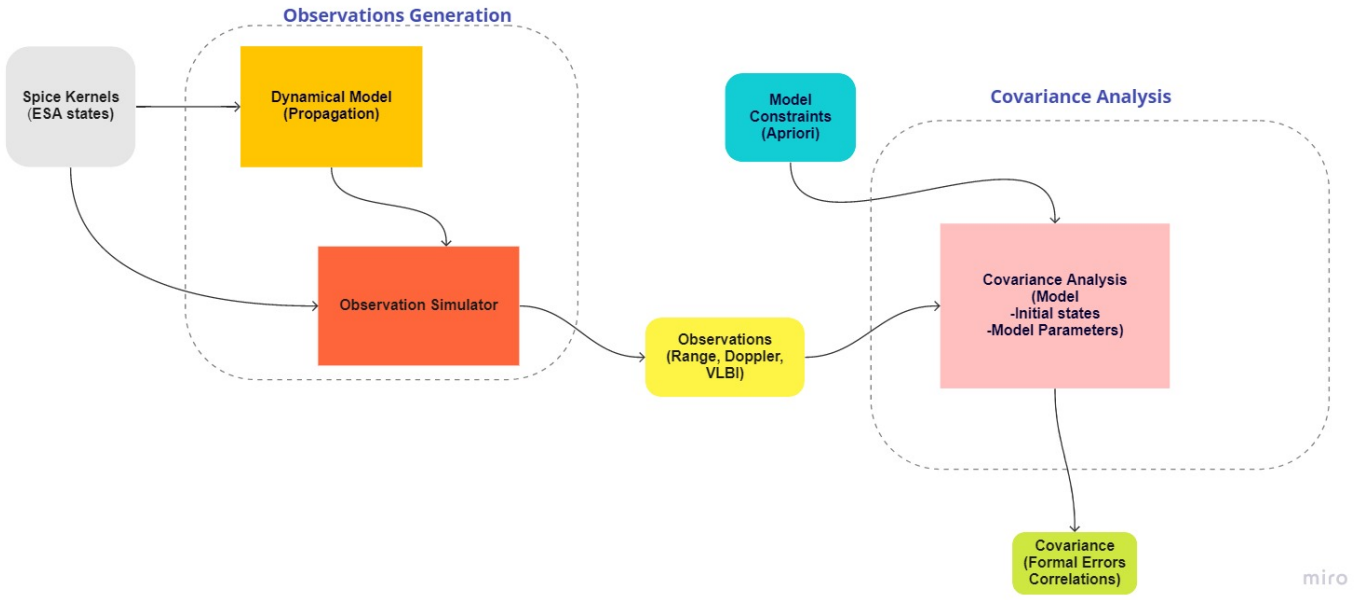

Figure 1: This figure illustrates the process of covariance analysis to obtain formal errors and uncertainties of spacecraft (initial) state and parameters. The first step is the "Observation Generation" where Initial conditions obtained from Spice Kernels are used to solve the equations of motion of the dynamical model. These are needed to generate the observations by the "Observation Simulator" (Range, Doppler and VLBI). The second step is the "Covariance Analysis" where the a priori uncertainty in initial states and parameters is propagated to obtain the formal errors and correlations of the (initial) states and parameters.

realistic and also helps to make the matrix invertible. The a priori uncertainties for the states and investigated parameters are summarized in table 1.

The W is the uncertainty in observations given by equation 8, it describes the statistical uncertainty (or measurement random noise) of observations. The uncertainty/noise of each data type is listed in table 2 . For uncorrelated observation errors W is a diagonal matrix with the weight of each observation type summarized in table 2. For example, for the range the uncertainty is 20 cm, which means that the range data has a precision of 20cm. As shown in equation 8 the weight will be a factor of 25 ($1/0.2^2 = 25$), meaning that the greater the precision the higher the weight. Underlying assumption with respect to the weight are that the observations are uncorrelated (as given by the zero non-diagonal terms of the W matrix) and the weight is constant for all observations of each observation type.

For the observations obtained from the simulation for a time period t, the design matrix ($\mathbf{H}$) is as follows (equation 9):

$$\mathbf{H}(t) = \frac{\partial h(t)}{\partial \mathbf{q}} \tag{9}$$

Here the numerator $\partial h(t)$ of the partial derivative is the change in uncertainty of observations and the denominator $\partial \mathbf{q}$ is the change in uncertainty of parameters

$$\mathbf{q} = [\mathbf{s}_0; \mathbf{p}] \tag{10}$$

Here $\mathbf{q}$ is the set of uncertainty of all parameters (See table 1 for a summary of the model parameters and their a priori uncertainty), where s_0 stands for initial states per arc as given in equation 11 and $\mathbf{p}$ stands for all other parameters.

$$\mathbf{s}_0 = \begin{bmatrix} x_0 \\ y_0 \\ z_0 \\ \dot{x}_0 \\ \dot{y}_0 \\ \dot{z}_0 \end{bmatrix} \tag{11}$$

3. Simulation Environment & Nominal Model

In this section the propagation and estimation settings are explained (section 3.1). Following this is the development of the nominal model (section 3.2) and some preliminary results obtained for the nominal model (section 3.3).

3.1. Simulation Environment

The simulation has been developed in tudat, by expanding on an existing code taken from the tudat . Tudat is an open-source library of simulation codes available with a free license.

3.1.1. Propagation Settings

The JUICE orbit is propagated w.r.t the centre of mass of Ganymede with the orientation fixed w.r.t the ICRF (J2000). The SPICE KERNEL Crema 4 is used to extract the initial state of JUICE per arc. Other kernels are used

Table 1: In this table, First two columns give a chronological list of parameters for which the uncertainty is propagated. These parameters form the matrix **q** as shown in equation 10. The third column indicates whether the parameter is a local (specific to each arc) or Global (common to all arcs). The empirical accelerations are local parameters when multiple arcs are implemented and global when a single arc is implemented. Kaula's constant (A) is defined in section 3.3 and l is the degree of the gravity field coefficient. The final column lists the a priori uncertainties for each parameter.

Name	Parameter	Type	A priori Uncertainty
JUICE State	Position	Local	100 m
	Velocity	Local	0.1 m/s
Solar Radiation Pressure		Global	0.12
Gravitational Parameter	μ	Global	170,000 m^3/s^2
Gravity Field	Spherical Harmonic Coefficients for degree & order 1-12	Global	A/l^2 ($A = 1 * 10^{-4}$)
Empirical Accelerations	Across-track, Along-track or radial	Local/Global	$2.5 * 10^{-8}$ m/s

Table 2: This table gives the values of the noise for each Date Type, as used for the Weight matrix (W).

Observation	Uncertainty
Range	20 cm
Doppler	10 $\mu m/s$
VLBI	1 nrad

to obtain gravitational parameters for all other perturbing bodies to include the weaker gravitational acceleration experienced by the spacecraft from these bodies. These perturbing bodies are Earth, Sun, Ganymede, Io, Europa, Callisto, Jupiter and Saturn. The simulation uses a variable stepsize integrator (RungeKuttaFehlberg78). Three random ground stations are used as transmitter and receiver of the radio signals, the position of which is not optimized as it is assumed to have little influence on the formal errors and correlations.

3.1.2. Estimation Settings

The simulation is based on a one-way range model but using the noise for a two-way range measurement system, since the JUICE instrument is designed for two-way measurement. For the covariance analysis this is possible since the uncertainty in measurements is required and not so much the measurements themselves. Biases are not included for the range measurements and Doppler data has very little bias. In practice two-way range measurements have the advantage that the large clock error is eliminated.

The settings also account for non-visibility of the spacecraft due to eclipse of Ganymede or Jupiter. Continuous tracking for 24 hours is not possible due to interruption in ground station visibility due to for instance solar body eclipse and technically the down link phase is 8 hours per day for the available ground stations This is quite challenging as large amount of data is down linked in real time, since no on-board data storage is possible with the JUICE mission ESA (2014).

The a priori uncertainty for the solar radiation pressure is taken to be 10% of its original value. This is reasonable and corresponds to the value 0.1 mentioned in (Montenbruck et al. (2002)). The Gravitational parameter has an a priori uncertainty as that given in table 1 and is estimated over a time span of 01-10-1600 to 01-10-2200 (Jacobson (2021)). This is the post-fit uncertainty obtained when obtaining the ephemerides for the Jovian system from astrometric data, including early measurements by Galileo himself. Both the solar radiation pressure and the gravitational parameters are estimated over the full arc of the mission duration, as they are assumed to be constant. The empirical accelerations on the other hand are short term disturbances in the accelerometer of the spacecraft and therefore these are implemented arc-wise to see how the arc-length of these acceleration influences the uncertainties in estimated parameters. The a priori uncertainty for empirical accelerations as given in table 1 is taken as an average value of the output of the noise of the non-gravitational accelerations shown in figure 1 of (Alessi et al. (2012)) and is assumed to be constant in along-track, cross-track and radial directions.

3.2. Nominal Model

In order to setup the nominal model, a number of simulations and analysis have been carried out as listed in table 3, not all simulations and results however are reported in the results section. These simulations runs are a part of the sensitivity analysis.

The nominal model and hence the simulation runs are setup as follows:

- Add Weights (precision) and a priori Covariance: To quantify how measurement noise impacts the solution in presence of a priori covariance by scaling the measurement noise by a factor 1, 5 or 10. This is done to compare to the expectations as explained in section 2.2.4. Ideally the formal errors will decrease with weight (W), but this might have little influence on the overall result depending on whether the a priori covariance has a greater influence than the data uncertainty.

- Investigate data Types (Range/VLBI/Doppler): Even though Doppler data is predicted to have a greater influence on the formal error due to its high precision compared to range and VLBI, this hypothesis

Table 3: Simulation runs and analysis done to develop the nominal model. The first column shows the abbreviation given to the type of run. The last column shows the setting which was chosen as a result of these runs. In the nominal model 20cm measurement noise is used for the range even though noise of 1cm shows promising results.

Abbreviation	Description	Simulation Runs	Conclusion
DT	Data Type	VLBI/Doppler/Range	Doppler
DW	Data Weights	Weight Factor 1,5,10	Weight factor 10
		Doppler Only	
OI	Observation Interval	0.5,1,2,5,10 min	10 min
AL	Arc Length	1,2,3,4,5 days	5 days
MD	Mission Duration	1,2,3,3.5 months for	3.5 months
		Fixed AL (5 days)	
		Fixed no. of arcs (5 arcs)	
WR	Weight Ratio	Weight 20cm Range	20cm Noise
		Weight 1cm Range	
OP	Observation Planning	Hour shifts	Not applied
		0,4,8,12,16,24 hours	

is still tested nonetheless. In general the more data types the better, because this will increase the number of measurements which provide useful information. Also, including different data types provides more realistic settings for a simulation.

- Arc length trade off & no. of arcs: Arc length is a significant factor in determining orbit determination accuracy. Whether it affects the gravity field needs to be determined in this case. A fitting arc length for the spacecraft (initial) states is specified and kept constant throughout the simulation. In general, a longer arc length will give more data and better accuracy, whereas a shorter arc length will increase computational time of the simulation.

- Observation interval for fixed total observation duration: Observation interval is decreased meaning less data is generated for the same total time period of observations per day. Less measurements will be needed by the instrument if no affect is observed in formal errors.

- Observation planning: This analysis is performed to investigate whether there is loss of data due to the spacecraft not being visible and whether there is a need to implement this criteria in the simulation.

- Weight ratio range measurements only: Range measurement noise is 20 cm for the JUICE mission, but better precision of 1cm is reported by Cappuccio et al. (2019). This is investigated to see whether this influences the spacecraft state uncertainty or the gravity field uncertainty and more importantly whether range measurement noise can be added as well as Doppler noise.

- Mission duration (months): This is to quantify how the formal error will decrease by adding more data to the simulation. Longer missions come at cost of higher fuel consumption. At some point the decrease in formal error of gravity field or spacecraft uncertainty might be insignificant and not worth the cost of adding extra time to the mission duration. Two scenarios are investigated, keeping the arc length fixed or fixing the number of arcs.

The final set of nominal settings as a result of these simulations can be found in column 4 of table 3. For convenience the relevant settings for subsequent analysis are once again summarized in table 4.

3.3. Degree variance of Gravity Field

The a priori uncertainty for the gravity field coefficients is given by the Kaula's rule (equation 12, which is a function of the degree (l) and is independent of the order (m) of the gravity field coefficient. These are denoted

$$\delta_{l,m} = \frac{A}{l^2} \tag{12}$$

A is the Kaula's constant which differs per body and is not known for Ganymede, it is found in the range of 10^{-3} and 10^{-5}. For this study, Kaula's constant is taken to be $1.0 * 10^{-4}$. The Kaula constant for Earth is 10^{-5} and can be scaled to other bodies by their relative gravity's, this gives for Ganymede a value of $5 * 10^{-4}$, 5 times larger than the value used in this study for earth, as a comparison (McMahon et al. (2016)).

From the gravity field coefficients uncertainty the degree variance for degree and order is calculated as given in equation (7) of Yan et al. (2019). This is then plotted with the a priori uncertainty, in a so-called 'degree variance' plot. The degree variance plot (figure 2 for nominal setting for degree and order 60 shows that the a priori uncertainty almost converges with the formal errors at higher degrees. This is also in line with Kaula's rule which mainly applies to higher degrees. For lower degrees the observations weigh more and a priori uncertainty has lesser influence on the output. At around degree 30 both the data and a priori equally influence the output. Simulating to

Table 4: Nominal Settings as obtained from the simulations performed while developing the nominal model.

Abbreviation	Settings
NS	3.5 months Degree 2-12
(Nominal Settings)	Observations Interval 10 min
	Doppler Only
	Arc length 5 days

higher degrees is always favourable to get an accurate representation of the gravity field. For this paper, it is chosen to take degree 12 (according to JUICE mission goals) as a baseline and later this can be extrapolated to degree 60.

For degree 60 the correlations may be higher. For this reason correlation plot for degree 60 simulation has been plotted for the nominal settings (figure 3). This plot shows that the states are correlated (top left corner). This is to be expected because due to numerical integration the states are calculated step by step therefore the next state is dependant on the previous state. The plot also shows that all estimated parameters are correlated with themselves (diagonal elements of correlation matrix), the radiation pressure coefficient (C_r) is slightly correlated with the states and that the gravity field parameters are not correlated with the states and other than a few exceptions are not correlated with other gravity field parameters either. Therefore we can fairly assume that the a priori uncertainty is not correlated under nominal setting and all parameters are estimated independent of each other.

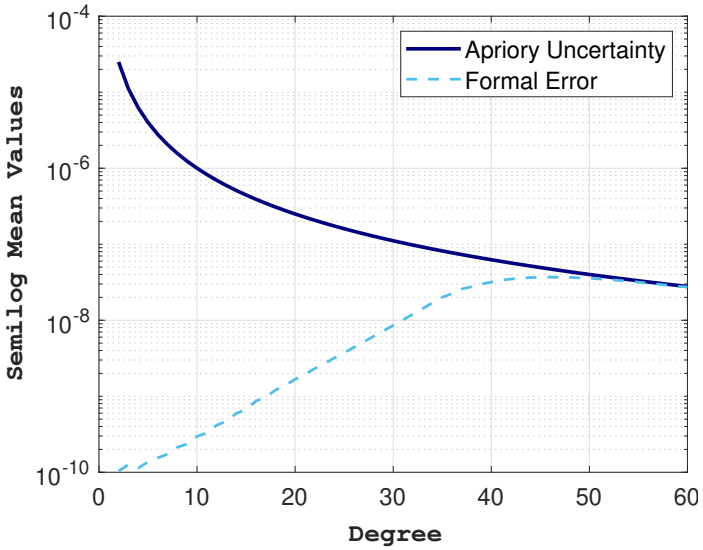

Figure 2: This figure illustrates the degree variance plot under nominal settings (NS). The plot shows that there is convergence at degree 50 for the a priori uncertainty and formal errors.

4. Results

The results presented in this section mainly concern the simulation runs performed after obtaining the Nominal model. The effects of adding these settings is discussed step wise in this section. These settings/parameters are listed in table 5. Each setting is given an abbreviation for quick reference (see column 1 of table 5).

Some interesting results while setting up the nominal model however are worth mentioning here. These two results are changing the arc length (AL) for Doppler only measurements and the increasing of a priori noise for range only measurements (WR as referred to in table 3). This discussion is presented first in sections 4.1 and 4.2, respectively.

4.1. Arc Length

Increasing the arc length while keeping the total simulation duration constant will decrease the number of arcs proportionally. Looking at figure 4 shows that the effect of increasing the arc length from 1 to 5 days is significant on the spacecraft (initial) states. The spacecraft (initial) states are represented by the top part of the figure. The change in formal error on gravity field coefficients on the other hand is less significant. The bottom part of the figure shows the shift of the gravity field coefficients from right to left. This result is to be expected since the spacecraft state is effected directly by the arc length of measurements and for 5 days more measurements will result in a better estimate of the uncertainty as more data is available as compared to 1 day arc length. On the other hand, the gravity field is not changed by the short term perturbations on the spacecraft. The gravity field will change if the mass composition on the surface of the moon changes for instance, which will not happen unless some significant natural phenomena causes the mass to shift, such as in the case of an earthquake or other tectonic movement. Such movement will be detected in years as a one time event. Under normal circumstances not much significant change in the gravity field is expected.

Further investigation into the effect on the gravity field is done by comparing the difference in degree variance for all arc lengths compared to arc length of 1 day. The results are plotted in figure 5. The percentage difference in degree variance for all arcs is less than 10 percentage, except for degree 2 variance. This difference w.r.t 1 arc increases slightly for higher degree coefficients. A 4 day arc gives highest change in degree variance w.r.t 1 day arc, however a 5 day arc is chosen for the nominal settings, as the degree variance values between 4 day and 5 day arc differ by a small 1% on average.

Further analysis on the arc length can be found in section 4.1 of the discussion.

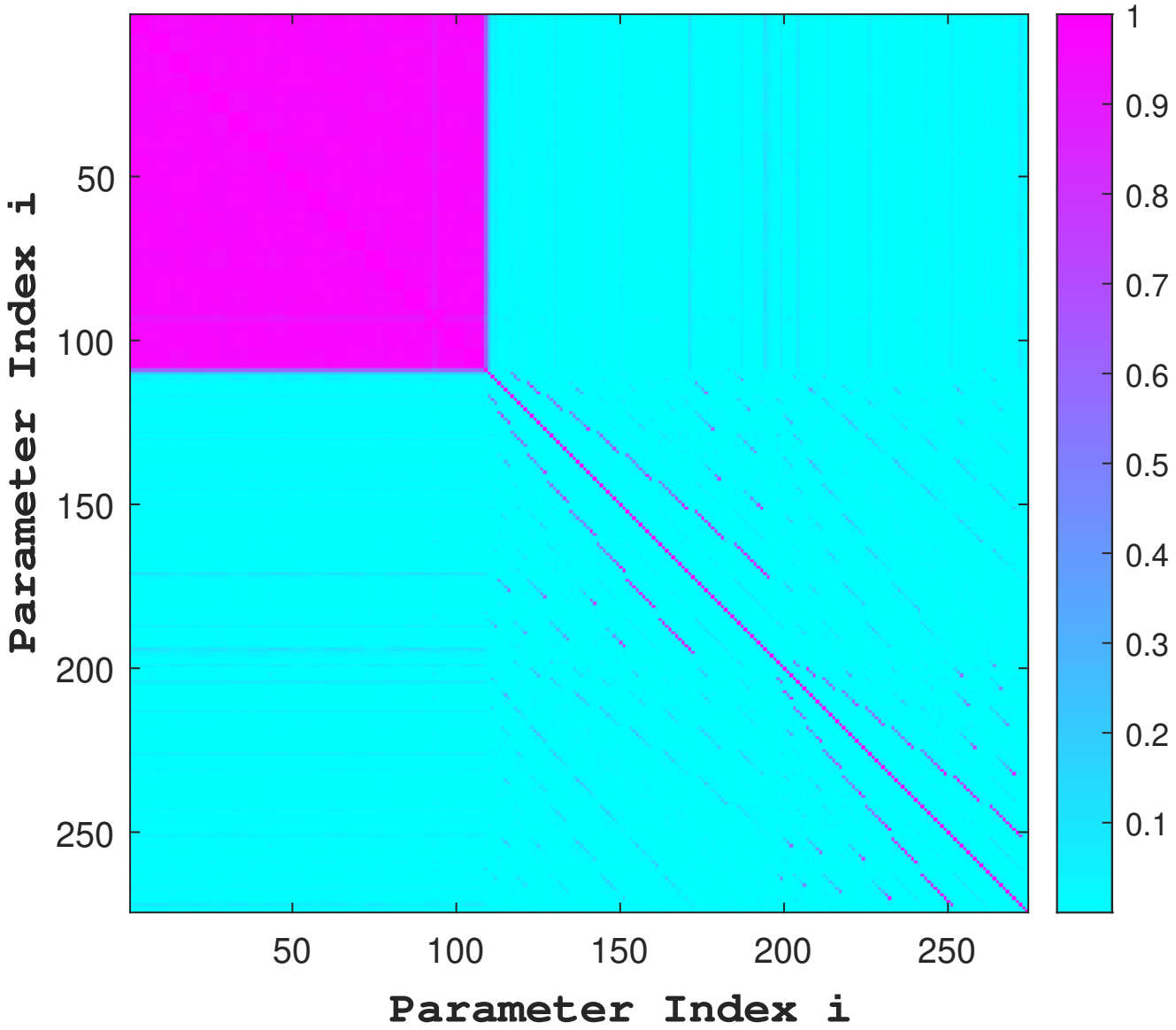

Figure 3: This figure illustrates the correlations for the estimated parameters under nominal settings (NS). Parameters 1 to 108 represent the states for each arc. There are a total of 18 arcs with 3 values for position (x,y,z) followed by 3 values for velocity (v_x,v_y,v_z). The correlation between the states form the symmetrical block in the top left corner of the correlation matrix. Parameter number 109 stands for the Solar radiation Pressure (C_r). Parameters 110 to 198 stand for the Cosine coefficients of the gravity field ($C_{n,m}$) starting with degree 2 (n) and increasing order (m) in the following manner ($C_{2,0}$, $C_{2,1}$, $C_{2,2}$, $C_{3,0}$, ..., $C_{12,12}$). Parameters 111 to 174 stand for the Sine Coefficients of the gravity field ($S_{n,m}$) in the following manner ($S_{2,1}$, $S_{2,2}$, $S_{3,1}$,...., $S_{12,12}$). The correlation matrix is symmetric and the diagonal entries should be ideally equal to 1, they represent the parameters correlated with themselves.

Table 5: Simulation runs performed with parameters/ settings added to the nominal settings. Abbreviations in column one are used in the text for quick reference.

Abbreviation	Description	Simulation Runs
D1	Degree 1 addition to NS (Nominal Settings)	
CR	Solar Radiation Pressure Removal from D1	
EA1	Empirical Acceleration added to CR	1 arc 3.5 months
EA3		3 arcs 35 day arc length
EA5		5 arcs 21 days arc length
EA21		21 arcs 5 days arc length
GP1	Gravitational Parameter addition	Add μ to CR Settings
GP2		Add μ to EA1 Settings
GP3		Add μ to EA21 Settings
GP4		Add μ to D1 Settings
GF60	Degree 60 simulation for GP2 settings	
GF60-2	GF60 for 2 min Observation interval	
GF60-5	GF60 for 5 min Observation interval	

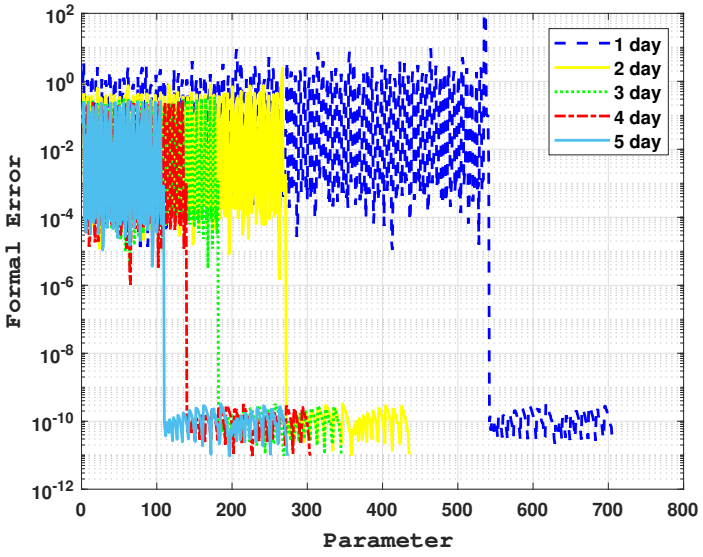

Figure 4: This figure illustrates the change in formal error for arc lengths of 1 to 5 days. The upper block of curves shows the gradual decrease in formal error for the spacecraft (initial) state arcs, from right (1 day arc) to left (5 day arc). The parameters at the bottom part of the figure are the gravity field coefficients. Here the change in formal errors is less prominent. The x axis shows the total number of parameters estimated, the number of parameters decreases with arc length. For larger arc length the number of arc decreases but the total number of gravity field coefficients remains the same, the figure shows that the curves shift to the left. For arc length of 1 day Parameters 1 to 540 represent the states for each arc, parameter 541 is the Solar radiation Pressure (SRP) and parameters 542 to 706 are the gravity field coefficients. For a 2 day arc, parameters 1 to 270 represent the states of each arc, parameter 271 is the SRP and parameters 272 to 436 are the gravity field coefficients. For arc length of 3 days, parameters 1 to 180 are the state arcs, parameter 181 is SRP and parameters 182 to 346 are the gravity field coefficients. For 4 day arc, parameters 1 to 138 are the state arcs, parameter 139 is SRP and parameters 140 to 304 stand for the gravity field coefficients. Finally, for 5 day arc length, parameters 1 to 108 are state arcs, parameter 109 is the SRP and parameters 110 to 274 are the gravity field coefficients.

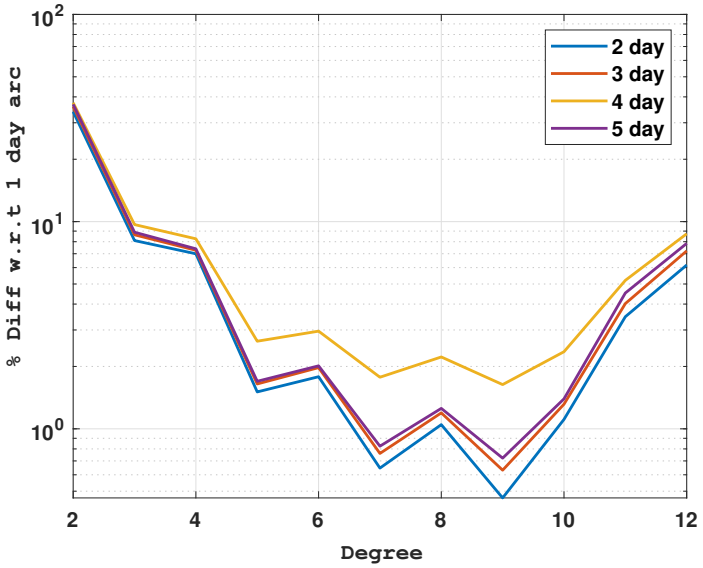

Figure 5: This figure illustrates the % change in degree variance of the gravity field uncertainty for different arc lengths with respect to the 1 day arc. This means that the average value of the degree field uncertainty decreases with increasing degree.

4.2. Range Noise 1*cm* & 20*cm*

Although a weight of 20*cm* is used for the range measurements. Range accuracy of 1*cm* has also been reported for the BepiColombo mission (Iess et al. (2021)). The Mercury orbiter radio science experiment (MORE) onboard BepiColombo is comparable to that of JUICE. Two-way microwave links at X (7.2-8.4 GHz) and Ka-band (32-34 GHz) to calibrate the dispersive plasma noise component are used Cappuccio et al. (2020), which is the same frequency range as the instrument specifications on 3GM (as reported in section 2.1.1). The design accuracy for the range for Bepicolombo was the same as that of JUICE, namely 20*cm*. The reported noise uncertainty of 1*cm* means that it is much better than the design accuracy of 20*cm* of the instrument.

This weight of $1cm$ was also simulated, the result of which is given in figure 6. The first part of the figure shows a somewhat constant difference in formal error of about 45% w.r.t weight of $20cm$, for the spacecraft (initial) states. However, the second part of the figure shows that Formal error difference can fluctuate up to 60 %, this represents the gravity field uncertainty. Therefore both states uncertainty as well as gravity field estimation can significantly be improved by decreasing the weight/noise of the range measurements. The possible implications of this are to be found in section 5.2 of the discussion.

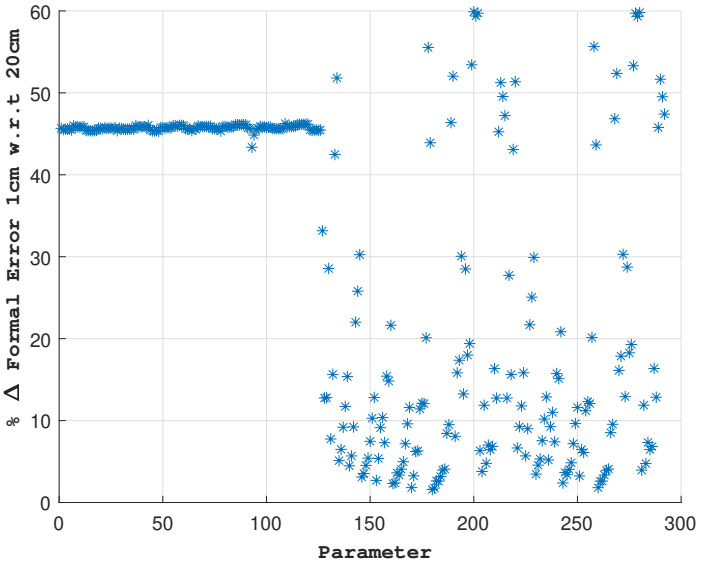

Figure 6: This figure illustrates the % difference in formal error for $W = 1cm$ w.r.t $W = 20cm$ for range only measurements under nominal settings. The horizontal set of the measurement in the first half of the figure apply to the spacecraft (initial) states. The random error distribution in the second half of the figure applies to the gravity field coefficients. Parameters 1 to 126 stand for the (initial) state arcs. Parameter 127 is for the Solar radiation pressure. Parameters 128 to 292 represent the gravity field coefficients.

*4.3. Ganymede Centre of Mass [**D1**]*

Addition of degree 1 coefficient uncertainty helps estimate the uncertainty in the centre of mass of the body. Kaula's rule is applied to estimate the a priori uncertainty for degree 1 for lack of better information, however this application might not be realistic since this rule mostly holds for higher degrees. The resulting degree variance is plotted in figure 7. From the plot it seems that the degree 1 variance is closer to the a priori uncertainty than higher degrees and does not follow the upward slope trend of higher degrees. It is 3 orders of magnitude below the a priori and 3 orders of magnitude above the degree 2 values. This means that both a priori as well as formal uncertainty play out equally with this value.

Plotting the correlations show that compared to the (NS), the correlation plot has changed little except for values for which the correlations have increased slightly.

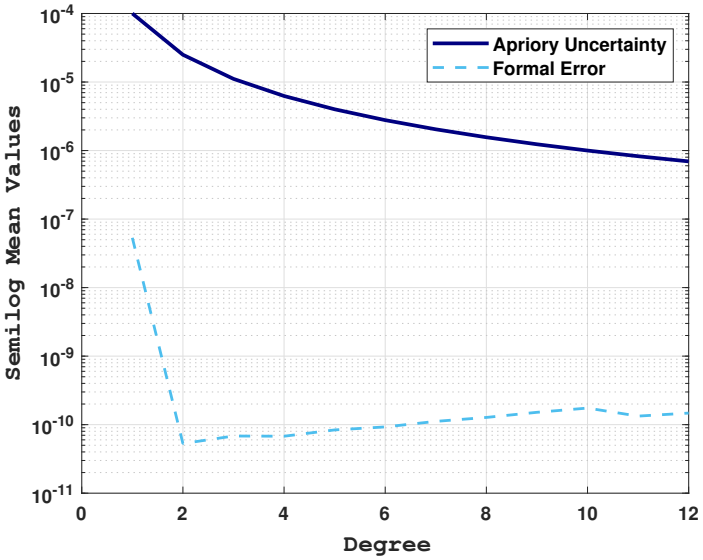

Figure 7: This figure illustrates the change in degree variance plot once the degree 1 values are added to the estimation.

Table 6: Formal uncertainties obtained for degree 1 coefficients. The a priori uncertainty is estimated with Kaula's rule.

Abbreviation	Formal Uncertainty	a priori
$C_{1,0}$	$9.228e-08$	10^{-4}
$C_{1,1}$	$1.332e-09$	10^{-4}
$S_{1,1}$	$1.397e-09$	10^{-4}

The addition of degree 1 has a minimal affect on the gravity field coefficients compared to the nominal case for all degree coefficients except for degree 1. Plotting this difference between (Deg1) and (NS) shows a change of less than 0.1% (plot not shown here). The degree 1 formal uncertainties obtained with this simulation run are summarized in table 6 alongside the a priori uncertainty. The formal error uncertainty reduces more for $C_{1,1}$ and $S_{1,1}$ compared to $C_{1,0}$.

The formal error for D1 settings is plotted in figure 9 and this plot shows the distribution of the magnitude of the formal errors. The inner part of the pyramid shows that the formal error is higher for higher degree and lower orders. Exception is degree 1 coefficients which shoot way above the range of maximum uncertainty shown. Also it can be seen that the distribution of uncertainties is symmetrical for both cosine and sine coefficients.

4.4. Solar Radiation Pressure C_r

Solar Radiation pressure C_r is estimated throughout all simulations of the nominal settings (in table 3) until the empirical accelerations are added (before CR in table 5). Table 7 shows that the formal error in C_r is estimated to be 0.00071 for nominal settings (NS). Adding degree 1 (D1) has no affect on this estimated value. Whereas, the formal error becomes much worse when empirical accelerations and C_r are estimated simultaneously (case CR

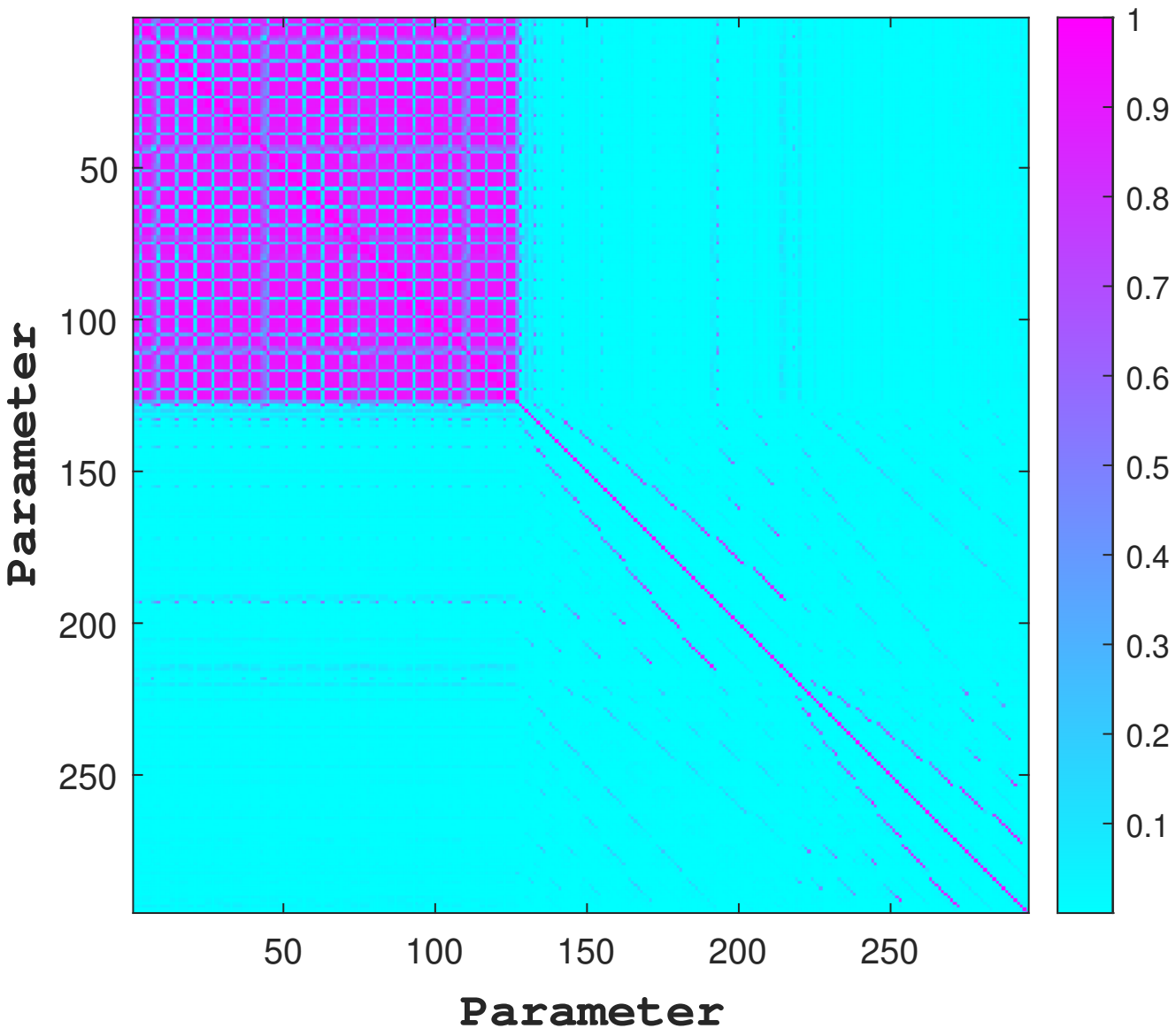

Figure 8: This figure illustrates the correlations for the estimated parameters after simulation run D1 in table 5, which represents Degree 1 coefficient addition to nominal settings (NS). Parameters 1 to 126 represent the states for each arc. There are a total of 21 arcs with 3 values for position (x,y,z) followed by 3 values for velocity (v_x,v_y,v_z). The correlation between the states form the symmetrical block in the top left corner of the correlation matrix. Parameter number 127 stands for the Solar radiation Pressure (C_r). Parameters 128 to 217 stand for the Cosine coefficients of the gravity field ($C_{n,m}$) starting with degree 1 (n) and increasing order (m) in the following manner ($C_{1,0}$, $C_{1,1}$, $C_{2,0}$, $C_{2,1}$, $C_{2,2}$ $C_{3,0}$, ..., $C_{12,12}$). Parameters 218 to 295 stand for the Sine Coefficient of the gravity field ($S_{n,m}$) in the following manner ($S_{1,1}$, $S_{2,1}$, $S_{2,2}$, $S_{3,1}$,...., $S_{12,12}$). The correlation matrix is symmetric and the diagonal entries should be ideally equal to 1, they represent the parameters correlated with themselves.

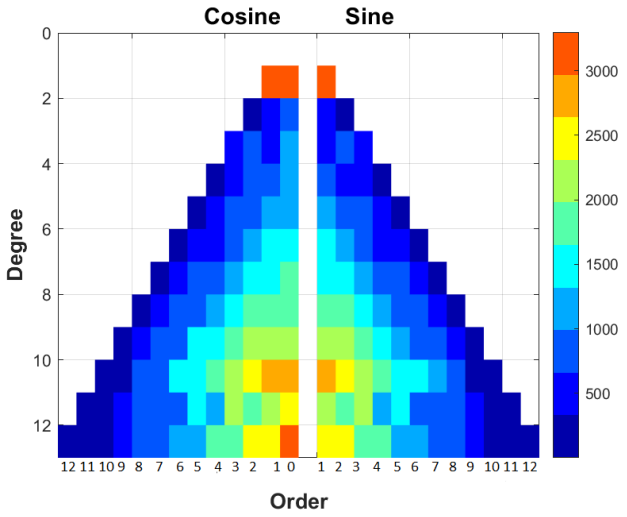

Figure 9: This figure illustrates the distribution of formal errors in the gravity field coefficients. The left half of the pyramid represents cosine and the right half the sine coefficients. The scale is such that all the values are multiplied by a factor 10^{12} to be able to plot such small values. The degree 1 coefficients (top row) exceed the scale limit but in order to plot them they have been assumed to be at the upper end of the scale bar.

Table 7: Formal error in C_r obtained for 3 different simulation cases. The results are rounded off to 2 significant figures.

Case	Formal Error
D1	0.00071
CR + EA	0.0013
NS	0.00071

Table 8: Correlation between empirical acceleration and C_r for simulation run **EA1**. The results are rounded off to 4 decimal places.

Direction	Correlation
Across-track	-0.8256
Along-track	0.0441
Radial	0.07563

+ EA). It is interesting to investigate what would happen in case both empirical accelerations and C_r are estimated to see if they can be determined independently. The results suggest otherwise, possibly due to correlation between empirical accelerations and Solar Radiation pressure coefficient. In fact the results in table 8 show that there is a high negative correlation for the across-track direction, and low correlation in the other two directions, therefore it is a good idea to exclude the C_r from the EA estimation. In all 3 cases, the formal error values are much smaller than the a priori uncertainty.

4.5. Empirical Accelerations

Adding empirical acceleration uncertainties eliminates the need to estimate the solar radiation pressure separately, therefore all following simulations (after CR in table 5) do not estimate the formal error for C_r. As shown in table 5 four different cases are studied to investigate the affect of the arc-length of the arc-wise empirical accelerations on the gravity field. First a single-arc empirical acceleration for the length of the simulation is added, afterwards the arc-length is gradually decreased till it is the same as the arc length for the states (5 days). Figures 11 and 12 show the correlations for 1 arc (EA1) and 21 arcs (EA21) only. Both figures show that there is correlation between empirical acceleration with the states of the s/c, but no correlation between the empirical accelerations and the gravity field.

In figure 10 the percentage difference in formal errors w.r.t to 1 arc settings are plotted. This plot shows that the formal error difference for the states can reach up to 100%, this might be due to the correlation between empirical accelerations and states which was observed in the correlation plots. Secondly, the change in formal error of the gravity field coefficients (the right half of the figure) due to different arc length of empirical accelerations is on average below the 1% line, there are some exceptions to this however, as shown by the peaks above the 1% line. Although insignificant, the difference in formal error for 21 arcs is larger than that for 3 arcs, w.r.t 1 arc of empirical accelerations. From this it can be concluded that the change in formal error is so small such that it makes little difference for the gravity field coefficient uncertainty if empirical accelerations were to be estimated over 1 large arc or 21 smaller arcs. The 100% difference for the states is a change to be noted, however, despite correlations. For accurate determination of spacecraft and hence improve accuracy of navigation, 21 smaller arcs are more feasible.

In the same plot, the final 3 parameters, show that the percentage difference in formal error for the empirical accelerations for 21 arcs (final arc values) can reach beyond 100%. These values are summarized in table 9 and it can be seen that the biggest change corresponds to formal errors in the Along-track direction (see section 5.5 for further discussion). Also the same along-track direction has the highest precision for the formal errors in empirical acceleration for all arc lengths. Comparing the radial uncertainty with the across-track uncertainty, shows a factor 2 difference for all arc lengths.

Table 9: Empirical accelerations uncertainties for the final arc for different arc lengths. The results are rounded off to 3 decimal places

Track	1 arc 3.5 months	3 arcs 35 days	5 arcs 21 days	21 arcs 5 days
Across	1.259e-09	1.484e-09	1.469e-09	1.568e-09
Along	2.002e-14	2.759e-14	3.338e-14	1.068e-13
Radial	3.054e-09	3.313e-09	3.150e-09	3.191e-09

4.6. Estimating Gravitational parameter

Estimating Gravitational parameter μ uncertainty for Ganymede helps to estimate the mass uncertainty and therefore make a more accurate estimate of error bound

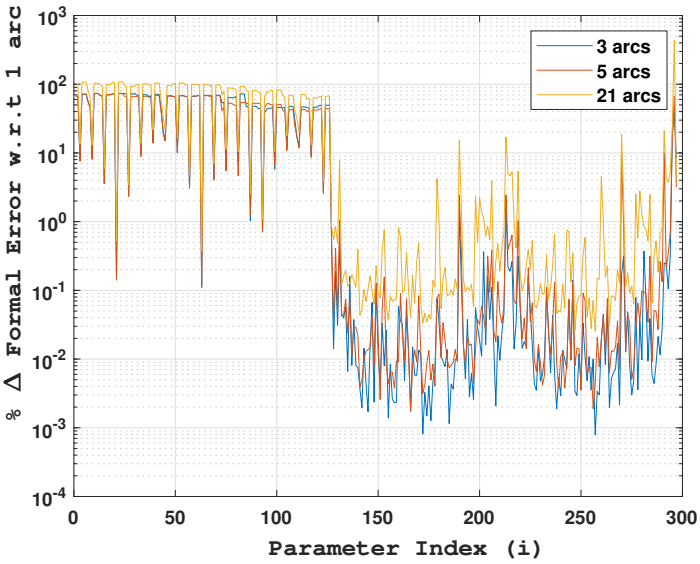

Figure 10: This figure illustrates the % difference in formal error compared to the 1 arc case for given parameters. Parameters 1 to 126 represent the states for each arc. There are a total of 21 arcs with 3 values for position (x,y,z) followed by 3 values for velocity (v_x,v_y,v_z). Parameters 127 to 216 stand for the Cosine coefficients of the gravity field ($C_{n,m}$) starting with degree 1 (n) and increasing order 0 (m) in the following manner ($C_{2,0}$, $C_{2,1}$, $C_{2,2}$, $C_{3,0}$, ..., $C_{12,12}$). Parameters 217 to 294 stand for the Sine Coefficient of the gravity field ($S_{n,m}$) in the following manner ($S_{2,1}$, $S_{2,2}$, $S_{3,1}$,...., $S_{12,12}$). Parameters 294 to 297 stand for the empirical accelerations.

in which the mass of Ganymede lies. In this simulation formal error in μ is estimated for 4 different cases as summarized in table 10. Figure 13 is plotted to find out if the Gravitational parameter uncertainty is correlated with other parameter. Apart from being correlated with itself, there is correlation with spacecraft (initial) states, but no correlation with gravity field coefficient uncertainty or empirical acceleration uncertainty. This parameter is therefore estimated independently.

Table 10 shows that that the formal error decreases from case GP3 (21 EA arcs) to GP2 (1 EA arc). The formal error is lowest for the case GP1, where neither C_r nor empirical accelerations are added to the estimation. The formal error is highest for case GP4 where empirical accelerations are not added yet and C_r is not yet removed from the estimation, but the % difference in values is too small to base any conclusions from these results. All four cases the uncertainty is about 99% of the a priori uncertainty meaning that a priori uncertainty is very accurate and the data has very little influence on the formal error of the gravitational parameter. The conclusion is that gravitational parameter uncertainty can be estimated almost accurately in all cases. This is also confirmed by the zero correlations as shown figure 13 for all parameters other than the (initial) states of the spacecraft.

4.7. Ganymede Gravity Field Uncertainty

Even though the degree 12 requirement is set for JUICE instrument specifications higher degree simulations can be

Table 10: Gravitational parameter μ uncertainty for four different cases. For Abbreviation see table 5. The results are rounded off to 2 decimal places.

Case	μ	% of a priori
GP1	168911.59	99.36
GP2	169221.88	99.54
GP3	169763.97	99.86
GP4	169233.32	99.55

run to get maximum return from the data. This is shown in figure 2 where convergence between a priori covariance and formal error starts at degree 40. Therefore simulations for degree 60 are run. Figure 3 already showed minimum correlations for degree 60 simulation. Now, the final settings can be run for degree 60 to see the actual change in the gravity field uncertainty for high degrees. As demonstrated by Figure 10 the gravity field formal error difference between EA21 and EA1 settings remains less than 1% on average, therefore it is chosen to run the degree 60 case for EA1 settings. Even for degree 60, and with the new settings compared to the nominal settings, the correlation plot shows no change in correlations between gravity field parameters (plot not shown here). Plotting the degree variance plot for this case shows that except for the addition of degree 1 coefficients the degree variance plot looks very similar to the plots shown in figure 2. In fact the average difference in formal error is again less than 1% as depicted in figure 14.

However, some further investigation can be done to look at the actual values of the correlation, even though the correlation plot doesn't show any correlation. The correlation between $C_{2,0}$ and $C_{2,2}$ is significantly higher for simulation GF60, GF60-2 and GF60-5 compared to the correlation for cases CR, GP2 and GP3. This shows that contrary to what the correlation plots for degree 60 suggest, there are more correlations for a degree 60 simulation than a degree 12 simulation. Also, note that the correlations for observation interval of 10 min (GF60), 5 min (GF60-5) and 2 min (GF60-2) are more or less the same suggesting the observation interval has no influence on the correlations.

Table 11: Correlation coefficient between $C_{2,0}$ and $C_{2,2}$ for simulation runs as given in table 5.

Case	Correlation Coefficient
CR	0.035229
GP2	0.024676
GP3	0.01672
GP4	0.031556
GF60	0.174837
GF60-2	0.175904
GF60-5	0.174837

At this point it is wise to make comparison with other work. Anderson et al. (1996) reported correlations of 0.7339

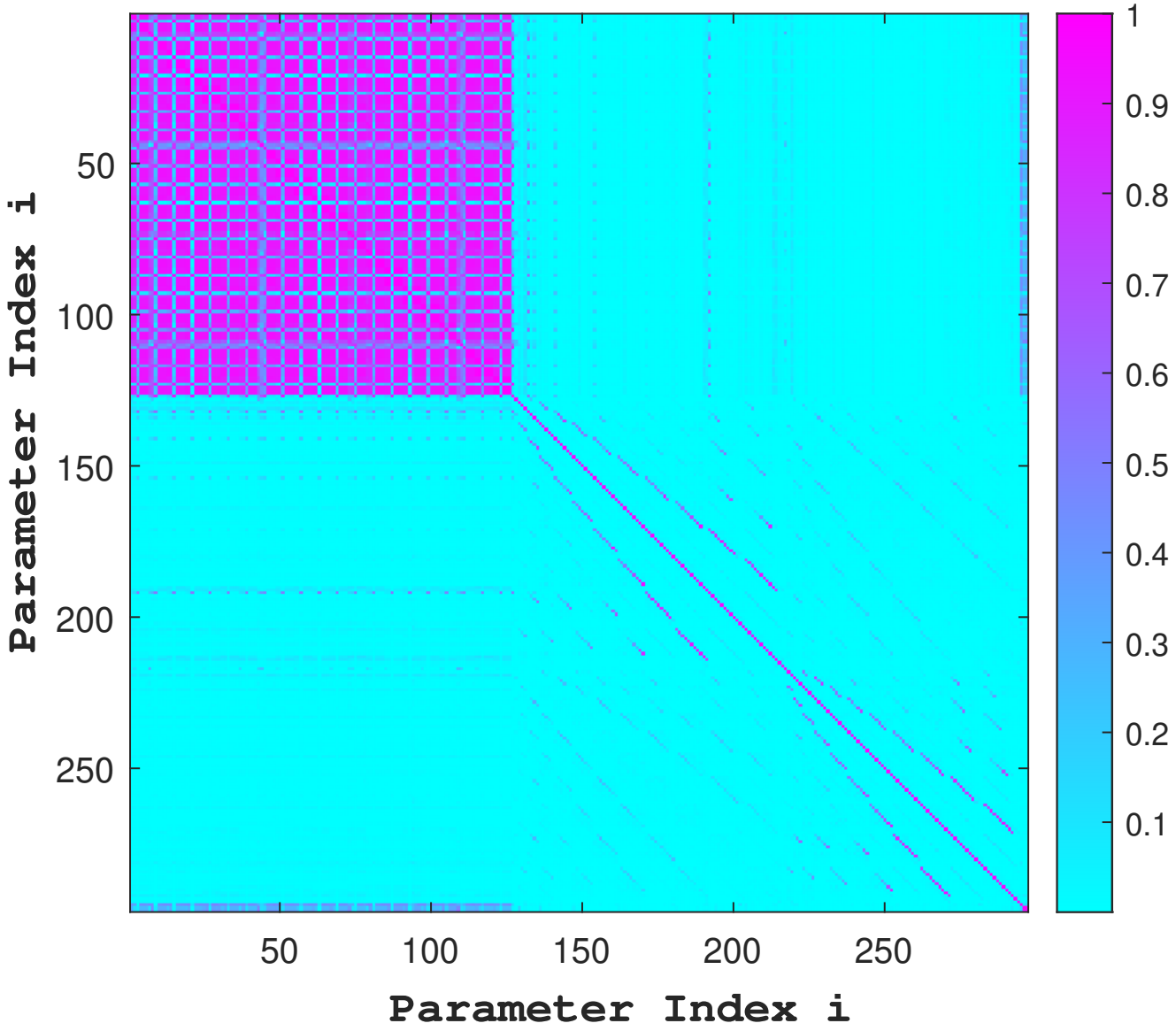

Figure 11: This figure illustrates the correlations of parameters with addition of empirical accelerations for the case of 1 arc for the entire length of the mission (EA1). Parameters 1 to 126 represent the states for each arc. There are a total of 21 arcs with 3 values for position (x,y,z) followed by 3 values for velocity (v_x,v_y,v_z). The correlation between the states form the symmetrical block in the top left corner of the correlation matrix. Parameters 127 to 216 stand for the Cosine coefficients the gravity field ($C_{n,m}$) starting with degree 1 (n) and increasing order 0 (m) in the following manner ($C_{1,0}$, $C_{1,1}$, $C_{2,1}$, $C_{2,2}$, $C_{3,0}$, ..., $C_{12,12}$). Parameters 217 to 294 stand for the Sine Coefficient of the gravity field ($S_{n,m}$) in the following manner ($S_{1,1}$, $S_{2,1}$, $S_{2,2}$, $S_{3,1}$,...., $S_{12,12}$). Parameters 295 to 297 represent the 3 values of the empirical accelerations for the single arc. The correlation matrix is symmetric and the diagonal entries should be ideally equal to 1, they represent the parameters correlated with themselves.

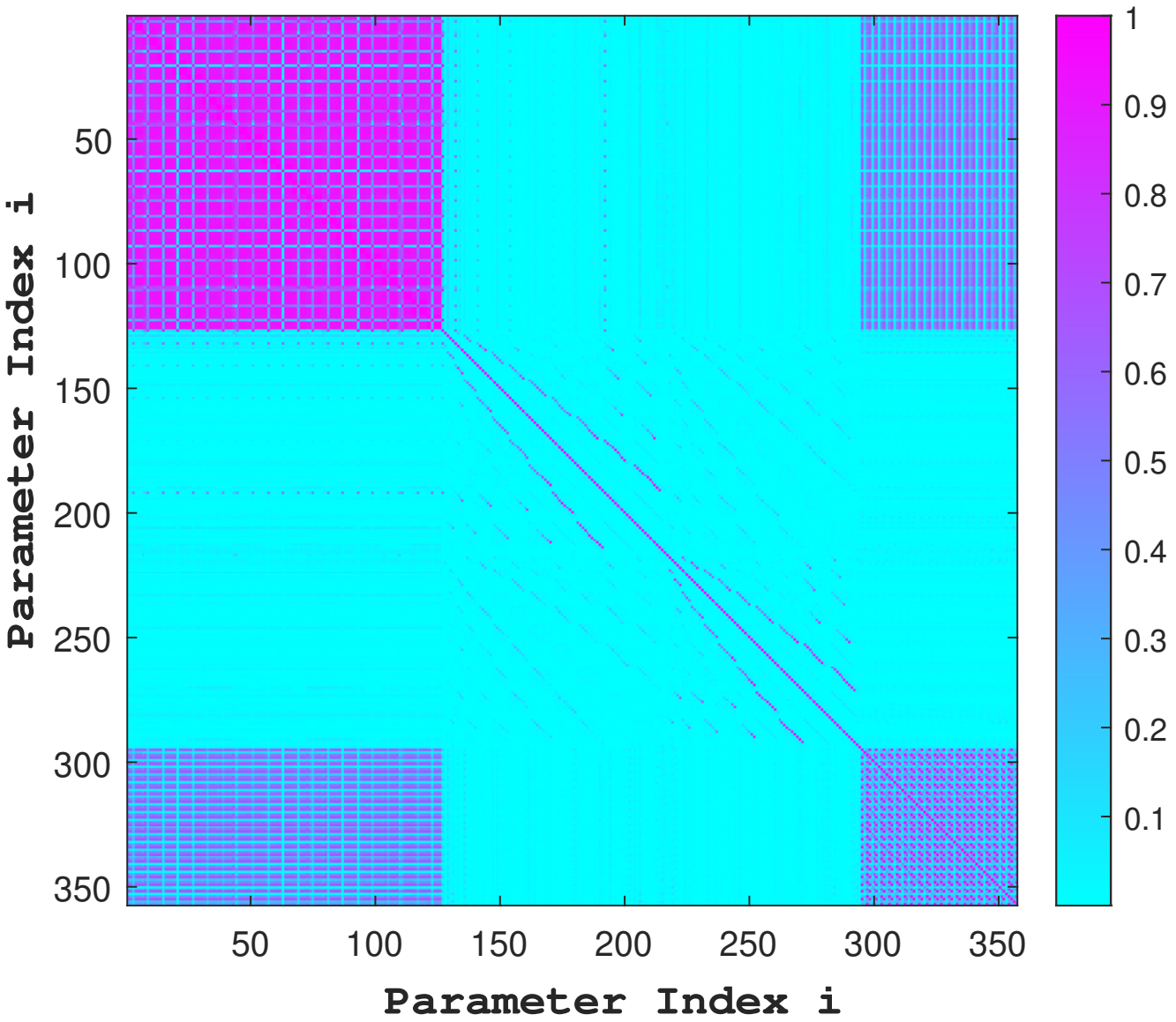

Figure 12: This figure illustrates the correlations with addition of empirical accelerations for the case of 21 arcs for the entire length of the mission. Parameters 1 to 126 represent the states for each arc. There are a total of 21 arcs with 3 values for position (x,y,z) followed by 3 values for velocity (v_x,v_y,v_z). The correlation between the states form the symmetrical block in the top left corner of the correlation matrix. Parameters 127 to 216 stand for the Cosine coefficients of the gravity field ($C_{n,m}$) starting with degree 1 (n) and increasing order 0 (m) in the following manner ($C_{1,0}$, $C_{1,1}$, $C_{2,1}$, $C_{2,2}$, $C_{3,0}$, ..., $C_{12,12}$). Parameters 217 to 294 stand for the Sine Coefficient of the gravity field ($S_{n,m}$) in the following manner ($S_{1,1}$, $S_{2,1}$, $S_{2,2}$, $S_{3,1}$,...., $S_{12,12}$). Parameters 295 to 357 represent the values of the empirical accelerations for the 21 arcs. The correlation matrix is symmetric and the diagonal entries should be ideally equal to 1, they represent the parameters correlated with themselves.

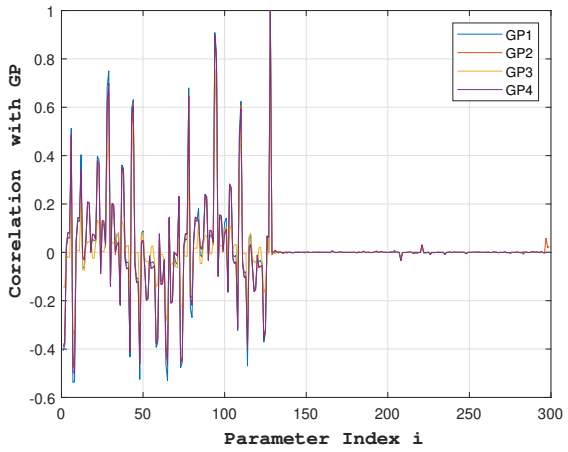

Figure 13: This figure illustrates the correlations of given parameters with the Gravitational parameter. Parameters 1 to 126 represent the states. Parameters 127 to 216 stand for the Cosine coefficients of the gravity field and Parameters 217 to 294 stand for the Sine Coefficients of the gravity field. The last 3 parameter 294 to 297 are the empirical accelerations.

and 0.5870 between $C_{2,0}$ and $C_{2,2}$ for two different encounters of Ganymede (Figure 15) after fitting the data. The results by Anderson et al. (1996) show that the correlation is much less compared to the a priori assumption of hydrostatic equilibrium in theory. The formal errors were obtained from a covariance analysis without applying the hydrostatic equilibrium assumptions, the same way it is done in this paper. The correlations obtained for this study are mostly less than 0.05 for nominal settings and on average .175 for degree 60 analysis as shown in table 11. Figure 15 does show a priori uncertainty estimated to be $1.8*10^{-6}$ and $1.0*10^{-6}$ for $C_{2,2}$ for the two encounters. The formal error values obtained for degree 2 coefficients in this study are shown in table 12. Comparing $C_{2,2}$ value of $2.98e-11$ with above mentioned values of the two encounters, a significant lowering of formal error is observed. Keep in mind that former results are based on flybys at closest approaches, whereas results in this study hold for a 3.5 month Ganymede orbit phase.

Table 12: Formal uncertainties for case GP2, a degree 12 simulation.

Parameter	Formal Error
μ (km^3/s^2)	$1.69e-04$
$C_{2,0}$	$8.59e-11$
$C_{2,1}$	$5.04e-11$
$C_{2,2}$	$2.98e-11$
$S_{2,1}$	$5.13e-11$
$S_{2,2}$	$3.02e-11$

A more recent study by Magnanini (2021), based on the JUICE mission, reports results for the uncertainty in Gravitational parameter as well as $C_{2,1}$ and $C_{2,2}$. These values are summarized in table 13. Comparison with results show that in this study results are factor 10^4 smaller roughly, but the a priori uncertainty used is also a factor 2 larger in this study (for $C_{2,1}$, as reported in section 3.3, compared to the values used by Magnanini (2021).

Table 13: Ganymede a priori and expected uncertainties as reported by Magnanini (2021) based on the JUICE mission.

Parameter	Apriori	Results
mu (km^3/s^2)	0.04	$1.3e-04$
$C_{2,1}$	$5.0e-05$	$5.7e-07$
$S_{2,1}$	$5.0e-05$	$6.8e-07$
$C_{2,2}$	$1.0e-04$	$1.3e-07$
$S_{2,2}$	$5.0e-04$	$1.5e-07$

5. Discussion

In the course of this research, a sensitivity analysis is performed where several model design choices were made and insights were gained. Numerous settings are investigated to understand the relation between the input variables and the outcome as to realistically predict the results and help make improvements for the mission in the future. This does not say anything about the value that JUICE is going to determine in practice, one can only predict.

First the settings listed in table 3 were carried out to build the nominal model. The second set of runs as listed in table 5 were investigated which accounted for the addition of the onboard accelerometer (in the form of empirical accelerations), as well as estimating the gravitational parameter uncertainty. Degree 1 estimation was also included to provide a wholesome picture of the gravity field uncertainty.

The results obtained have been presented in section 4. . In this section a discussion of the obtained results is presented.

5.1. Arc length

In section 4.1, it was shown that decreasing the arc length influences the formal error of spacecraft states more than it influences the formal error of the gravity field coefficients. In both cases, it is however recommended to keep the arc length constant when investigating the affect of changing other parameters. The difference in formal error for 1 to 5 arcs is so small for the gravity field that an arc of 5 days chosen as opposed to 1 day, to reduce the computation time of the simulation. It is safely assumed that this small difference is reason enough not to decrease the arc length when extrapolating the results of the nominal settings (degree 12) to degree 60. It is expected that the difference in formal errors will remain less than 1% in the gravity field coefficients at degree 60 and hence a 5 day arc is used even at higher degree 60 analysis for nominal settings. In case the difference in formal error in the gravity field had been 10% or more for shorter arc length, then this would have indeed be a case to investigate at degree 60 level.

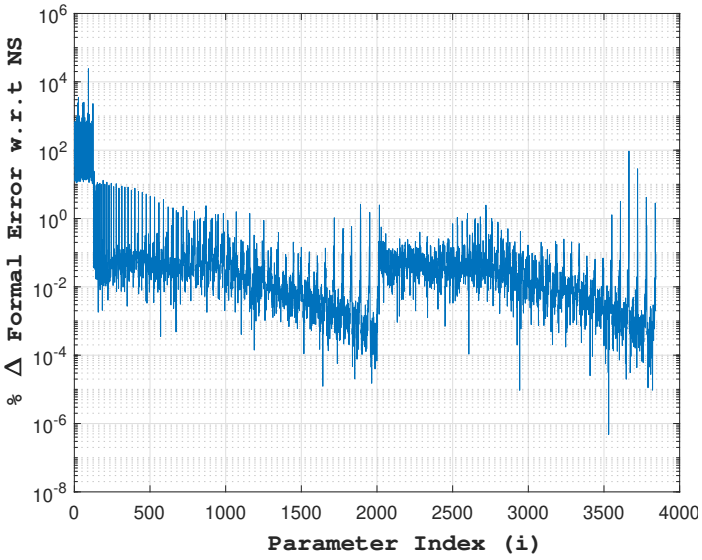

Figure 14: This figure illustrates the % difference in formal error for the final settings GF60 w.r.t the nominal settings NS. Parameters 1 to 126 represent the states. Parameters 127 to 2017 stand for the Cosine coefficients of the gravity field and Parameters 2017 to 3843 stand for the Sine Coefficients of the gravity field.

TABLE 1 Ganymede gravity results

	Encounter 1	Encounter 2
J_2	$(126.0 \pm 6.0) \times 10^{-6}$	$(127.8 \pm 3.0) \times 10^{-6}$
C_{22}	$(37.8 \pm 1.8) \times 10^{-6}$	$(38.3 \pm 1.0) \times 10^{-6}$
μ	0.7399	0.5870

J_2 and C_{22} are defined in the text; μ is the correlation coefficient.

Figure 15: This figure illustrates the Gravity Results for Ganymede as reported by JPL in 1996 (Anderson et al. (1996)). Here μ stands for the correlation between $C_{2,0}$ and $C_{2,2}$ after fitting the data. The hydrostatic equilibrium constraint of 10/3 had been imposed a priori in this study.

5.2. Range $1cm$ *vs* $20cm$

The range noise analysis in section 4.2 shows a significant change in formal error for gravity field coefficients as well as spacecraft states. Nominal value of $20cm$ range Noise as used aboard the JUICE mission, shows that range and VLBI measurements weigh much less compared to Doppler data. This is why range and VLBI measurements are predominantly used in ephemeris determination for celestial bodies as the changes are measured over longer period of time, whereas Doppler data which is measured with higher frequency and short time intervals is more applicable to spacecraft orbit determination. The results of $1cm$ range noise seem to suggest that this might change and range measurements could be included in spacecraft orbit determination in the future. This will eventually require greater data processing on ground. In terms of data load transmitted to ground, this can be handled well, since 3GM takes a small percentage of the link budget.

As shown in Figure 6 a 50% improvement in spacecraft (initial) state is observed for a $1cm$ range noise. Adding more data to existing Doppler data will improve the accuracy of the orbit determination. Better orbit determination improves the overall results related to orbit determination. In terms of spacecraft navigation more accurate maneuvers can be performed leading to less disturbances in the spacecraft position and as a result in the accelerometer position, meaning that effect of empirical accelerations can be mitigated properly.

5.3. Degree 1

Addition of degree 1 makes shows that degree variance deviates from upward positive slope trend set by the higher degrees, in figure 7. This is due to the kaula's assumption which does not hold for lower degrees. In this case the variance shoots towards the a priori uncertainty. However, the gravity field is not affected for higher degrees, so the estimation is not sensitive to this additional parameter. Given that the gravity field model would be incomplete without degree 1 coefficients, it is in the end essential to estimate it as well.

5.4. Solar Radiation Pressure

Even though solar radiation pressure C_r coefficient uncertainty is estimated in all the simulations, it is not the main point of concern of this study as its value is known relatively better than the gravity filed coefficients. It is a good piece of knowledge however given the large JUICE solar panels. The Radiation pressure model used is the cannonball radiation pressure model and improving this model by for instance making a better estimation of the area of the solar panels will have little affect on the covariance analysis, since implementing a better model will minutely change the position estimation of the spacecraft, which however in the larger scale of celestial measurements does not influence the sensitivity towards the gravity field

coefficients, as it is a long periodic affect. Moreover, the accelerometer on board the JUICE mission can accurately estimate C_r along-side other non-gravitational accelerations and the uncertainty in this accelerometer is estimated in the form of empirical acceleration uncertainties.

5.5. Empirical Accelerations

Unlike C_r, the empirical accelerations are implemented in an arc-wise fashion. The C_r uncertainty could in theory also be estimated arc-wise but due to above reasoning it is deemed to make no difference. The output will need some post processing in case the individual measurements (C_r, propellant sloshing, atmospheric drag) need to be determined separately. The empirical accelerations have constant a priori uncertainty in all 3 directions ($along-track$, $cross-track$ and radial). From the results in section 4.5 it became obvious that the propagation resulted in most accurate estimate of empirical acceleration uncertainty in along-track direction. This is because atmospheric drag or any other non-gravitational perturbation mainly works in the $along-track$ direction and reduces the orbital energy, since the $along-track$ force acts in the direction of the orbital plane as opposed to working against it or perpendicular to it and there will be a build up of perturbation. $Along-track$ direction is in the direction of the orbital plane, but not exactly the same as the velocity vector, due to slight orbital eccentricity. This suggests that the accelerometer is more prone to pick up accurate measurements in the $along-track$ direction due to its greater sensitivity to a perturbation. This also means that a perturbation in this direction will require the least amount of fuel and result in a relatively higher orbital correction maneuver, assuming that the orbital plane is not drifting.

The change in the gravity field coefficient formal error for 21 arc compared to 1 arc is minimal, therefore 1 arc of empirical accelerations will suffice to estimate the gravity field coefficient uncertainty. The overall improvement in gravity field due to empirical accelerations is also expected to be minimal. The differences are small but the addition of the empirical acceleration and all other parameters for that matter always improves the model and make it more realistic. The empirical acceleration correlations with the gravity field do seem to suggest that they are constant despite changing the arc length, therefore they are independent of the arc length as well. This is illustrated in figure 11 and 12, there is very little correlation between empirical acceleration and the gravity field coefficients. The same figures illustrate the visible correlation between the state arcs and empirical accelerations. In these figures the correlation of the state arcs with themselves become stronger as well compared to the nominal model. Therefore the state is affected by both the arc length of the states as well as the arc length of the empirical acceleration. This is important set of results when considering the accelerometer operation. The fact that the gravity field uncertainty is independent of the number of arcs of states or the number of arcs of empirical accelerations, provides an extra degree of freedom when considering accurate state determination or orbit determination for the spacecraft. As figure 10 illustrated up to 100% difference is seen in formal errors for 3,5 or 21 arcs compared to 1 arc for empirical accelerations. Therefore, implementing multiple arcs will improve the state estimation (POD) and help improve the navigation of the spacecraft and accuracy of all other systems which are related to this, as well as therefore performing better trajectory correction maneuvers, without jeopardizing the gravity field uncertainty estimation.

The consequence of having 1 arc for the entire mission is that the accelerometer will be turned on once and calibrated once. In practice this will mean that the accelerometer is using power even when no measurements are being done during downtime, as the measurement window is only 8 hours and the other 16 hours of the day the accelerometer will be redundant, the simulation does not account for this time gap between measurements. As the results show there is some flexibility in deciding between 3,5 or 21 arcs in terms of percentage change in formal error for the (initial) states, since they are almost 100% for all three cases. In the end the optimal choice will be to coincide the arc length of the empirical acceleration to the arc length of the states, namely 5 day arc length with 21 arcs in total. This will ensure that when results of these two settings are compared the time period of measurements will be consistent with each other. Accelerometers and other equipment are tested for continuous on/off cycles as to avoid malfunction of the equipment, therefore increasing the number of cycles to 21 arcs should accommodate for the this and this will not be a factor in deciding against large number of arcs.

In general, re-calibration for each arc will lead to constant improvement in accelerometer measurement and account for any new disturbing perturbations which which were not accounted for in the previous calibration. Therefore, in practice it is recommended to implement several arcs, ideally the same as the states, however a better power budget and link budget analysis as well as instrument capabilities are needed to actually test this hypothesis and quantify the advantages and disadvantages to make a proper trade-off. Since the accelerometer operations can be changed when in flight, this area gives a lot of potential for future simulations as to come up with an innovative plan of accelerometer use during the JUICE mission. It should be mentioned that a calibrated parameter does not necessarily represent reality as reality is much more complex.

5.6. Gravitational Parameter

Estimated values for the gravitational parameter as shown in table 10 are almost the same as the a priori uncertainty. The a priori uncertainty is obtained from the Jovian system ephemerides of JPL, Compared to this long time series of about 400 years, a few months of JUICE orbit data will increase the total time period of available data once the data is obtained after the end of the orbit

phase and flybys in the Jovian system in 2032. However there will be some gaps in between the previous mission (Juno) and the JUICE mission data. The JUICE mission data however, will be the most extensive set of data as it include the GCO-500 over a few months, but also flybys for the other Galilean moons as well as Jupiter itself.

5.7. Degree 60

For the final results in figure 14, the settings used are consistent with the basics of the nominal settings. However, propagating at such higher degrees, the correlations might not be visible for the given arc length. To see if there are actually any correlations at higher degrees it is therefore necessary to decrease the observation interval for Doppler data from 10 min to 2min. This is by a factor 5, which corresponds to five fold increase in the degree from degree 12 to degree and order 60. This is explained by equation 5 in section 2.2.2, where the cosine of the longitude (λ) will be multiplied by a factor 5 and the wavelength of the change in gravity field signatures will become 5 times more frequent. Therefore some final simulations runs are performed for GF60 with 5min and 2min observation interval, accordingly. The results (correlation plots not shown here) show that some correlations appear but in general there are very few correlations between empirical accelerations and gravity field. However, looking up the correlation values of $C_{2,0}$ and $C_{2,2}$ show that the figures can be deceptive due to large number of parameters depicted in them and numerical values of correlation exceeding a certain minimum value should be searched for instead.

The numerical results reported in 4.7 show some promising decrease in correlations for the JUICE mission compared to Anderson et al. (1996) and further decrease in formal uncertainties compared to Magnanini (2021). In figure 15 correlation of 0.7399 and 0.5870 were obtained for the two closest approaches reported by Galileo. Although the model of this study is more realistic due to the addition of the accelerometer and an orbit phase compared to flybys, therefore direct comparison can not be made between these studies. Nonetheless, table 11 shows the correlation obtained for this study for the different simulation runs. For degree 12 estimation the correlations are less than 0.04. The correlations increase to 0.174 for degree 60 simulations. These values are much higher compared to the degree 12 case but still low enough to conclude that the gravity field sensitivity to the added parameters and settings is low. And secondly these values are a significant improvement to the correlation between $C_{2,0}$ and $C_{2,2}$ as reported by Anderson et al. (1996) in figure 15. This implies that with this study there is considerable chance of differing from the a priori assumption of hydrostatic equilibrium and to predict that JUICE actual results will do the same, as was the goal of ESA for the JUICE mission.

With the given settings showing little sensitivity towards formal errors, the formal conclusion is that the chosen model is a good and stable foundation for estimating the uncertainty in the gravity field, as these settings are not prone to unexpected drastic changes. Moreover developing a reliable model for future processing of output once the actual mission has flown, serves as an important goal for research itself.

6. Conclusion

The main focus of this study has been to develop a numerical model based on mission and instrument specification from the JUICE mission and study settings and parameters which influence the gravity field uncertainty estimation during an extended orbit phase around Ganymede. The nominal model developed for degree and order 12 was eventually run to degree 60 to utilize all the data at hand and increase the science return of the mission.

The extensive sensitivity analysis has delivered some promising results with regards to including range measurements with $1cm$ range noise in future missions for spacecraft precise orbit determination. Presently, Doppler measurements are the only source of data for spacecraft state determination. The range and VLBI data are used when considering planetary ephemerides.

It was also demonstrated that the accelerometer can be utilized with different operation schedules during the mission with out having any loss of quality of the data with respect to the gravity field uncertainty estimation. On the other hand the percentage change in formal errors for spacecraft states can reach 100%. Therefore changing the arc length to be the same as arc length for (initial) state uncertainty estimation or implementing multiple arcs in general as opposed to a single arc, is highly recommended for POD purposes.

Increasing the arc length shows considerable influence on the spacecraft (initial) state uncertainties, both for state arcs as well as empirical acceleration arc lengths. The influence of the arc length on the gravity field uncertainty in comparison remains minimum for both cases. In general, with the model assumptions, limitation and choices made it is seen that the gravity field uncertainty is little or not at all sensitive to the given settings or model choices in terms of formal errors. A lower correlation between $C_{2,0}$ and $C_{2,2}$ is reported compared to previous, giving some statistical reason to believe in the revision of the hydrostatic equilibrium assumption and hence independent determination of the degree 2 gravity field coefficient uncertainties, as a result of the JUICE mission.

Some limitations of this study which can be addressed in the future are that no rotational model was added, the tidal potential could be an additional parameter which will make the model more realistic and help estimate the uncertainty in the tidal dissipation constant. This constant helps better constrain the internal water ocean and thickness of the overlying ice shell of Ganymede (Jara-Orué and Vermeersen (2016)).

References

Alessi, E. M., Cicalo, S., and Milani, A. (2012). Accelerometer data handling for the bepicolombo orbit determination. *Advances in the Astronautical Sciences*, 145:121–129.

Allahvirdi-Zadeh, A., Wang, K., and El-Mowafy, A. (2022). Precise orbit determination of leo satellites based on undifferenced gnss observations. *Journal of surveying engineering*, 148(1):03121001.

Anderson, J., Lau, E., Sjogren, W., Schubert, G., and Moore, W. (1996). Gravitational constraints on the internal structure of ganymede. *Nature*, 384(6609):541–543.

Asmar, S., Armstrong, J., Iess, L., and Tortora, P. (2005). Spacecraft doppler tracking: Noise budget and accuracy achievable in precision radio science observations. *Radio Science*, 40(2):1–9.

Cappuccio, P. and Cascioli, G. (2019). Esa's juice end-to-end orbit determination simulation to calibrate on-board accelerometer.

Cappuccio, P., Notaro, V., di Ruscio, A., Iess, L., Genova, A., Durante, D., di Stefano, I., Asmar, S. W., Ciarcia, S., and Simone, L. (2020). Report on first inflight data of bepicolombo's mercury orbiter radio science experiment. *IEEE Transactions on Aerospace and Electronic Systems*, 56(6):4984–4988.

Cappuccio, P., Notaro, V., Iess, L., Asmar, S., Border, J., Ciarcia Sr, S., Di Ruscio, A., Montagnon, E., De Vicente, J., Mercolino, M., et al. (2019). First results from cruise tests of the mercury orbiter radio science experiment (more) of esa's bepicolombo mission. In *AGU Fall Meeting Abstracts*, volume 2019, pages P34A–04.

Casajus, L. G., Zannoni, M., Tortora, P., Park, R., Buccino, D., Parisi, M., Levin, S., and Bolton, S. (2021). The gravity field of ganymede after the juno extended mission. Technical report, Copernicus Meetings.

De Pater, I. and Lissauer, J. J. (2015). *Planetary sciences*. Cambridge University Press.

Di Benedetto, M., Cappuccio, P., Molli, S., Federici, L., and Zavoli, A. (2021). Analysis of 3gm callisto gravity experiment of the juice mission. *arXiv preprint arXiv:2101.03401*.

Di Benedetto, M., Ciarcia Sr, S., Iess, L., Kaspi, Y., Mann Sr, R., and Shapira Sr, A. (2017). The 3gm radio science experiment on board the esa juice mission. In *AGU Fall Meeting Abstracts*, volume 2017, pages P12A–03.

Dougherty, M., Grasset, O., Erd, C., Titov, D., Bunce, E., Coustenis, A., Blanc, M., Coates, A., Drossart, P., Fletcher, L., et al. (2012). Jupiter icy moons explorer (juice): An esa l-class mission cadidate to the jupiter system.

ESA (2014). Juice (jupiter icy moon explorer): Exploring the emergence of habitable worlds around gas giants. Technical report, European Space Agency.

Frank, L., Paterson, W., Ackerson, K., and Bolton, S. (1997). Low-energy electron measurements at ganymede with the galileo spacecraft: Probes of the magnetic topology. *Geophysical research letters*, 24(17):2159–2162.

Giuseppe, M., Paolo, C., Luciano, I., et al. (2021). Observability of ganymede's gravity anomalies related to surface features by the 3gm experiment onboard esa's jupiter icy moons explorer (juice) mission. *Icarus*, 354:114003.

Hussmann, H., Sohl, F., and Spohn, T. (2006). Subsurface oceans and deep interiors of medium-sized outer planet satellites and large trans-neptunian objects. *Icarus*, 185(1):258–273.

Iess, L., Asmar, S., Cappuccio, P., Cascioli, G., De Marchi, F., di Stefano, I., Genova, A., Ashby, N., Barriot, J., Bender, P., et al. (2021). Gravity, geodesy and fundamental physics with bepicolombo's more investigation. *Space Science Reviews*, 217(1):1–39.

Iess, L., Asmar, S., and Tortora, P. (2009). More: An advanced tracking experiment for the exploration of mercury with the mission bepicolombo. *Acta Astronautica*, 65(5-6):666–675.

Iess, L. and Boscagli, G. (2001). Advanced radio science instrumentation for the mission bepicolombo to mercury. *Planetary and Space Science*, 49(14-15):1597–1608.

Jacobson, R. (2021). The orbits of the regular jovian satellites and the orientation of the pole of jupiter. In *JPL*, volume -, pages –.

Jara-Orué, H. and Vermeersen, B. (2016). Tides on jupiter's moon ganymede and their relation to its internal structure. *Netherlands Journal of Geosciences*, 95(2):191–201.

Kivelson, M., Khurana, K., Russell, C., Walker, R., Warnecke, J., Coroniti, F., Polanskey, C., Southwood, D., and Schubert, G. (1996). Discovery of ganymede's magnetic field by the galileo spacecraft. *Nature*, 384(6609):537–541.

Konopliv, A. S., Miller, J. K., Owen, W. M., Yeomans, D. K., Giorgini, J. D., Garmier, R., and Barriot, J.-P. (2002). A global solution for the gravity field, rotation, landmarks, and ephemeris of eros. *Icarus*, 160(2):289–299.

Luciuk, M. and Carlo, J. (2019). Hydrostatic equilibrium and planetary differentiation.

Magnanini, A. (2021). Estimation of the ephemerides and gravity fields of the galilean moons through orbit determination of the juice mission. *Aerotecnica Missili & Spazio*, 100(3):195–206.

McMahon, J., Farnocchia, D., Scheeres, D., and Chesley, S. (2016). Understanding kaula's rule for small bodies. In *47th Annual Lunar and Planetary Science Conference*, number 1903, page 2129.

Montenbruck, O., Gill, E., and Lutze, F. (2002). Satellite orbits: models, methods, and applications. *Appl. Mech. Rev.*, 55(2):B27–B28.

Nimmo, F., Bills, B., and Thomas, P. (2011). Geophysical implications of the long-wavelength topography of the saturnian satellites. *Journal of Geophysical Research: Planets*, 116(E11).

Saur, J., Duling, S., Roth, L., Jia, X., Strobel, D. F., Feldman, P. D., Christensen, U. R., Retherford, K. D., McGrath, M. A., Musacchio, F., et al. (2015). The search for a subsurface ocean in ganymede with hubble space telescope observations of its auroral ovals. *Journal of Geophysical Research: Space Physics*, 120(3):1715–1737.

Schubert, G., Zhang, K., Kivelson, M. G., and Anderson, J. D. (1996). The magnetic field and internal structure of ganymede. *Nature*, 384(6609):544–545.

Serra, D., Spoto, F., and Milani, A. (2018). A multi-arc approach for chaotic orbit determination problems. *Celestial Mechanics and Dynamical Astronomy*, 130(11):1–17.

Yan, J., Liu, S., Yang, X., Xiao, C., Ye, M., Jin, W., Li, F., and Barriot, J.-P. (2019). Mercury gravity recovery and analysis system (mergreas) and its performances from simulated four-way doppler measurements. *Astrophysics and Space Science*, 364(4):1–14.

3

Conclusion

This chapter addresses the conclusion to the research questions and research objective posed at the start of the thesis. The first question concerns the covariance analysis and model development to qualitatively define the benefit of the extended Ganymede orbit phase of the JUICE mission. The last two questions deal with the sensitivity analysis and how these results can be utilized for future missions.

The first research question:

- How well is the gravity field uncertainty of Ganymede simulated during GCO-500 phase of the JUICE mission.

Simulating the uncertainty in the gravity field of Ganymede is interesting from two points of view. First is that the uncertainty is only known for a few parameters but not good enough, therefore existing values can be improved. Secondly, the fact that an estimate for higher degree coefficients can be made is a first step in itself and will eventually determine the margin within which the actual gravity field coefficients will lie, once they are determined theoretically or practically after the JUICE mission has flown. It has been demonstrated in this simulation model that this analysis can be done independent of whether the gravity field coefficients and other parameters are known or not. From the results as discussed in the scientific paper, it has been shown that the Ganymede Orbit Phase will definitely improve the gravity field estimation. The correlations obtained show a significant decrease compared to previous studies of mainly flybys and therefore this is expected to be the case also for the extended orbit phase, as well as expect independent estimation without any a priori assumptions. It does become tricky to validate all other estimated uncertainties since the mission has not flown yet.

The results of a few months of data are somewhat optimistic since years of data is needed to come to presentable conclusions. Nonetheless these values are a good start to better answer the questions posed by ESA about harboring sub-surface oceans and existence of lifeforms on Ganymede. In general, modelling the GCO-500 has been successful especially due to possibility of adding of empirical accelerations as they represent the uncertainty in the onboard accelerometer.

Some assumptions and limitations are inherent to numerical modelling and covariance analysis. The covariance analysis uses a dynamical model to generate observations, however it ignores errors in the dynamical model as it is indirectly dependent on the dynamical model. The formal errors are an indication of the distribution of the observations only and not their actual values. Therefore most results are optimistic and indication of the behaviour of the error propagation and not exact representation of their values, as they indicate the order of magnitude of the values.

The dynamical model assumes that the motion of the spacecraft, Ganymede, Jupiter and sun is known perfectly. It assumes that the orbits are circular, in case of elliptical orbits this will not be accounted for. It also assumes perfectly uncorrelated noise, but this might not always be the case.

Second research question:

- What are the most sensitive settings/parameters and to what extent do they influence error estimation of gravitational and non-gravitational parameters.

In general, it has been concluded that the gravity field uncertainty is almost indifferent to parameter changes or model choices. The chosen settings have eliminated the need to investigate these settings

any further, however the question remains whether there are any other settings for which the gravity field uncertainty estimation is actually sensitive or has the analysis been exhaustive and any further decrease in uncertainty might not be possible. The maximum change in formal error of all cases has been about 1% which is a relatively small percentage to see any changes in the gravity field coefficients.

A larger sensitivity is observed for the (initial) state uncertainties due to arc length or the number of arcs of the states as well as empirical accelerations. Even though the gravity field uncertainty is the main focus of this study, POD can also benefit from this analysis. While the change in the formal error for gravity field remains below 1%, a 100% difference is observed when increasing a single arc of empirical acceleration to multiple arcs. A next step in the investigation would be to actually implement downtime of accelerometer in the simulation and observe whether this will worsen the formal error of the gravity field. At the moment this downtime is not implemented and the next arc starts as soon the previous arc finishes.

Another sensitive parameter is the rang noise for range only measurements. Almost 100% difference is observed for the initial states and up to 60% difference is observed for the gravity field uncertainty, when reducing the range noise from $1cm$ to $20cm$. The mission duration also has an influence on the formal errors. All other settings and parameters have least influence on the formal errors.

Third research question:

- How do the sensitivity results contribute to future mission operations of the JUICE mission.

As indicated in the scientific paper, some useful conclusions are made with regards to practical consequences of the sensitivity analysis. The insensitivity of the gravity field to arc length of empirical accelerations opens many possibilities for accelerometer operations. If the accelerometer can be turned off during downtime, without influencing the gravity field uncertainty, this will avoid unnecessary occupation of power and data handling subsystems of the spacecraft. Multiple arcs can be implemented during measurement time as to improve the spacecraft orbit determination accuracy and navigation. This will also lead to re-calibration of the accelerometer at each step, which will account for any new disturbances compared to the previous calibration. The analysis carried out for arc length of empirical accelerations is very basic and further possibilities in this aspect should be investigated.

The range only analysis shows that addition of range noise of $1cm$ for the JUICE mission is a promising aspect to include range measurements in spacecraft orbit determination. Range measurements are already carried out as part of the radio science measurements, but are generally applied to ephemeris determination. With these new insights it will be possible to include the range measurement noise without major modifications in the measurement system.

The Research Objective:

Determine the influence of model settings and parameters on the quality of the gravity field uncertainty estimation of Ganymede during the orbit phase of the JUICE mission.

It can be said that this objective has been fulfilled. A comprehensive analysis of model and parameter settings has characterized the uncertainties and the sensitivity of the model. A good foundational model is created, which opens up further possibilities of investigation, which are discussed in the recommendations section.

4

Recommendations

Recommendations for future work come in two forms. Either they are aspects that could have been investigated given more time or computational expertise were available for the given model or they are insights which could lead to a different model than the existing model. In whichever form, recommendations could potentially help future readers to formulate research goals which build upon this piece of work. Following are a few recommendations:

- Although the condition number for most simulation runs as well as matlab analysis of the results has been very high, in no case has there been a case of simulation terminating due to high condition number. It is recommended to keep a better track of the condition number in order to understand the consequences of having a larger covariance matrix or simulation and how to account for this. The result analysis at the moment has somewhat ignored the condition number and assumes that the results are accurate even with high condition numbers. This is however not the case, because a high condition number does not give accurate results and the matrix is called ill-conditioned. There are ways to make a matrix ”well-conditioned” and this will be applicable when considering more broader simulations.
- During the research it became apparent that a lot of studies have been performed on the flyby phases of Io and Callisto by using least squares instead of a covariance analysis. This has the advantage that the actual parameter values can be estimated and not just the formal errors. Doing a least squares might not be a good recommendation for the orbit phase due to the high condition numbers already obtained, but combining a flyby and applying well-conditioned matrices is an interesting follow up to covariance analysis.
- Alternatively another option worth considering is extending the current simulation by including the flyby phases of the JUICE mission tour, if possible. This is indeed challenging, as there is a time gap between the end of the flyby and the start of the orbit phase, but making well-founded assumption about the initial conditions of each phase might help to accomplish this extended version of the Covariance analysis for the JUICE mission tour.
- Rotational properties and tidal love numbers are not included in this simulation due to complexity of implementing a rotational model. This makes the uncertainties optimistic. It would be interesting to see the affect of the rotational dynamics on JUICE motion. The rotational model will make the gravity field estimation a little worse, as it is closer to reality.
- Add additional data types. Even though Doppler data is the main data type for estimating the error in the gravity field and from this study it is also recommended to add the range noise of 1 cm, another interesting application would be to investigate the contribution of ILR (interplanetary laser ranging). Study from Dirkx et al. (2019) suggest that it could be an option to include ILR with Doppler tracking system to study the influence of the gravity field on spacecraft dynamics.
- It is recommended to apply this model or the finding of this model to other outer planetary bodies in the solar system. A covariance analysis indeed is a good start and gives a lot of insight about

error propagation. One suggestion when interpreting the results would be to not only rely on a qualitative analysis of the correlation plots for higher degrees, but actually perform a better quantitative analysis about the increase in correlations.

- When using SPICE kernels from ESA, it is not possible to receive the actual dynamical model used by them to construct the model. Therefore underlying assumptions are not known. It would be recommended to request the original dynamical model if possible. In terms of covariance analysis this is not urgent but for proper parameter estimation the original dynamical model is important, assuming that the software at hand is capable of handling such a model.
- Optimize for initial time better. Orbit could have been 4 months instead of 3.5 months, although the result of this is predictable. Extend the length of the simulation by using the same SPICE. Alternatively, ESA could design a trajectory longer than 4 months or a few years.
- Consider different multi-arc strategies for empirical accelerations of the accelerometer. These could be more advanced compared to simply changing the arc length of empirical accelerations, as was the case in this work.

Appendices

A. Model Development

As stated in Table 3 of the scientific paper, a list of simulation runs have been performed to develop the nominal model. For convenience the table is presented here once again (1). Two of these runs have been discussed in the paper itself (Arc Length (AL) & Weight ratio (WR), the remaining runs and their outputs are presented here, in the same order with abbreviation for each run found in the Table 1. The settings for each simulation type may vary in this investigative phase as the nominal settings had not been determined yet.

Table 1: **Simulation runs and analysis done to develop the nominal model. The first column shows the abbreviation given to the type of run. The last column shows the setting which was chosen as a result of these runs.**

Abbreviation	Description	Simulation Runs	Conclusion
DT	Data Type	VLBI/Doppler/Range only VLBI/Doppler/Range ratio	Doppler
DW	Data Weights	Observations constant Observation Ratio	
OI	Observation Interval	0.5,1,2,5,10 min	10 min
AL	Arc Length	1,2,3,4,5 days	5 days
MD	Mission Duration	1,2,3,3.5 months for Fixed AL (5 days) Fixed no. of arcs (5 arcs)	3.5 months
WR	Weight Ratio	Weight 20cm Range Weight 1cm Range	Not applicable
OP	Observation Planning	Hour shifts 0,4,8,12,16,24 hours	Not applied

A.1. Data Type

The 3 Data types that are investigated in this simulation model are Range, Doppler and VLBI with the settings given in Table 2. Figure A.1b shows that under nominal settings Doppler data has the lowest formal error followed by range and VLBI, when each data type is simulated independently. Increasing the number of observations by a factor of 5 or 10 as shown in figure A.2a & A.2b has no affect on this result. For the Data Types to be simulated together as in Figure A.1a while giving a certain ratio to the number of observations for each data types, shows that despite increasing range and VLBI observations by tenfold compared to Doppler observations, the final formal error is in the same order of magnitude as in Doppler only results of Figure A.1b, A.2a or A.2b. This leads to the conclusion that Doppler measurements have the greatest influence on the results, followed by range and then VLBI. For this reason range and VLBI are considered negligible in the nominal settings for the given noise values of range and VLBI (20 cm & 1nrad (Dirkx et al. (2017)), respectively). Figure A.1b also shows that in terms of formal error Doppler formal error is roughly a factor of 10^4 smaller and for range it is a factor 10^2 smaller. For range observations given that a change in formal error for gravity field coefficients is observed when decreasing the noise to $1cm$, adding range observations might still improve the data. As shown in Figure 6. of the scientific paper, the percent change in formal error can fluctuate up to 60% and has a mean value of 29.67%. This would mean that decreasing the noise by a factor of 20 improves the gravity field formal uncertainty estimation by a factor of almost 30% on average. This would mean that 30^2 less observations will be needed for the range data to weigh as significant as Doppler data. But the total number of range observations might still be too high (a factor of 4900) for this to actually happen. Adding range data to Doppler data is slightly more realistic than adding VLBI to these measurements at the moment. In terms of VLBI measurements this will computationally not be possible, because a

Table 2: Nominal Settings of simulation runs performed to investigate the influence of Data Types and Hour Shifts.

Abbreviation	Settings
DTS	30 Days Degree 2-12
(Data Type Settings)	10 arcs
	Arc length 3 days
Range Noise	20 cm
Doppler Noise	0.33 E-13
VLBI Noise	1 nrad

Table 3: Nominal Settings for simulation runs to investigate the influence of the Observation Interval (OI).

Abbreviation	Settings
OI	90 Days Degree 2-12
(Observation Interval)	30 arcs
	Arc length 3 days
Doppler Noise	0.33 E-13

factor 10^4 difference would mean 100 million observations more are required, which is far too many observations for such a small scale system as a spacecraft orbit of a few months. For ephemeride generation of celestial bodies it might be more feasible, however this amount of measurements will significantly add to the computational effort to estimate the ephemerides accurately.

Adding data of different types means that the total number of measurements increase and consequently improved, assuming that the data is a good data set. A good data set is defined as a data set which is close to the real data and has least uncertainty. In this case VLBI data has the greatest uncertainty compared to Doppler and range. Doppler is more suitable for short period measurements and the whole orbit around Ganymede is covered in 3.08 hours (assume almost circular orbit with semi-major axis of $500km + Ganymderadius$), meaning that the total observation period of 8 hours as specified by esa, covers about 2.6 orbits around Ganymede. The angular uncertainty for VLBI is 1 nrad which at a distance of 628.3 million km to Ganymede, will mean uncertainty of 628.3 metres, which is roughly a factor 3141.5 greater than the uncertainty for range $(20cm)$. Factors which attribute to this inaccuracy of VLBI measurements is the no. of ground stations and the noise.

Doppler is a really good source information for parameters with fast variation, in this case less than a day. For Doppler data the frequency that is received looks like a sine wave and the oscillation immulates the period of JUICE around Ganymede, because the spacecraft is constantly moving away or towards the ground station with more or less the period of the s/c around Ganymede, which is a few hours and therefore Doppler is applicable to those short periods.

A.2. Observation Interval

Increasing the interval of observation means reducing the number of observations, while keeping the total time interval of observations constant. The noise used for Doppler data applies to 60 seconds integration time, when observations are generated for different time periods the noise level has to be scaled accordingly. For example, the observation interval to 5 minutes means that the noise has to be divided by a factor of square root of 5, since the number of observations is decreasing therefore the noise is decreasing accordingly.

The results and settings obtained for changing the observation interval are summarized in Figure A.3a and Table 3 respectively. Figure shows that for time intervals ranging from 30 seconds to 10 minutes for Doppler only observations the formal error is the same. The observation interval hardly makes any difference. Therefore, taking a longer observation interval might be more feasible in terms of saving computation time without increasing the formal error.

A.3. Data Weight

Data Weight is the statistical uncertainty of observations (measurement random noise). Biases on the other hand is deterministic noise and represents a constant offset in measurements. Doppler data does not have bias (measurement errors). Even though bias can be added to range and VLBI measurements,

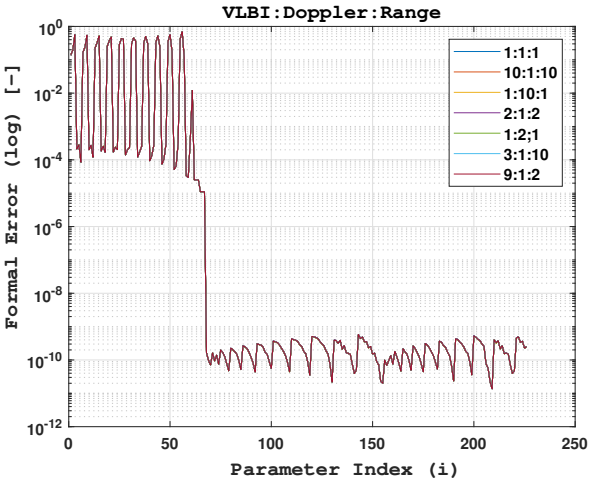

(a) This figure illustrates the Formal Error for each parameter, for given ratios of Data Types in the order (VLBI:Doppler:range). Parameters 1 to 60 represent the state arcs, parameter 61 is the solar radiation pressure. Parameters 62 to 226 are the gravity field coefficients (cosine followed by sine) for degree and order 12.

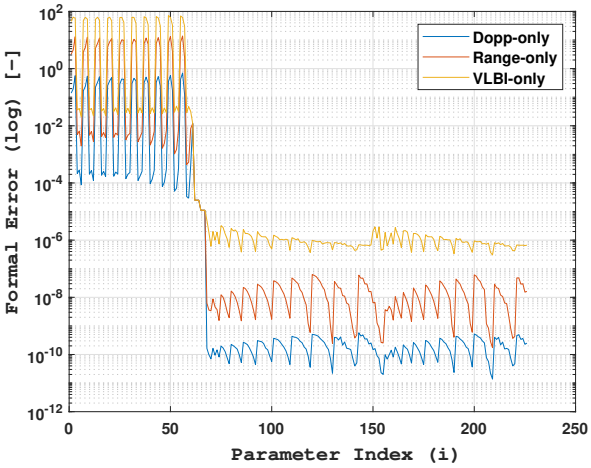

(b) This plot concerns Doppler only, range only and VLBI only measurements. Parameters 1 to 60 represent the state arcs, parameter 61 is the solar radiation pressure. Parameters 62 to 226 are the gravity field coefficients for degree and order 12.

Figure A.1

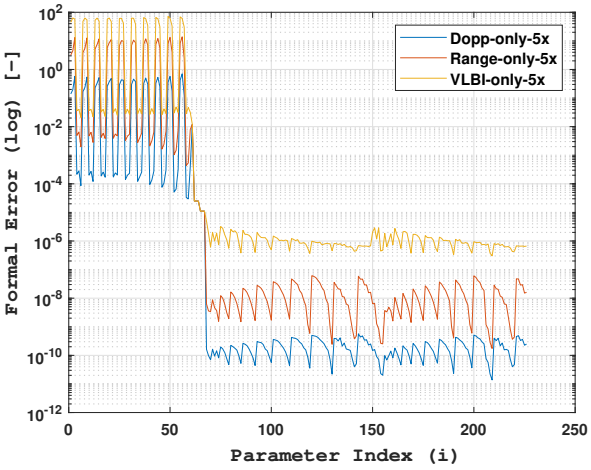

(a) This figure illustrates the Formal Errors obtained when 5 times more observations are generated for the given Data Types for the same total time interval of observations. Parameters 1 to 60 represent the state arcs, parameter 61 is the solar radiation pressure. Parameters 62 to 226 are the gravity field coefficients (cosine followed by sine) for degree and order 12.

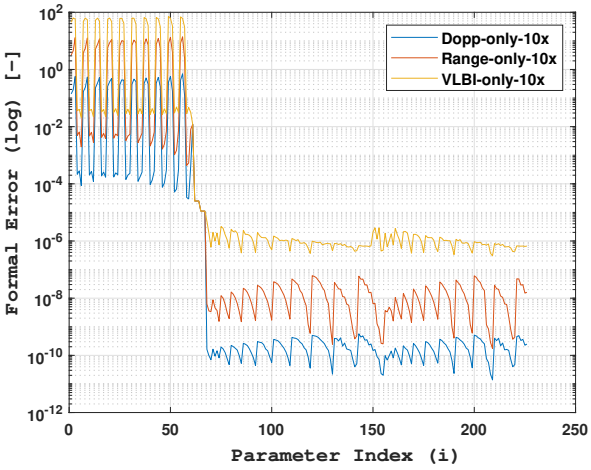

(b) This figure illustrates the Formal Errors obtained when 10 times more observations are generated for the given Data Types for the same total time interval of observations. Parameters 1 to 60 represent the state arcs, parameter 61 is the solar radiation pressure. Parameters 62 to 226 are the gravity field coefficients (cosine followed by sine) for degree and order 12.

Figure A.2

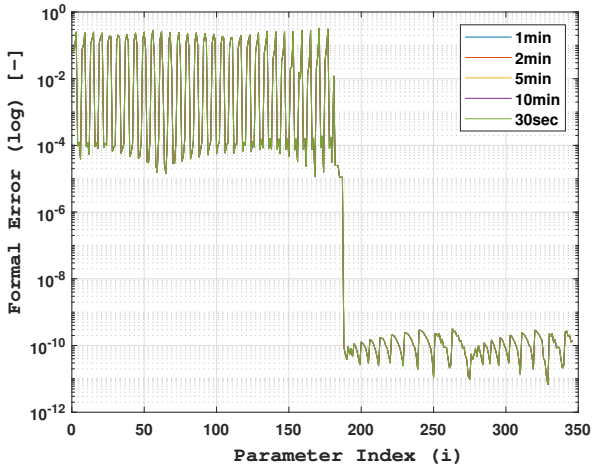

(a) This figure illustrates the Formal Error obtained for different observation intervals for the settings given in table 3. Parameters 1 to 180 represent the state arc, parameter 181 is the solar radiation pressure. Parameters 182 to 346 are the gravity field coefficients (cosine followed by sine) for degree and order 12.

Figure A.3

Table 4: **Nominal Settings of simulation runs performed to investigate the influence of Data weights (noise).**

Abbreviation	Settings
NS (Nominal Settings)	3.5 months Degree 2-12 Observations Interval 10 min Doppler Only Arc length 5 days

in this study no bias has been added. Data weight represent uncertainties originating from the 3GM instrument which specifies the accuracy of the range data. Currently this accuracy is set to 20cm.

Data Weights are investigated under nominal settings as given in the scientific paper (Table 4). Figure A.4a shows the affect of changing the weight factor while keeping the number of observations constant. When the weight is decreased, the data noise gets higher and formal errors should decrease by the same factor, given there is no a priori uncertainty. Higher precision does not mean that the data gets better, data is only better if it has no correlations. Decreasing the Weight by a factor 10 (hence square root 10) will decrease the formal error, as the weight is inversely proportional to the formal error. Figure A.4b shows what happens when the number of observations is modified disproportionately. It shows that the formal error is lower for the case when the weight is decreased by a factor of 15 and 3 times more observations are generated (W15Obs3). It is concluded that weight and number of observations don't influence the formal error greatly. This is because a priori uncertainty also has to be considered. A plot of the degree variance as shown in figure A.5a shows that the formal error is the lowest for the case of high weight and low observations (W15Obs3),therefore decreasing the weight (and therefore increasing the noise) makes the result deviate from the a priori curve, meaning that the data influences the result more than the apriori knowledge of parameters. The case the where the weight is the lowest and observations of factor 1 (W1Obs1), is closest to the a priori curve as expected (here the weight is lower for the same number of observations and the data influences the formal error slightly more than (W5Obs1) for instance).

A.4. Observation Planning

While orbiting Ganymede, the JUICE spacecraft will not be visible to the ground station when it is at the dark side of the moon, this occurrence will happen multiple times daily (2 or 3 times for a 3 hour orbit and 8 hour measurement window). Therefore accounting for these eclipses is part of the nominal model. Another major source of occultation could be Jupiter itself when it comes in between Ganymede and the ground station (Ganymede has an orbital period of about 7.17 days around Jupiter), therefore less

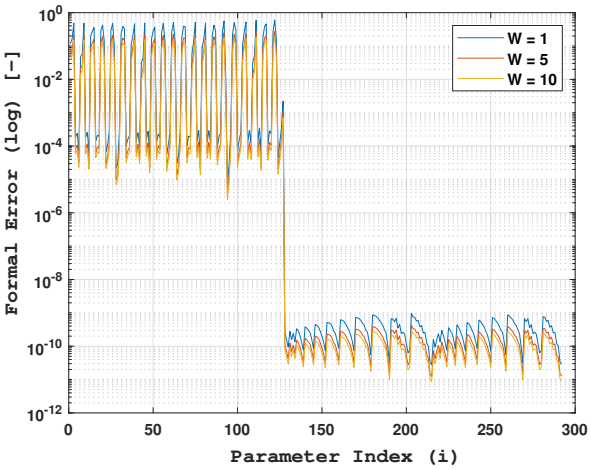

(a) This figure illustrates the formal error obtained for given Weight factors for Doppler Measurements only. Parameters 1 to 126 represent the state arcs, parameter 127 is the solar radiation pressure, Parameters 128 to 294 are the gravity field coefficientsfor degree and order 12.

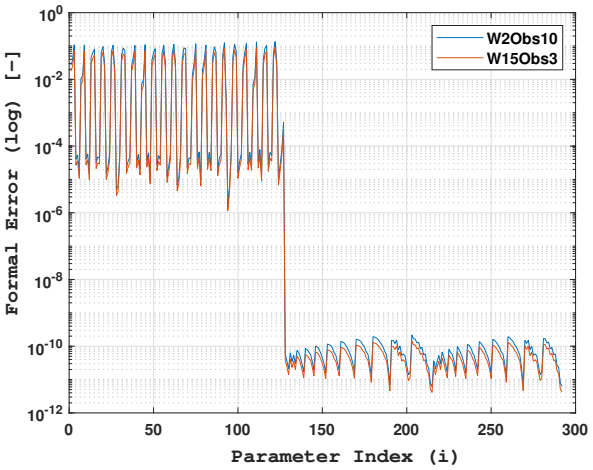

(b) This figure illustrates formal error obtained when the weight ratio and number of observations are as given in the legend. W2Obs10 means that the weight or noise is decreased by a factor 2 and the number of observations is increased by a factor 10.

Figure A.4

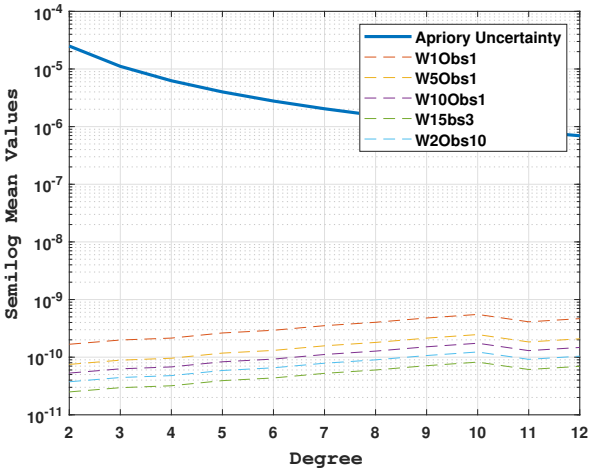

(a) This figure illustrates the Degree variance plot for data weights and number of observation ratios. For example, W2Obs10 means that the weight is decreased by a factor 2 and number of observations are increased by a factor of 10.

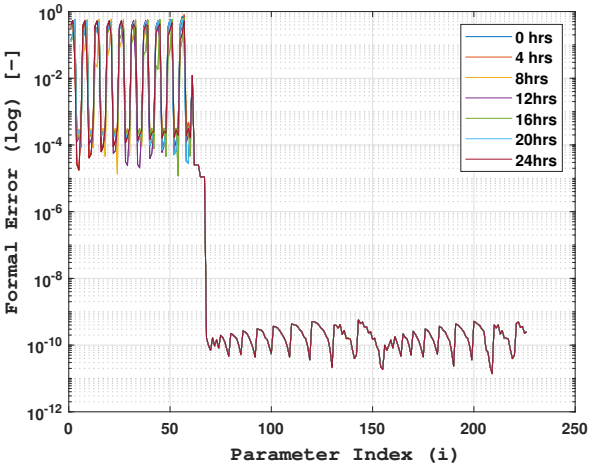

(b) This figure illustrates the formal error obtained for different hour shifts accounting for change in the initial ephemeris time.

Figure A.5

than half of the time both JUICE and Ganymede will not be ”visible” to the ground station. To prune these measurements, observation viability settings take into account the occultation of Jupiter and Ganymede. Eclipses from other Galilean moons or outer moons of Jupiter are not taken into account. When implementing the viability settings, a visible decrease in the total number of observations is observed, but total reduction in number of observations is a small portion because the orbital period around Ganymede is only 3 hours and the dark side is only a fraction of that so not all observations will be thrown out in 8 hours. This only is the case for long mission duration and the reduction in number of observations will only be visible for a simulation of 2 weeks or more. The reduction is equally proportional for all data types, since equal numbers of each data type are generated. In the Doppler only measurements this will not be applicable. Adding observation viability means that a list of times is generated for which observations are simulated and this list fulfills certain constraints, namely that there should not be a third body obscuring the measurement. This is different than the viability settings which accounts for the ground station being on the dark side of Earth. Therefore, when the ground station it is invisible to the spacecraft without eclipse conditions. This process is a bit more tedious to implement and a simple check is done to see whether it will add to the model.

This check is done by performing hour shifts as shown in figure A.5b, with settings as given in Table 2. Shifting the start time of the simulation by a few hours will allow to see the affect on the formal error. So whether, the station is visible in one simulation or not, the affect on the formal error can nonetheless be investigated. The results indeed show that for different hour shifts the formal error shows no change at all and the states do fluctuate a bit as expected. From these results, some conclusions are drawn. First that implementing a check for ground station or spacecraft visibility is not worth it for the little change that is observed. Consequently, adding an elevation angle viability check is also expected to hardly have any influence on the formal error of the gravity field coefficients. This will save unnecessary removal of valuable data which does not comply with these viability checks, if they were to be implemented. Shifting the simulation by 12 hours for instance, the earth has rotated by 180 degrees, therefore one simulation has ground station visible and the other does not. So the model is made sufficiently reasonable, but adding these constraints will result in a huge loss of data for little change in formal error in return due to observation planning. Therefore this aspect is not included in the simulation.

A.5. Mission Duration

For any mission, the longer the mission the more data is obtained hence the lower the formal error is expected to be. For mission duration, two cases are investigated. These are keeping the arc length fixed (figures A.8a and A.8b) or keeping the number of arcs fixed (figure A.6a and A.6b). In the first case, the number of arcs is fixed to 5 arcs per mission duration. In the second case, the arc length is fixed to 5 days. In both cases, the results show that increasing the mission duration decreases the formal errors. However, the change in formal error w.r.t that of 1 month is greater for changing the arc length (figure A.7a) as opposed to fixed arc length (A.9a). Fixed arc length gives a maximum of 32 percent change in formal error for the full 3.5 months mission duration, compared to 48 percent maximum difference achieved when the arc length is changed. This is because the arc length will be larger than 5 days compared to fixed arc length, providing more data to to lower the formal error. In practice, however it is more feasible to keep the arc length constant.

B. Verification & Validation

In this section verification of the simulation model and validation of the results is presented. The simulation model is not built from start, an example application from the Tudat library is taken as a basis and modified/expanded to obtain the desired functionality. Tudat is an open-source program available with free license. These example applications have already been verified by the creators and therefore do not need verification. Instead the added functionalities are verified if needed. In fact each step taken is carefully examined and verified.

B.1. Verification: Model Functionalities

In this section the verification of the correct orbit phase (GCO-500), Degree variance implementation, empirical acceleration implementation and the results of the degree 60 analysis are presented.

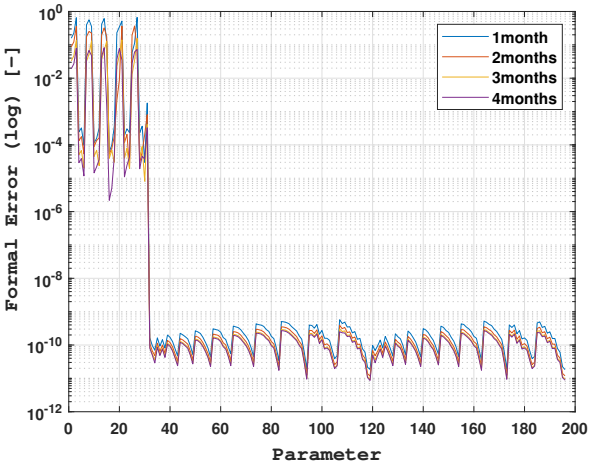

(a) This figure illustrates the Formal Error obtained for different mission duration for fixing the number of arcs to 5. Parameters 1 to 18 stand for the states, 19 is the solar radiation pressure and parameters 20 on wards are the gravity field coefficients.

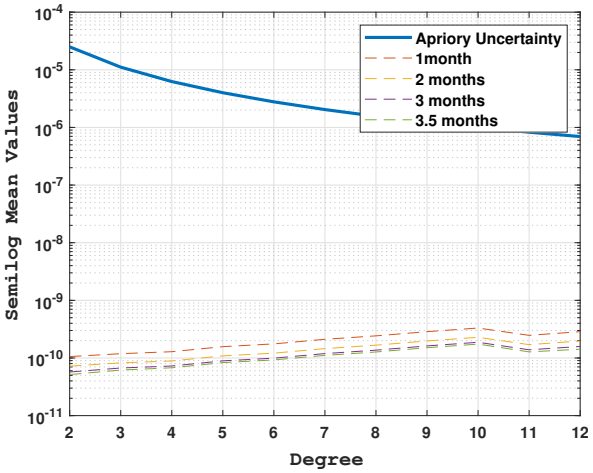

(b) This figure illustrates the Degree Variance plot for different mission duration for fixed number of arcs (5).

Figure A.6

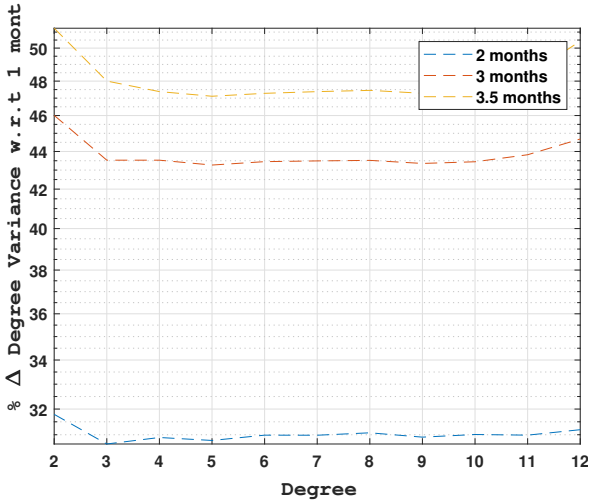

(a) This figure illustrates the % difference in degree variance when increasing the mission duration w.r.t 1 month for fixed number of arcs (5).

Figure A.7

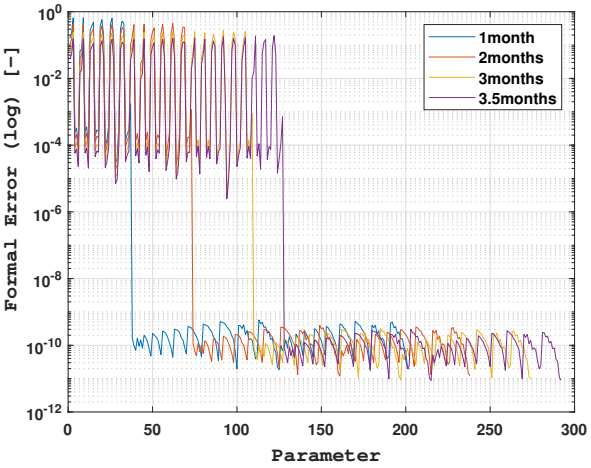

(a) This figure illustrates the formal error for different mission duration and a fixed arc length of 5 days (number of arcs will change accordingly), the arc length changes accordingly.

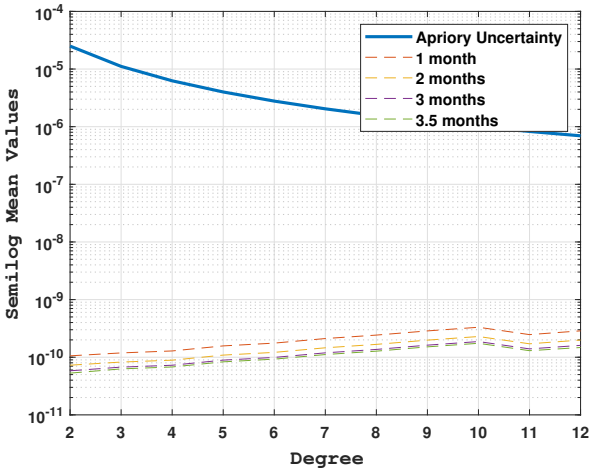

(b) This figure illustrates the degree variance for mission duration with a fixed arc length

Figure A.8

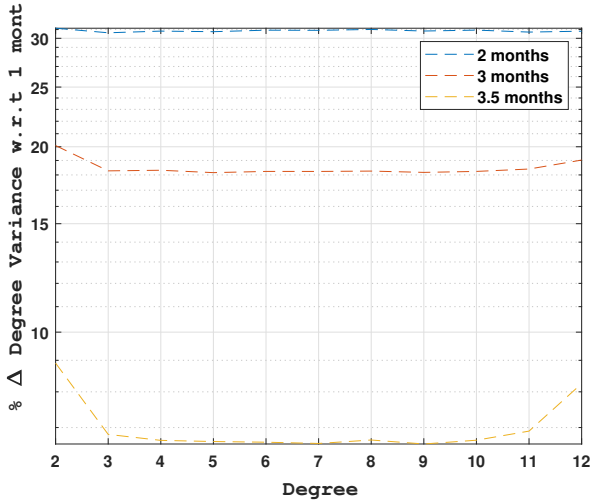

(a) This figure illustrates the degree variance difference for fixed arc length w.r.t 1 month.

Figure A.9

Table 5: Initial Ephemeris times to determine orbit eccentricity and altitude at GCO-500. The Ganymede Circular Orbit phase starts around IET 2 and continues for a maximum of 4 months. The simulation terminates for IET 4 and therefore no eccentricity or Altitude is plotted for that case. This coincides with the planned ending of the JUICE mission by end of June 2033 and final crash into Ganymede surface.

IET no.	InitialEphemerisTime (IET)	Approximate Date
1	1045240200.0	14 Feb 2033
2	1046055600.0	21 Feb 2033
3	1047712320.0	14 March 2033
4	1057179600.0	1st July

GCO-500

The aim of this study is to propagate the uncertainty in the GCO-500 phase of the Juice mission. It is therefore important to ensure that the initial ephemeris time (IET) is correct and corresponds with the right orbit. This is done checking the output for the altitude and the eccentricity at the start of the model development (See example of selected times in table 5. The plots show that the orbit has an eccentricity less than 0.1 and therefore is almost circular. The altitude is also correct, at 500 km above surface of Ganymede.

Degree Variance

To verify the implementation of the degree variance calculations in matlab, an excel sheet is created which would manually take the values for each degree and calculate the average sum of the degree and order, to finally add it all up. Even then there was a small percent difference and the difference was not entirely zero percent. However, overall the values calculated by matlab and those calculated by the excel matched. This is done because it is very easy to make a mistake with the degrees and order and with this extra check the proper implementation of the degree variance loop in the matlab script is verified.

Empirical Accelerations

When implementing empirical accelerations it is important to check whether the arc-wise empirical accelerations are implemented correctly. This is done by plotting the partial derivative of the observations with respect to the empirical acceleration arc. Alternatively, the H-matrix can also be plotted to see the evolution of the partials for each arc. Basically in an arc-wise fashion the uncertainty in Doppler observations is a function of parameters of the arc and zero for all other parameters in that arc. As seen in figures B.13b to B.19b, this gradual sequence can be observed in the H-matrix plots. Plotting these partials for each arc, confirms that all other elements other than the arc partials are exactly zero. The partials show a sinusoidal behaviour. For the case of 21 arcs only 4 partials plots are added in this appendix to demonstrate that the empirical acceleration is implemented correctly. Plotting the correlations for 3 arcs as wells as 5 arcs as shown in Figures B.24 and B.25 shows that there is correlation between empirical accelerations and the states but no correlation between empirical acceleration and gravity field coefficient uncertainty, this was the case as described and discussed in the scientific paper.

Degree 60 Analysis

Although in section on observation interval it was demonstrated that the formal error is not affected at all for observation intervals ranging from 10 minutes to 30 seconds. Nonetheless, it was argued in the paper that certain correlations might become visible when reducing the observation interval is reduced. For degree 60 analysis the correlations become higher indeed. This is not visible from the correlation plots, but as demonstrated in the scientific paper in the results section, looking up the correlation values showed an increase in correlations for gravity field coefficients $C_{2,0}$ and $C_{2,2}$. Figures B.26 and B.27 show the correlation plots for these two cases, which were not included in the paper.

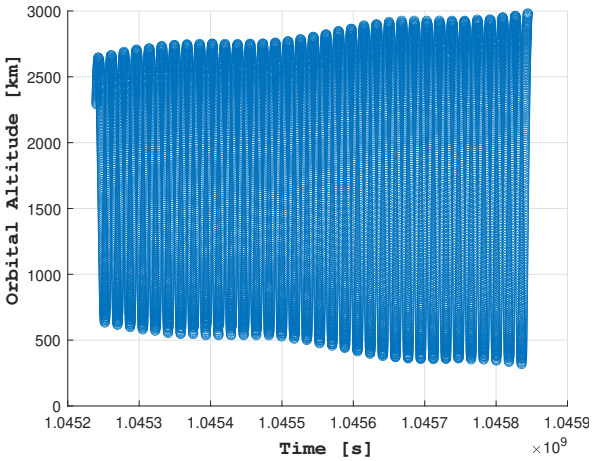

(a) This figure illustrates the orbital altitude h (km) plotted as a function of time for case IET 1 (as given in table 5). The altitude is gradually increasing and is above the desired GCO-500 phase and below the elliptical orbit phase of 5000km. It is most likely transitioning from elliptical to circular orbit.

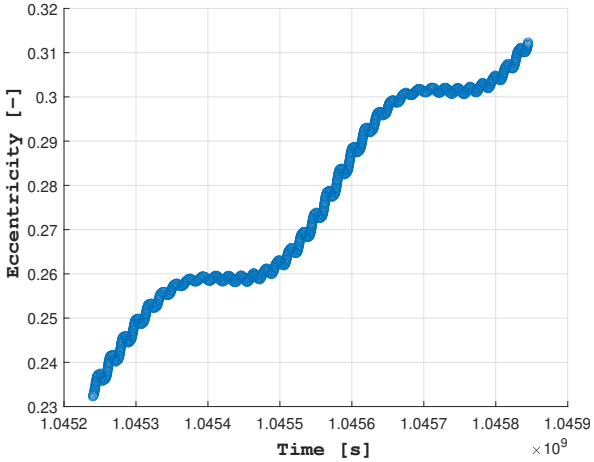

(b) This figure illustrates the eccentricity (e) of the orbit plotted as a function of time for the case of IET 1 (as given in table 5). The eccentricity is increasing with time and clearly too high to be in a circular orbit.

Figure B.10

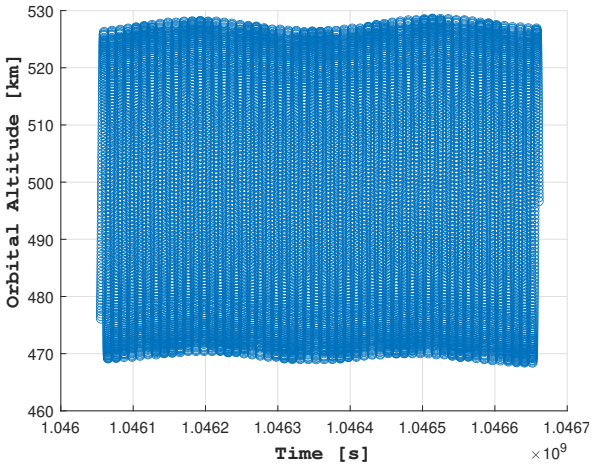

(a) This figure illustrates the orbital altitude h (km) plotted as a function of time for case IET 2 (as given in table 5). The altitude fluctuates between 470 to 530 km, indicating that with this initial ephemeris time the orbit lies within the GCO-500 phase.

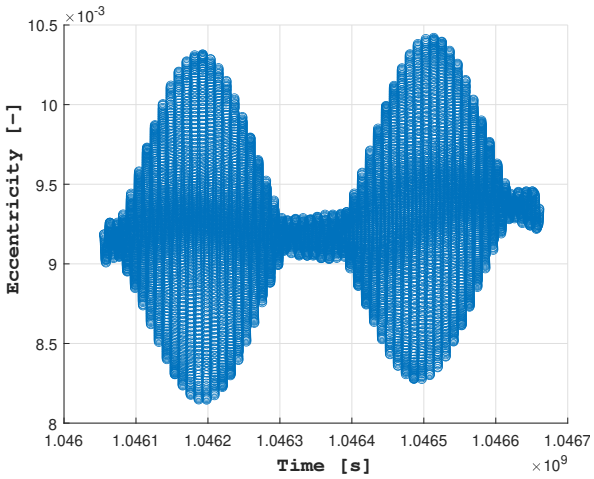

(b) This figure illustrates the eccentricity (e) of the orbit plotted as a function of time for the case of IET 2 (as given in table 5). There is a gradual sinusoidal increase in the eccentricity. The final eccentricity remains lower than 0.011, hence it is safe to assume that the orbit is circular.

Figure B.11

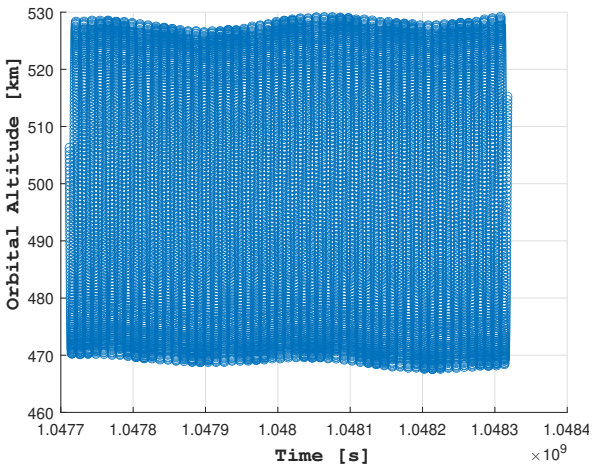

(a) This figure illustrates the orbital altitude h (km) plotted as a function of time for case IET 3 (as given in table 5). The altitude fluctuates between 470 to 530 km, indicating that with this initial ephemeris time the orbit lies within the GCO-500 phase.

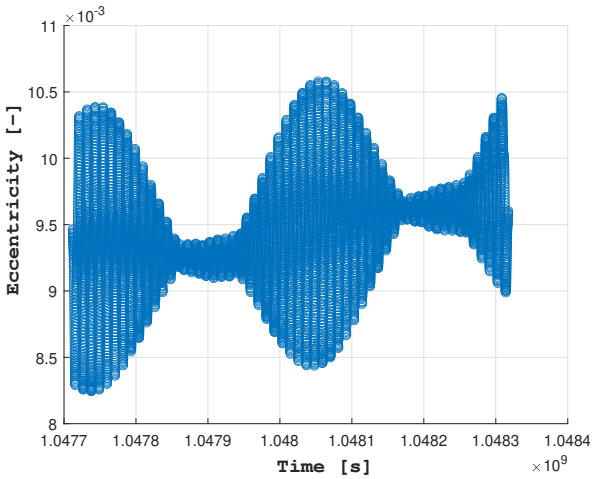

(b) This figure illustrates the eccentricity (e) of the orbit plotted as a function of time for the case of IET 3 (as given in table 5). There is a gradual sinusoidal increase in the eccentricity. The final eccentricity remains lower than 0.011, hence it is safe to assume that the orbit is circular.

Figure B.12

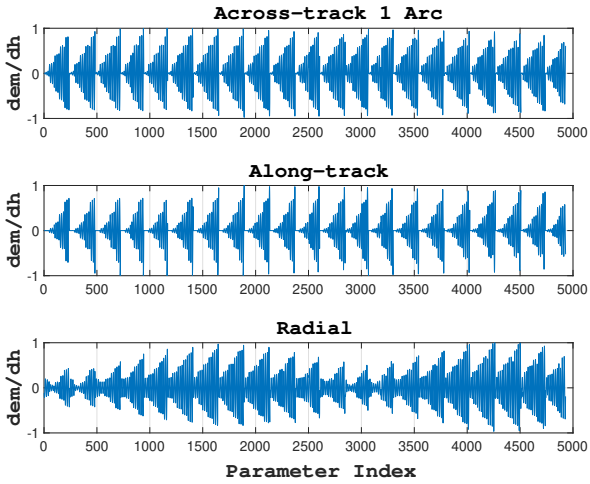

(a) This figure illustrates the partials for a single arc of 3.5 months.

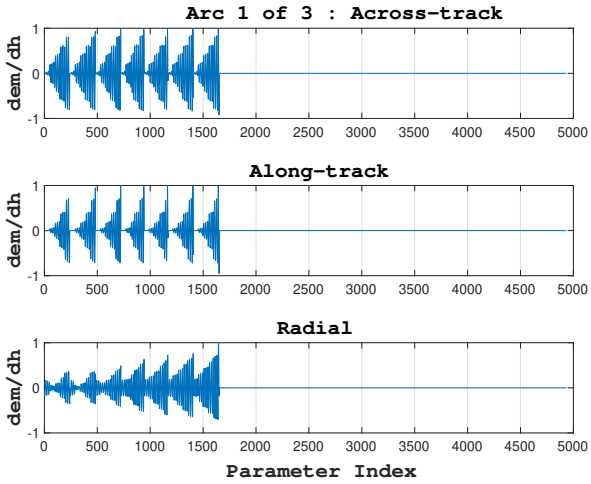

(b) This figure illustrates the partials for arc 1 of 3 arcs.

Figure B.13

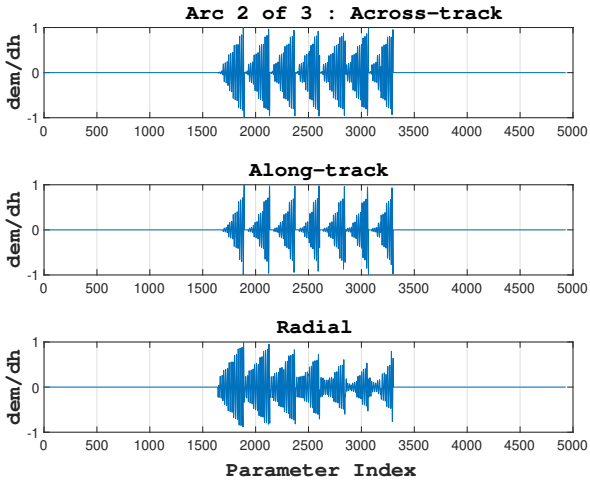

(a) This figure illustrates the partials for arc 2 of 3 arcs.

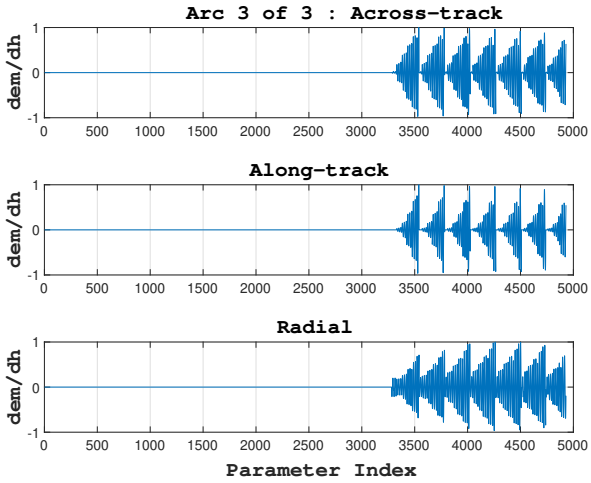

(b) This figure illustrates the partials for arc 3 of 3 arcs.

Figure B.14: The three figures above show a gradual shift in the partials for arcs 1,2 and 5 for the multi-arc implementation of the empirical accelerations. There are a total of 3 arcs with arc length of 35 days each. This is to verify if the empirical accelerations have been implemented properly. Partials for all other arcs are zero. The partials are obtained from the H matrix, representing uncertainty in empirical accelerations w.r.t uncertainty in Doppler observations ($\frac{\partial em}{\partial h}$). This gradual shift in partials for each arc can also be observed in the form of the H matrix. In this figure vertical components from the H matrix are plotted horizontally. The empirical accelerations have 3 components, namely Across-track, Along-track and radial. The horizontal axis represent the total number of Doppler Observation generated.

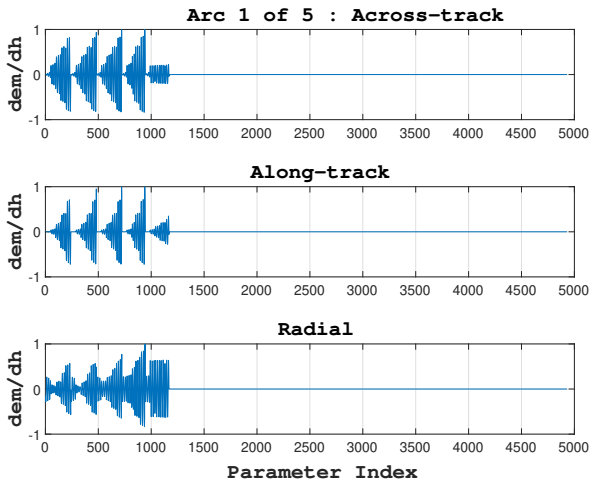

(a) This figure illustrates the partials for arc 1 of 5 arcs.

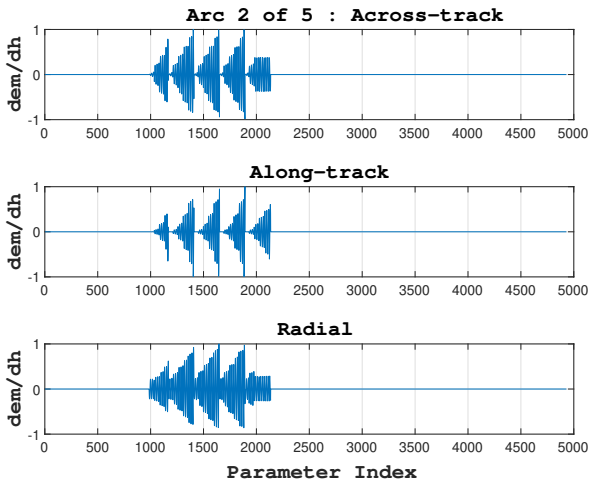

(b) This figure illustrates the partials for arc 2 of 5 arcs.

Figure B.15

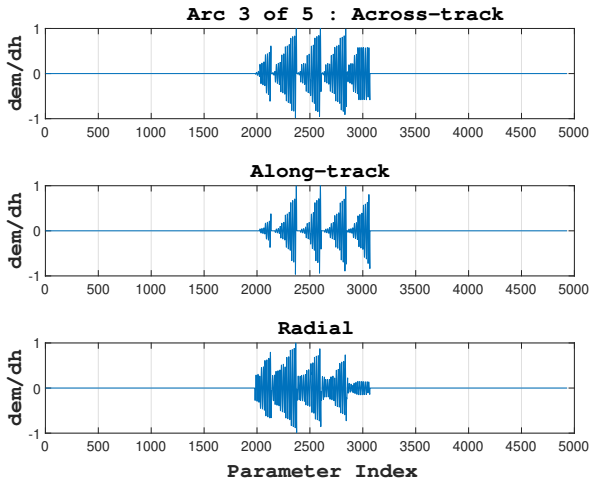

(a) This figure illustrates the partials for arc 3 of 5 arcs.

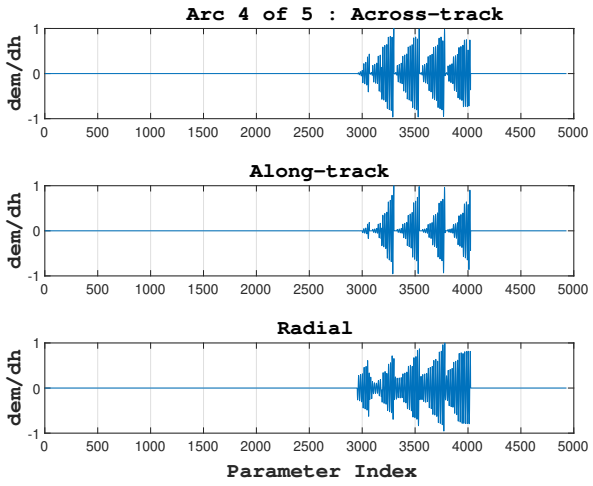

(b) This figure illustrates the partials for arc 4 of 5 arcs.

Figure B.16

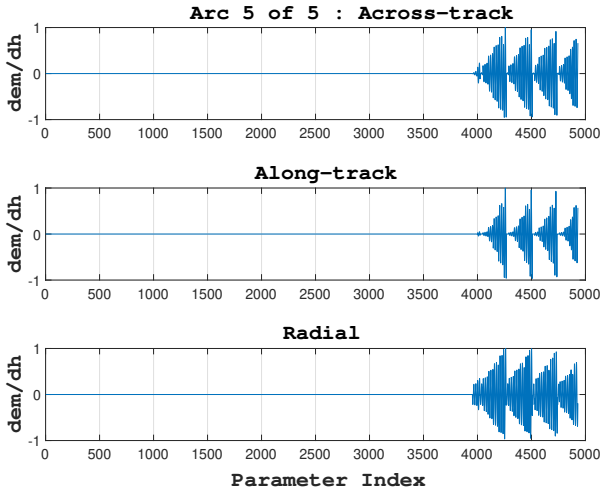

Figure B.17: The previous five figures show a gradual shift in the partials for arcs 1,2, 3, 4 and 5 for the multi-arc implementation of the empirical accelerations. There are a total of 5 arcs with arc length of 21 days each. This is to verify if the empirical accelerations have been implemented properly. Partials for all other arcs are zero. The partials are obtained from the H matrix, representing uncertainty in empirical accelerations w.r.t uncertainty in Doppler observations ($\frac{\partial em}{\partial h}$). This gradual shift in partials for each arc can also be observed in the form of the H matrix. In this figure vertical components from the H matrix are plotted horizontally. The empirical accelerations have 3 components, namely Across-track, Along-track and radial. The horizontal axis represent the total number of Doppler Observation generated.

B.2. Validation: Model Output

Two sets of outputs are validated in this section. First the degree variance as a function of degree, which is a basis for the covariance analysis. Secondly, the behaviour of the gravity field formal error as a function of spherical harmonic degree.

Degree Variance

In a study of 3GM for the JUICE mission by Di Benedetto et al. (2021) the degree variance for a Callisto flyby trajectory is presented (Figure B.28a). The degree variance plot makes it possible to compare the a priori uncertainty with the formal errors in the covariance analysis. This is to see how far the formal uncertainties lie from the a priori uncertainty and at what point do they converge, to understand how far or close the model output lies from the a priori information. Therefore, the degree variance plot has been used as an initial check to validate the output of the simulation. Figure B.28b shows that the initial degree variance obtained for the Doppler only simulations conforms with the results obtained by Di Benedetto et al. (2021) in Figure B.28a. A same upwards trend in the formal uncertainty curve is seen, even though the magnitudes of the Mean values are different.

Gravity field

While doing the formal error analysis during this project, a recurring observation was the decrease in formal error for increasing spherical harmonic degree. This can be seen both for range and Doppler only measurements. These two cases are shown in figures B.29b and B.29c respectively. This means that the formal error is estimated better as the degree increases. As the degree increases, the amount of data increases as well, which will statistically reduce the formal error of higher degrees, as the errors in lower degrees due to lower quality and quantity of data will spread out more.

Figure B.29b is compared to B.29a, as reported in work by Dirkx et al. (2019). In this paper it is shown that when comparing range and Doppler data, as the degree of the gravity field increases the contribution of range to the solution goes down, which means that for higher degrees including range will have less affect, this is due to higher correlations of the range data compared to the Doppler data. Range data also has bias and the Doppler data has almost no bias (Dirkx et al. (2019)). This should be kept in mind when adding $1cm$ range noise to include the range observations in Doppler only observations, when determining the gravity field. Nonetheless it should not be reason to exclude the 1 cm range noise altogether.

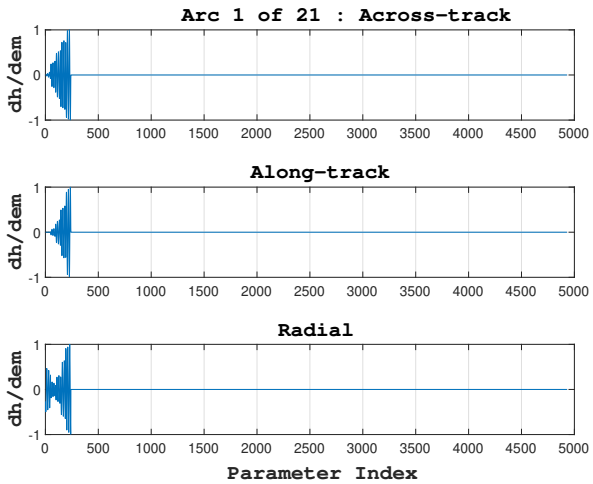

(a) This figure illustrates the partials for arc 1 of 21 arcs.

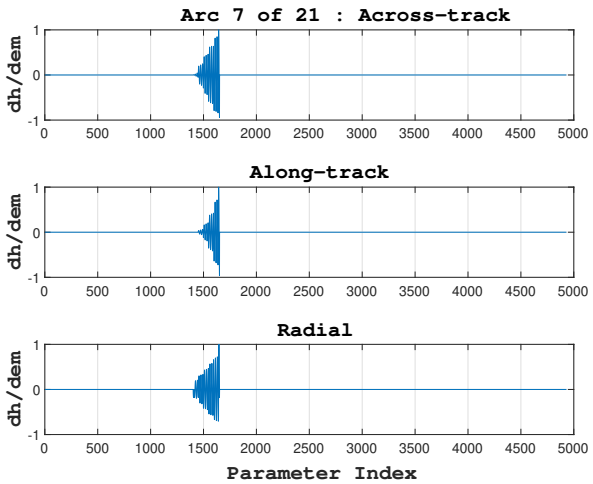

(b) This figure illustrates the partials for arc 7 of 21 arcs.

Figure B.18

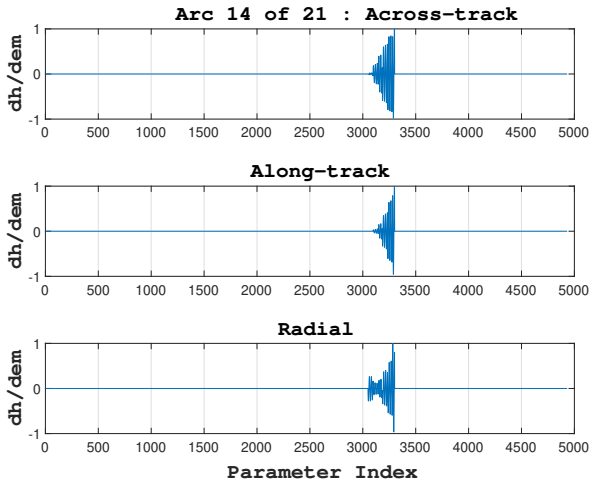

(a) This figure illustrates the partials for arc 14 of 21 arcs.

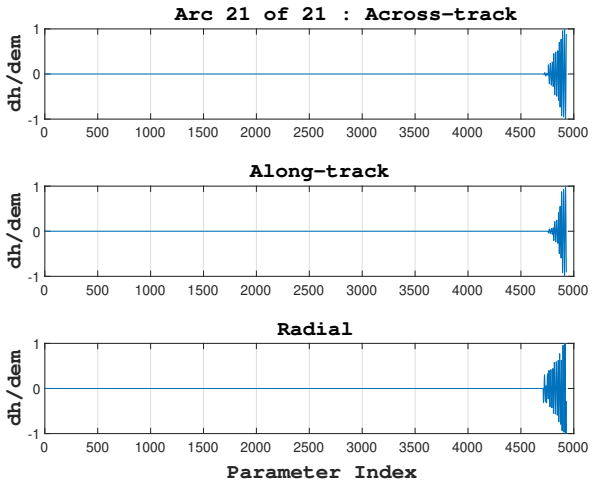

(b) This figure illustrates the partials for arc 21 of 21 arcs.

Figure B.19: The four figures above show a gradual shift in the partials for arcs 1,7, 14 and 21 for the multi-arc implementation of the empirical accelerations. There are a total of 21 arcs with arc length of 5 days each. This is to verify if the empirical accelerations have been implemented properly. Partials for all other arcs are zero. The partials are obtained from the H matrix, representing uncertainty in empirical accelerations w.r.t uncertainty in Doppler observations ($\frac{\partial em}{\partial h}$). This gradual shift in partials for each arc can also be observed in the form of the H matrix. In this figure vertical components from the H matrix are plotted horizontally. The empirical accelerations have 3 components, namely Across-track, Along-track and radial. The horizontal axis represent the total number of Doppler Observation generated.

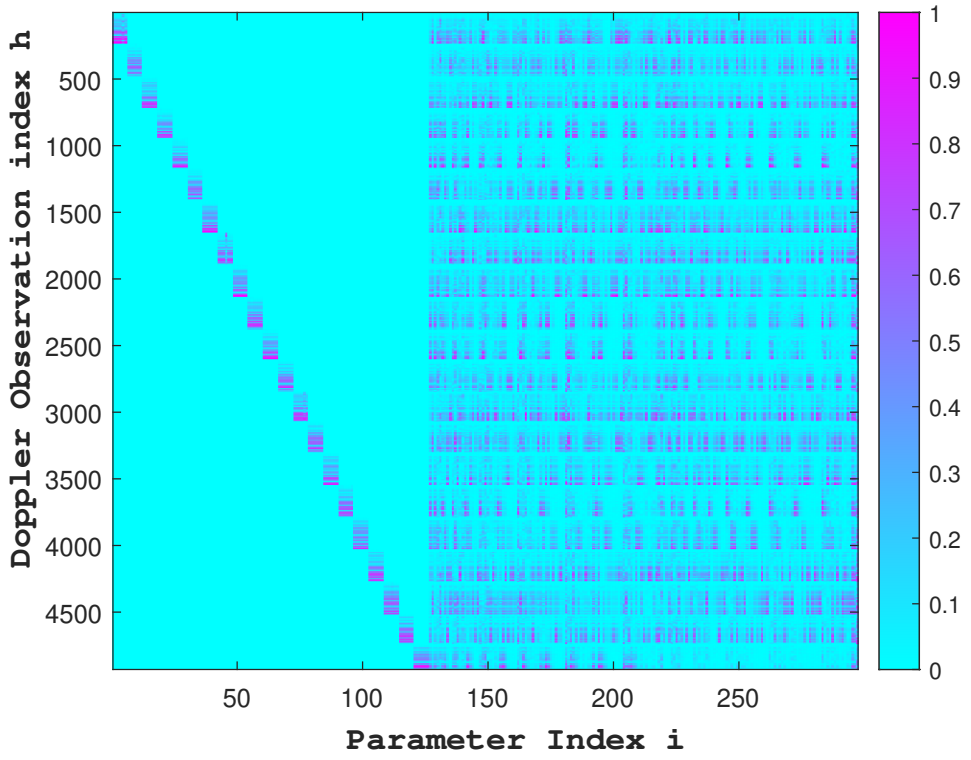

Figure B.20: This figure illustrates the H matrix for empirical accelerations of 1 arc. The H matrix contains partial derivatives, representing uncertainty in Doppler observations w.r.t uncertainty in parameters ($\frac{\partial h}{\partial i}$). The vertical axis represents the total number of Doppler observations generated. The parameters on the horizontal axis represent the states (1 to 126), the gravity field coefficients (127-294) and the empirical accelerations (295-297).

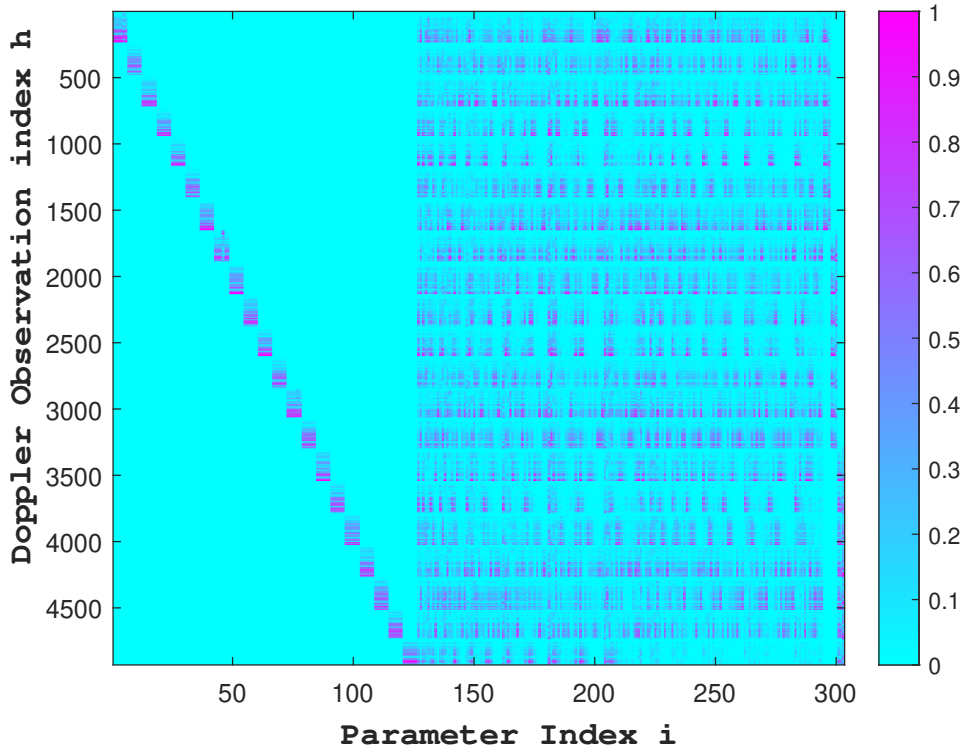

Figure B.21: This figure illustrates the H matrix for empirical accelerations of 3 arc. The H matrix contains partial derivatives, representing uncertainty in Doppler observations w.r.t uncertainty in parameters ($\frac{\partial h}{\partial i}$). The vertical axis represents the total number of Doppler observations generated. The parameters on the horizontal axis represent the states (1 to 126), the gravity field coefficients (127-294) and the empirical accelerations (295-303).

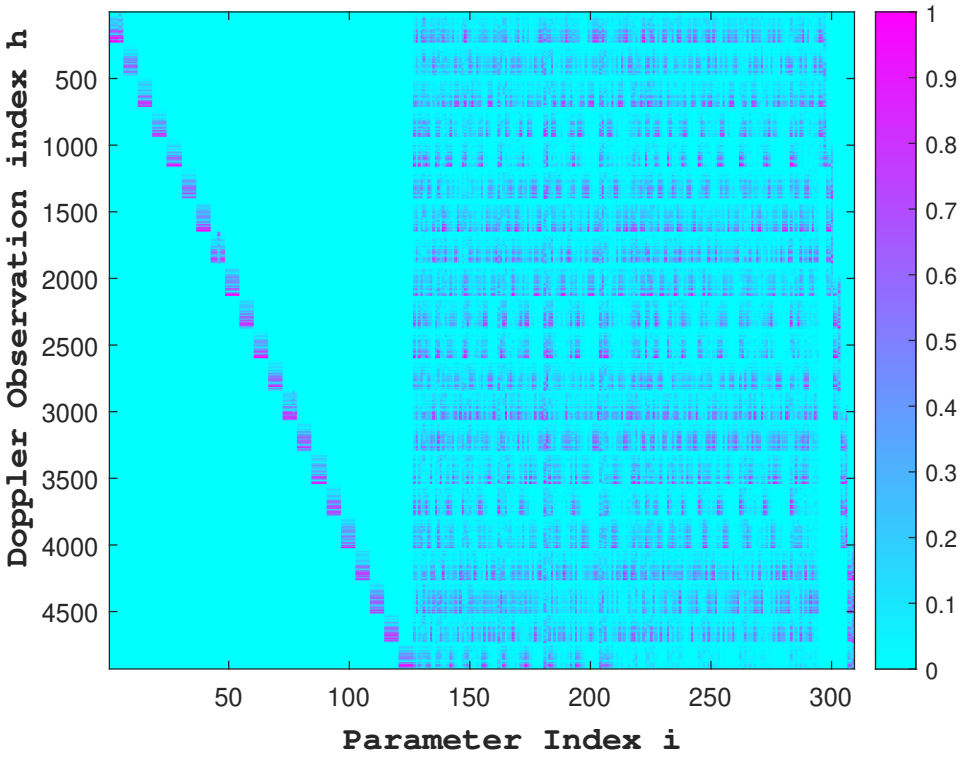

Figure B.22: This figure illustrates the H matrix for empirical accelerations of 5 arcs. The H matrix contains partial derivatives, representing uncertainty in Doppler observations w.r.t uncertainty in parameters ($\frac{\partial h}{\partial i}$). The vertical axis represents the total number of Doppler observations generated. The parameters on the horizontal axis represent the states (1 to 126), the gravity field coefficients (127-294) and the empirical accelerations (295-309).

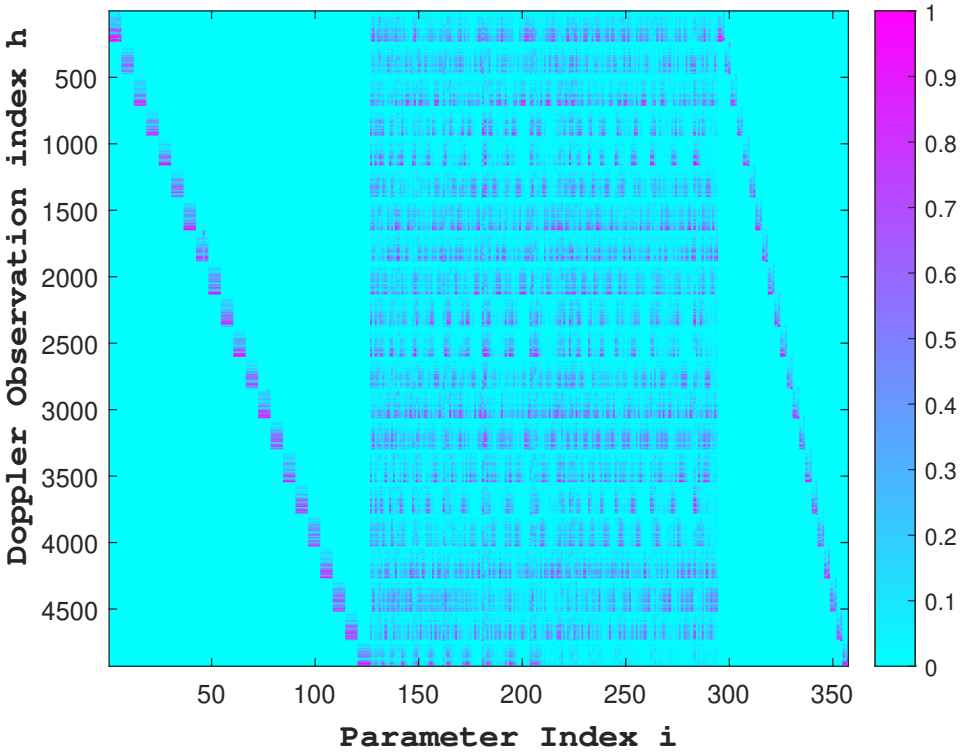

Figure B.23: This figure illustrates the H matrix for empirical accelerations of 21 arcs. The H matrix contains partial derivatives, representing uncertainty in Doppler observations w.r.t uncertainty in parameters ($\frac{\partial h}{\partial i}$). The vertical axis represents the total number of Doppler observations generated. The parameters on the horizontal axis represent the states (1 to 126), the gravity field coefficients (127-294) and the empirical accelerations (295-357).

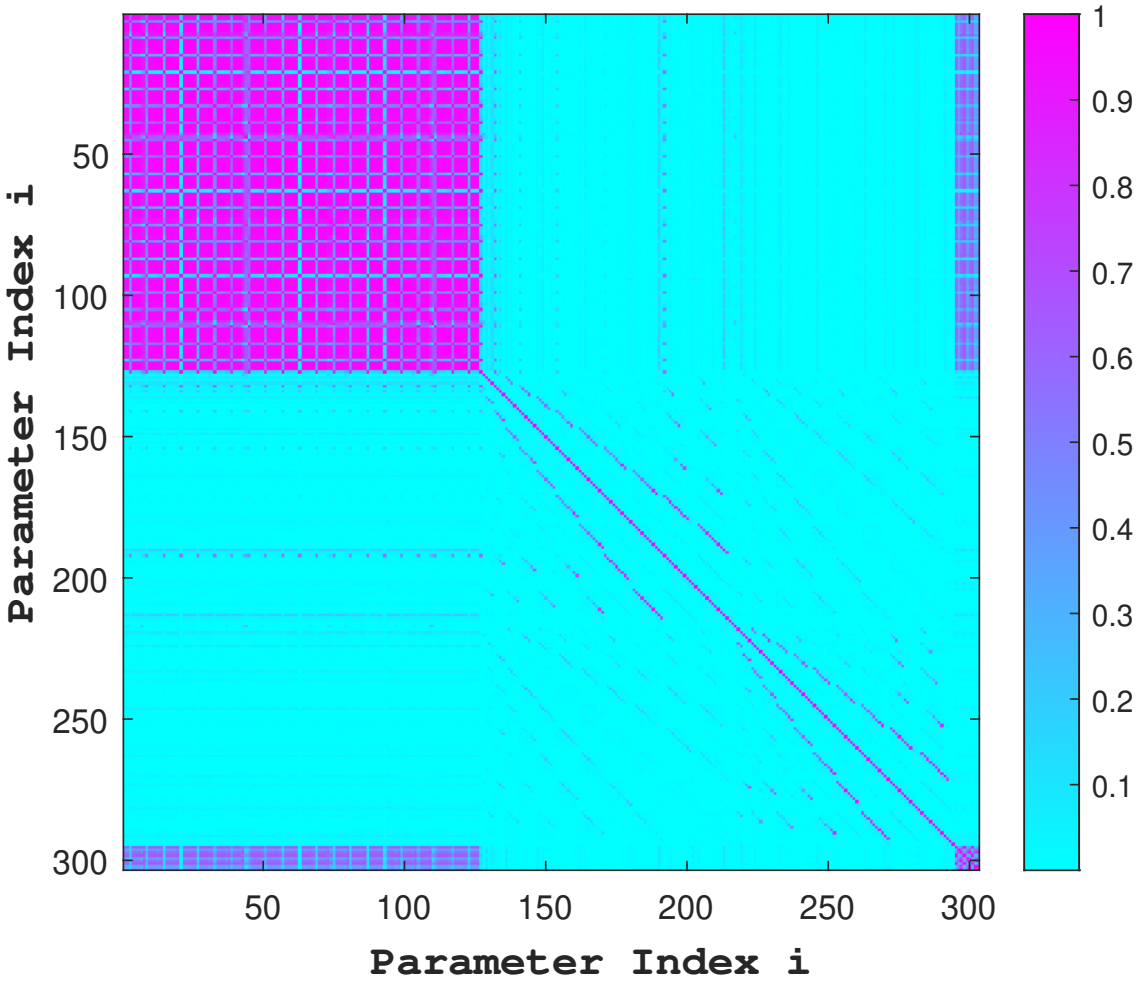

Figure B.24: This figure illustrates the correlations with addition of empirical accelerations for the case of 3 arcs. Parameters 1 to 126 represent the states for each arc. There are a total of 21 arcs with 3 values for position (x,y,z) followed by 3 values for velocity (v_x,v_y,v_z). The correlation between the states form the symmetrical block in the top left corner of the correlation matrix. Parameters 127 to 294 stand for the Cosine and Sine coefficients of the gravity field. For the Cosine coefficient ($C_{n,m}$) starting with degree 1 (n) and increasing order 0 (m) in the following manner ($C_{1,0}$, $C_{1,1}$, $C_{2,1}$, $C_{2,2}$, $C_{3,0}$, ..., $C_{12,12}$). The Sine Coefficient of the gravity field ($S_{n,m}$) in the following manner ($S_{1,1}$, $S_{2,1}$, $S_{2,2}$, $S_{3,1}$,...., $S_{12,12}$). Parameters 295 to 303 represent the values of the empirical accelerations for the 3 arcs. The correlation matrix is symmetric and the diagonal entries should be ideally equal to 1, they represent the parameters correlated with themselves. The figure also shows that the states as well as the empirical accelerations are correlated with themselves, top left and bottom right corner respectively.

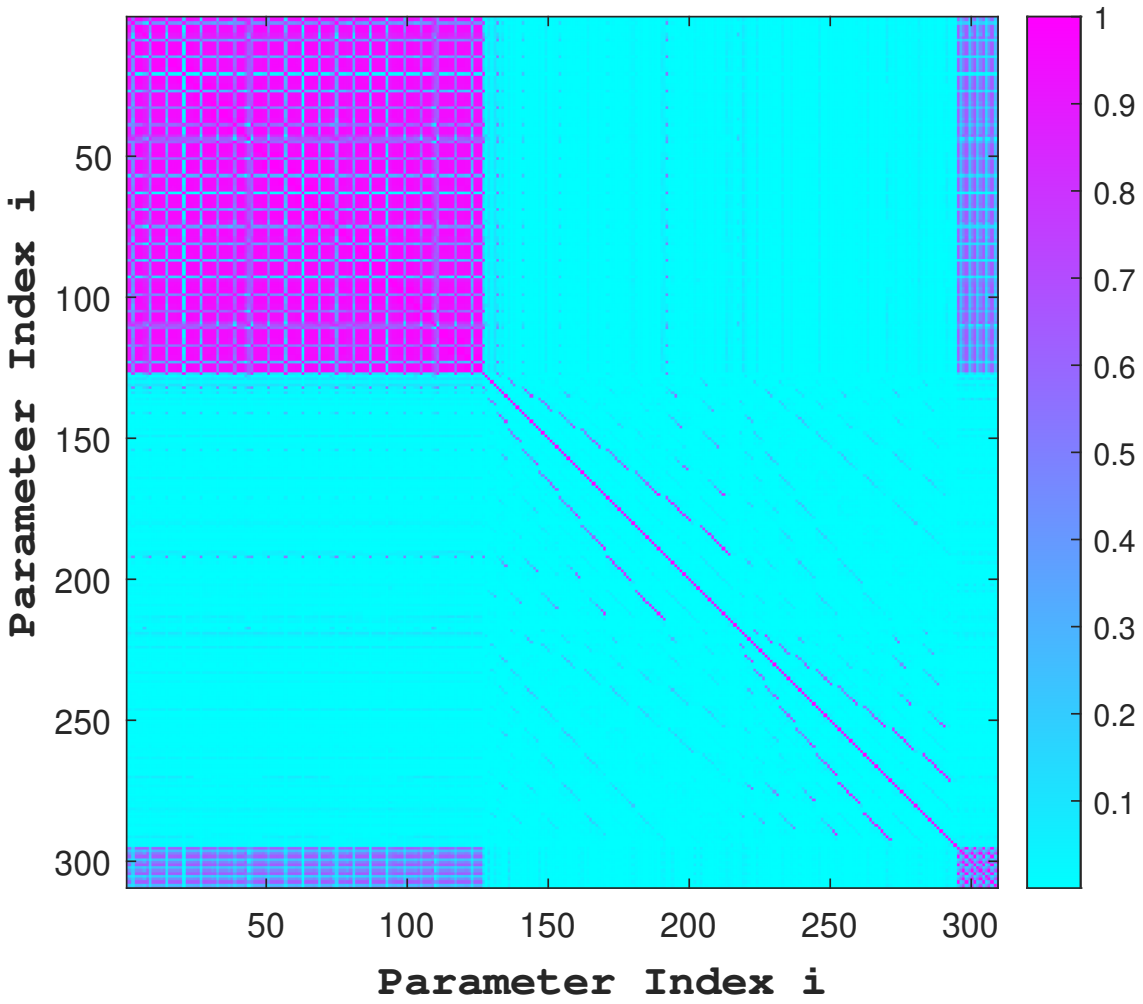

Figure B.25: This figure illustrates the correlations with addition of empirical accelerations for the case of 5 arcs. Parameters 1 to 126 represent the states for each arc. There are a total of 21 arcs with 3 values for position (x,y,z) followed by 3 values for velocity (v_x,v_y,v_z). The correlation between the states form the symmetrical block in the top left corner of the correlation matrix. Parameters 127 to 294 stand for the Cosine and Sine coefficients of the gravity field. For the Cosine coefficient ($C_{n,m}$) starting with degree 1 (n) and increasing order 0 (m) in the following manner ($C_{1,0}$, $C_{1,1}$, $C_{2,1}$, $C_{2,2}$, $C_{3,0}$, ..., $C_{12,12}$). The Sine Coefficient of the gravity field ($S_{n,m}$) in the following manner ($S_{1,1}$, $S_{2,1}$, $S_{2,2}$, $S_{3,1}$,...., $S_{12,12}$). Parameters 295 to 309 represent the values of the empirical accelerations for the 5 arcs. The correlation matrix is symmetric and the diagonal entries should be ideally equal to 1, they represent the parameters correlated with themselves. The figure also shows that the states as well as the empirical accelerations are correlated with themselves, top left and bottom right corner respectively.

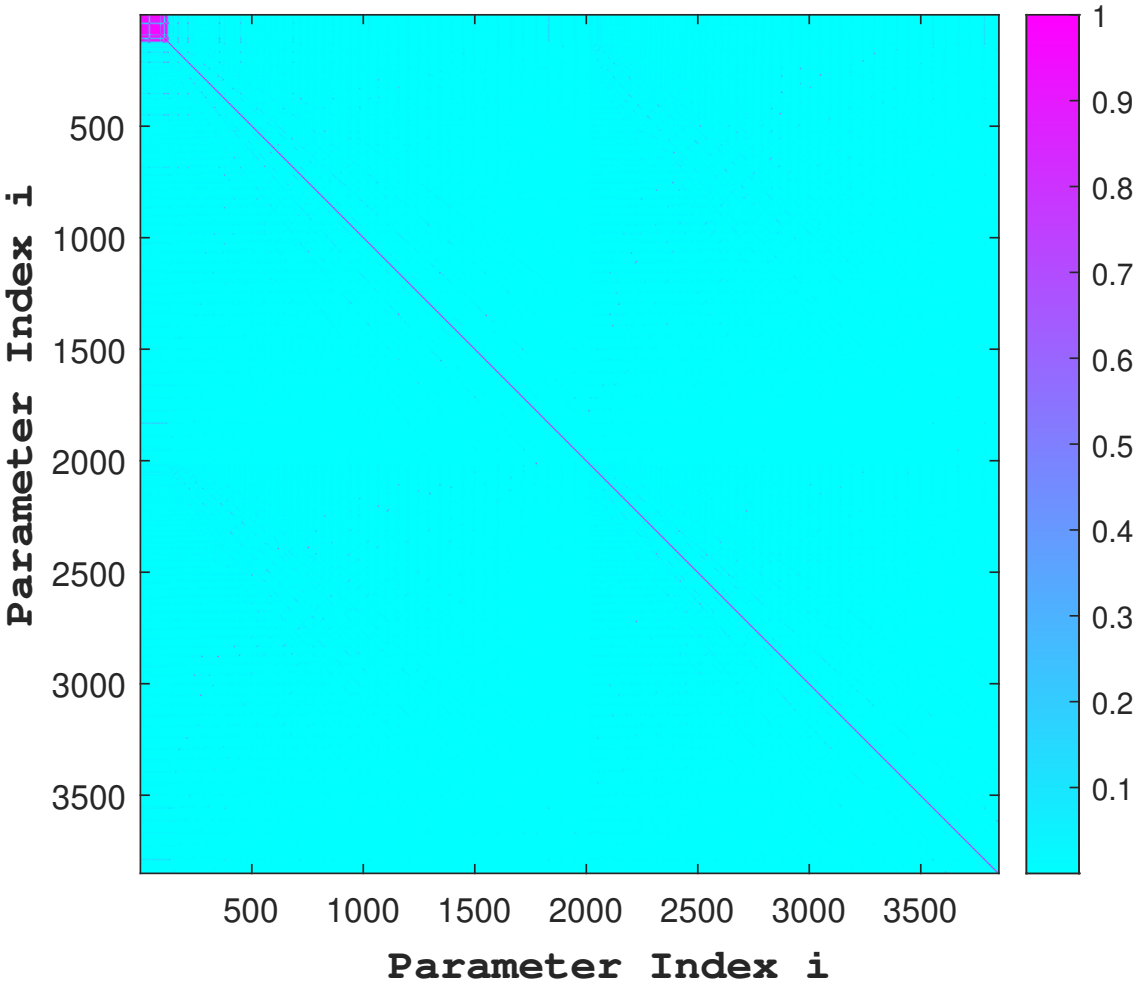

Figure B.26: This figure illustrates the correlations for degree 60 for observation interval of 2 min. Parameters 1 to 126 represent the states for each arc. Parameter 127 stands for the Gravitational parameter. There are a total of 21 arcs with 3 values for position (x,y,z) followed by 3 values for velocity (v_x,v_y,v_z). The correlation between the states form the symmetrical block in the top left corner of the correlation matrix. Parameters 128 to 3847 stand for the Cosine and sine coefficients respectively of the gravity field. The cosine coefficients are represented as follows: ($C_{n,m}$) starting with degree 1 (n) and increasing order (m) in the following manner ($C_{1,0}$, $C_{1,1}$, $C_{2,0}$, $C_{2,1}$, ..., $C_{60,60}$). Almost similar for the sine coefficients: ($S_{n,m}$) in the following manner ($S_{2,1}$, $S_{2,1}$, $S_{2,2}$, $S_{3,1}$,...., $S_{12,12}$). The correlation matrix is symmetric and the diagonal entries should be ideally equal to 1, they represent the parameters correlated with themselves.The final 3 parameters 3848-3850 stand for the empirical acceleration of the single arc.

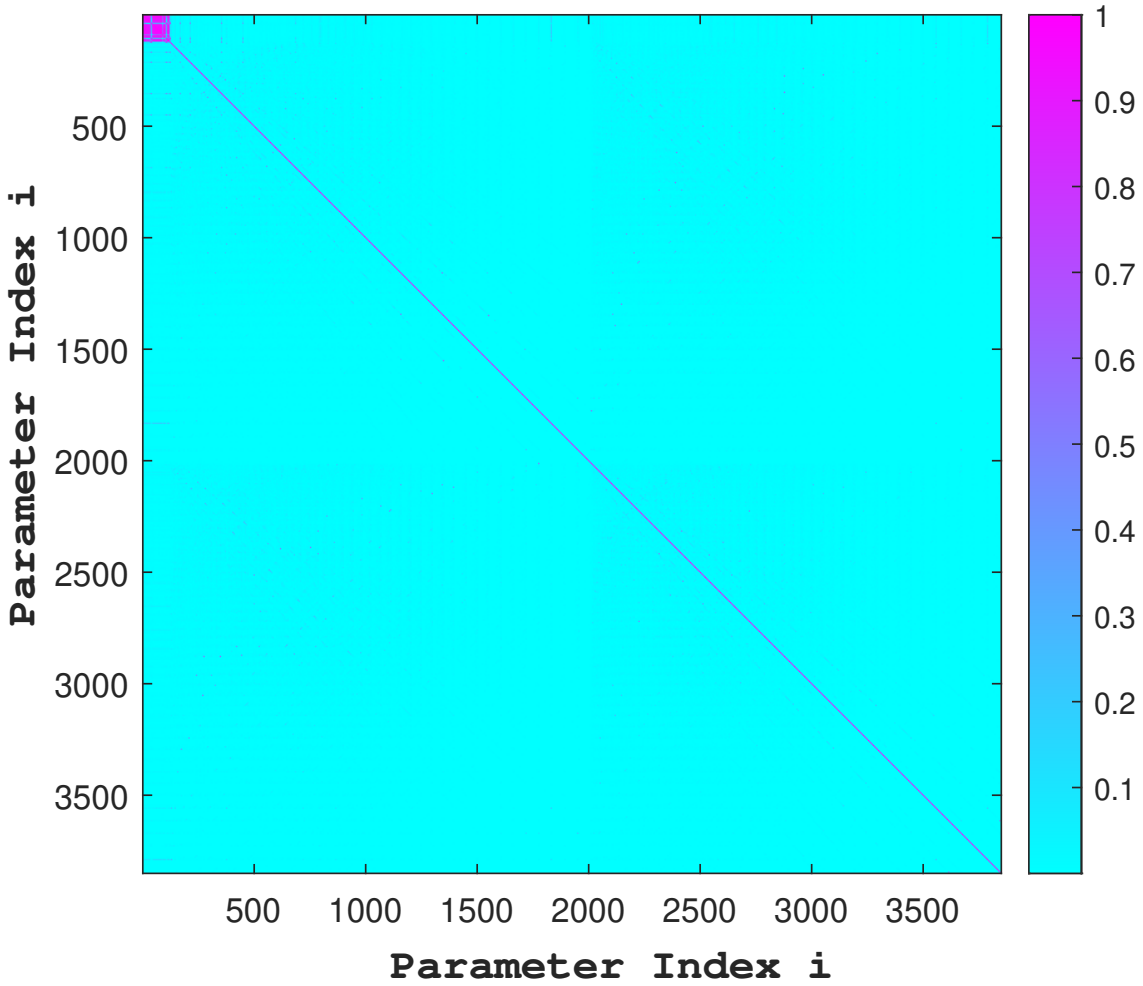

Figure B.27: This figure illustrates the correlations for degree 60 for observation interval of 5 min. Parameters 1 to 126 represent the states for each arc. Parameter 127 stands for the Gravitational parameter. There are a total of 21 arcs with 3 values for position (x,y,z) followed by 3 values for velocity (v_x,v_y,v_z). The correlation between the states form the symmetrical block in the top left corner of the correlation matrix. Parameters 128 to 3847 stand for the Cosine and sine coefficients respectively of the gravity field. The cosine coefficients are represented as follows: ($C_{n,m}$) starting with degree 1 (n) and increasing order (m) in the following manner ($C_{1,0}$, $C_{1,1}$, $C_{2,0}$, $C_{2,1}$, ..., $C_{60,60}$). Almost similar for the sine coefficients: ($S_{n,m}$) in the following manner ($S_{2,1}$, $S_{2,1}$, $S_{2,2}$, $S_{3,1}$,...., $S_{12,12}$). The correlation matrix is symmetric and the diagonal entries should be ideally equal to 1, they represent the parameters correlated with themselves.The final 3 parameters 3848-3850 stand for the empirical acceleration of the single arc.

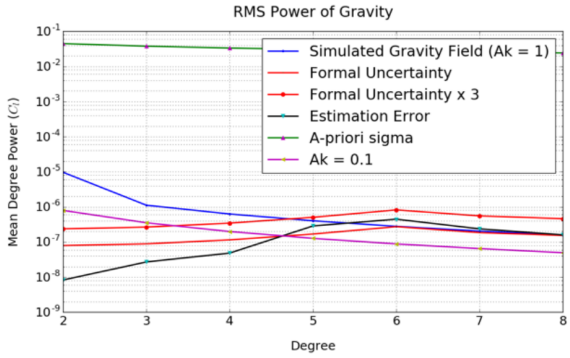

(a) This figure illustrates the degree variance obtained by Di Benedetto et al. (2021) for flyby of Callisto. Point of interest is the formal error uncertainty curve.

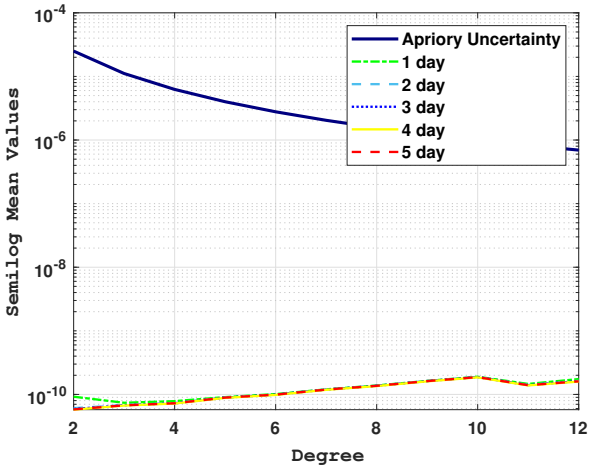

(b) This figure illustrates the Degree variance for different arc length for a 12x12 gravity field, Doppler observations only.

Figure B.28

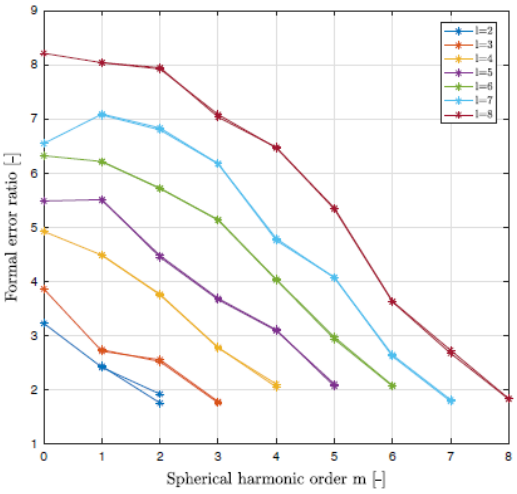

(a) This figure illustrates the decrease in formal error ratio of range to Doppler observations with increasing spherical harmonic order (m) as reported by Dirkx et al. (2019).

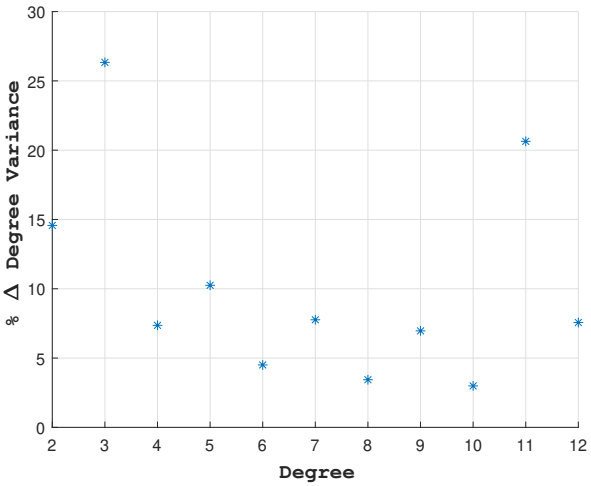

(b) This figure illustrates the percentage change in degree variance as a function of spherical harmonic degree for range only observations. The percentage difference is calculated as a difference in the degree variance for 1cm and 20cm noise, w.r.t 20cm noise in range only observations.

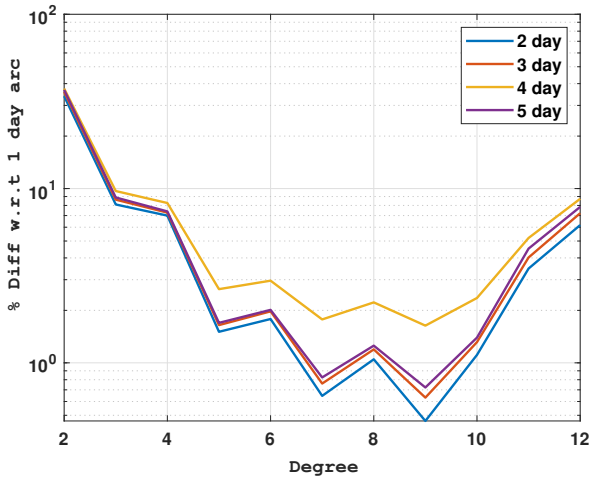

(c) This figure illustrates the % change in degree variance of the gravity field uncertainty for different arc lengths with respect to the 1 day arc, for doppler only observations. This means that the average value of the degree field uncertainty decreases with increasing degree.

Figure B.29

Bibliography

Paolo Cappuccio, Mauro Di Benedetto, Gael Cascioli, and Luciano Iess. Report on juice 3gm gravity experiment performance. In *European Planetary Science Congress*, pages EPSC2018–1066, 2018.

G Cimò, D Dirkx, DA Duev, G Molera Calvs, TM Bocanegra Bahamon, and LI Gurvits. Pride: Ground-based vlbi observations for the juice mission. In *European Planetary Science Congress*, volume 11, 2017.

Mauro Di Benedetto, Paolo Cappuccio, Serena Molli, Lorenzo Federici, and Alessandro Zavoli. Analysis of 3gm callisto gravity experiment of the juice mission. *arXiv preprint arXiv:2101.03401*, 2021.

Dominic Dirkx, V Lainey, LI Gurvits, and PNAM Visser. Dynamical modelling of the galilean moons for the juice mission. *Planetary and Space Science*, 134:82–95, 2016.

Dominic Dirkx, Leonid I Gurvits, Valery Lainey, Giacomo Lari, Andrea Milani, Giuseppe Cimò, TM Bocanegra-Bahamon, and PNAM Visser. On the contribution of pride-juice to jovian system ephemerides. *Planetary and Space Science*, 147:14–27, 2017.

Dominic Dirkx, Ivan Prochazka, Sven Bauer, Pieter Visser, Ron Noomen, Leonid I Gurvits, and Bert Vermeersen. Laser and radio tracking for planetary science missions—a comparison. *Journal of Geodesy*, 93(11):2405–2420, 2019.

ESA. Juice (jupiter icy moon explorer): Exploring the emergence of habitable worlds around gas giants. Technical report, European Space Agency, 2014.

Andrea Magnanini. Estimation of the ephemerides and gravity fields of the galilean moons through orbit determination of the juice mission. *Aerotecnica Missili & Spazio*, 100(3):195–206, 2021.